Analysis, Modeling and CAE Validation of Vehicle Crashes using Advanced Signal Processing Tools

Zuolong Wei

Analysis, Modeling and CAE Validation of Vehicle Crashes using Advanced Signal Processing Tools

A dissertation submitted to the University of Agder for the degree of
Doctor of Philosophy, Specialization in Mechatronics

University of Agder
Faculty of Engineering and Science
2017

Doctoral Dissertation at the University of Agder 159
ISSN: 1504-9272
ISBN: 978-82-7117-854-3

Printed by Wittusen & Jensen
Oslo

Acknowledgments

In the August of 2013, I came to Grimstad with dreams of my future. Three years have past and I received a lot: knowledge, friendship and love. For me, this is an excellent experience, which is infinitely precious and worth saving.

I wish to express my sincere gratitude to my supervisor, Prof. Kjell G. Robbersmyr, for his priceless advice, encouragement and patience in guiding my research life. He introduced me to the world of science, created chances for me to broad the view and offered me powerful support. He also conducted a physical crash test to support my research. All his help benefit my PhD work a lot.

I would like to thank my co-supervisor Prof. Hamid R. Karimi. In the three years, he attended all regular meetings and gave me helpful suggestions all the way along my research. From the discussions with him, I learned not only scientific knowledge but also useful skills in analyzing and dealing with problems. Without his insightful comments, my PhD project will not be proceeded smoothly.

I am grateful to the faculty members in Dynamics Research Group, Prof. Geir Grasmo, Assoc. Prof. Jan Henriksen, Assoc. Prof. Morten K. Ebbesen and Assoc. Prof. van Khang Huynh, who are qualified scientists with rich knowledge and professional attitude. I learned a lot from them. And I thank my office colleagues, Åse Linn, Emma and Sissel, who gave me a lot of help during the past three years.

I am thankful to my PhD colleagues, Witold, Jesper, Jannik, Surya, Jagath, Knut, Magnus, Øyvind, Andreas and Bernard. I am proud to work together with them. I also thank to my friends in the university, Ilya, Morten, Charly, Souman, Lei, Xuan, Huihui, Indika, Lakshmikanth, Mohamed, Meisam, Renée and Vimala. We have a good time together.

Least, but certainly not the last, I want to express the most sincere gratitude to my family for all their love and encouragement. In Grimstad, I met my wife, Tian, and we married on the Christmas Day in 2014. She accompanied me in the alien land and shared with me all the good and bad moments. I should also be grateful to my mother, who raised me with a love of science and supported me in all my pursuits.

Zuolong Wei

Grimstad, March 21, 2017

Thesis Details

Thesis Title: Analysis, Modeling and CAE Validation of Vehicle Crashes using Advanced Signal Processing Tools

PhD Student: Zuolong Wei

Supervisors: Prof. Kjell G. Robbersmyr, University of Agder
Prof. Hamid R. Karimi, Politecnico di Milano

The main body of this thesis consist of the following papers:

[A] Z. Wei, H. R. Karimi, and K. G. Robbersmyr, "A model of vehicle-fixed barrier frontal crash and its application in the estimation of crash kinematics," *24th Enhanced Safety of Vehicles Conference (ESV2015)*, Paper Number 15-0161, 2015.

[B] Z. Wei, H. R. Karimi, and K. G. Robbersmyr, "EEMD based analysis of vehicle crash responses," in *IECON 2015 - 41st Annual Conference of the IEEE Industrial Electronics Society*, pp. 005206–005210, 2015.

[C] Z. Wei, H. R. Karimi, and K. G. Robbersmyr, "Analysis of the relationship between energy absorbing components and vehicle crash response", *SAE Technical Paper*, Paper No. 2016-01-1541, 2016.

[D] Z. Wei, K. G. Robbersmyr, and H. R. Karimi, "Data-based modeling and estimation of vehicle crash processes in frontal fixed-barrier crashes", submitted to *Journal of the Franklin Institute*, 2016.

[E] Z. Wei, K. G. Robbersmyr, and H. R. Karimi, "An EEMD aided comparison of time histories and its application in vehicle safety", *IEEE Access, Special Section: Recent Advances on Modelling, Optimization and Signal Processing Methods in Vehicle Dynamics and Crash-worthiness*, 2016.

In addition to the main papers, the following publications have also been made:

[1] Z. Wei, S. Yin, and H. R. Karimi, "A subspace based fault diagnose method and its application on mechatronics systems," in *2014 IEEE 23rd International Symposium on Industrial Electronics (ISIE)*, pp. 2410–2415, 2014.

The scientific articles listed above form the basis of the thesis.

Contents

Abstract

Road safety is one of the hot-spot issues in modern society and covers many aspects of traffic system. Vehicle safety plays an important role in reducing the casualties and saving the accident cost. Up to now, a lot of efforts have been made to improve vehicle safety on both passive and active aspects, such as optimizing the vehicle structure, updating the vehicle dynamic control algorithm and developing driving assistant system. Considering the fact that traffic accidents cannot be completely avoided, passive safety of vehicle are seriously concerned by researchers, manufactures and consumers.

Modeling of vehicle crash process is a challenging problem, which has been widely studied and will remain a topic of interest in the future. With the developing of Computer Aided Engineering (CAE) technology (e.g. multi-body theory, nonlinear finite element method), detailed numerical models are used in various areas of vehicle safety. However, the development and utilization of numerical models are generally time consuming and costly. At the same time, mathematical models are usually built without clear physical interpretation, although they have advantages in some applications. The existing mathematical models have limitations in adaptation to different crash conditions.

This thesis is mainly about the investigation of vehicle crash process based on the time-frequency analysis of the crash responses (i.e. the accelerations of vehicle structure). The essential idea of this work is to building the mathematical relationship between vehicle structures and crash responses. The data used in this work come from the NCAP crash tests and finite element crash simulations of Toyota Yaris. Paper A illustrates the typical load paths of vehicle frontal structure firstly. According to the energy absorbing features of crashworthiness components, a piecewise model is proposed to represent frontal crashes. The proposed model is built by analyzing the crash response, engine accelerations and external barrier force. Moreover, the model variance in different cases, including crashes with different impact velocities and oblique crashes, are also discussed. Papers B and C introduce Ensemble Empirical Mode Decomposition (EEMD) method into crash response analyzing. EEMD is a time-frequency analysis technology, which is suitable for nonlinear and non-stationary signals. Paper B studies the signal transmission in vehicle components and illustrates how the deformations of components influence the crash responses. Paper C proposes an integrated algorithm to identify the performance of energy absorbing components during crashes by both low frequency trend and high frequency oscillations of the response signal. Two cases, low speed crash and oblique crash, are also studied in this work. Paper D presents a modeling scheme of vehicle crash, as well as an estimation method of crashes with different velocities. Specifically, the parameters of proposed model are identified from

the data of corresponding NCAP 56km/h frontal crash test, which is available for most vehicles. For the crash process estimation, the crashes are catalogued into light, moderate and sever types, according to the deformed components. For the crashes in different catalogues, the structures and parameters of piecewise models may vary consequently. For this reason, the estimation algorithms of three types of car crashes are developed separately. Examples are also given for these three cases. Finally, Paper E discusses the application of EEMD in the validation of CAE simulations. The proposed scheme compares the trend and oscillations of original signal separately and involves more features to achieve better validation performance.

In conclusion, this thesis involves the signal processing technologies into the analysis, modeling and CAE model validation of vehicle frontal crashes. It benefits the understanding of vehicle crash processes and helps to achieve better safety design of vehicle. Some future work should be continued for car crashes in more complex conditions.

Part I

Preliminaries

1 Introduction

1.1 Background

1.1.1 Vehicle Safety

Since firstly developed in 1886, the automobiles play an important role in modern society and offers great benefits, including on-demand transportation, travelling convenience, as well as independence [1, 2]. On the other hand, automobile safety has become an issue from the birth of road vehicles. According to the report of World Health Organization (WHO), the road traffic accident is one of the largest causes of injury-related deaths worldwide [3]. Every year, road traffic accidents may cause 1.25 million death and more sustaining serious injuries. It is the ninth leading cause of death across all age groups and the first reason of young people aged between 15 and 29 years.

Up to now, the whole society has made a lot of efforts, in various aspects, to improve vehicle safety. The governments put forwards specific laws and rules to reduce unsafe driving practices of drivers, such as speeding, drunk driving, etc. In road constructions, speed bumps, roundabouts and other safety designs are added in the traffic system. In addition, the standard safety tests, such as the New Car Assessment Program (NCAP) and tests by the Insurance Institute for Highway Safety (IIHS), are mandatory for new vehicle designs to evaluate their performance against safety threats.

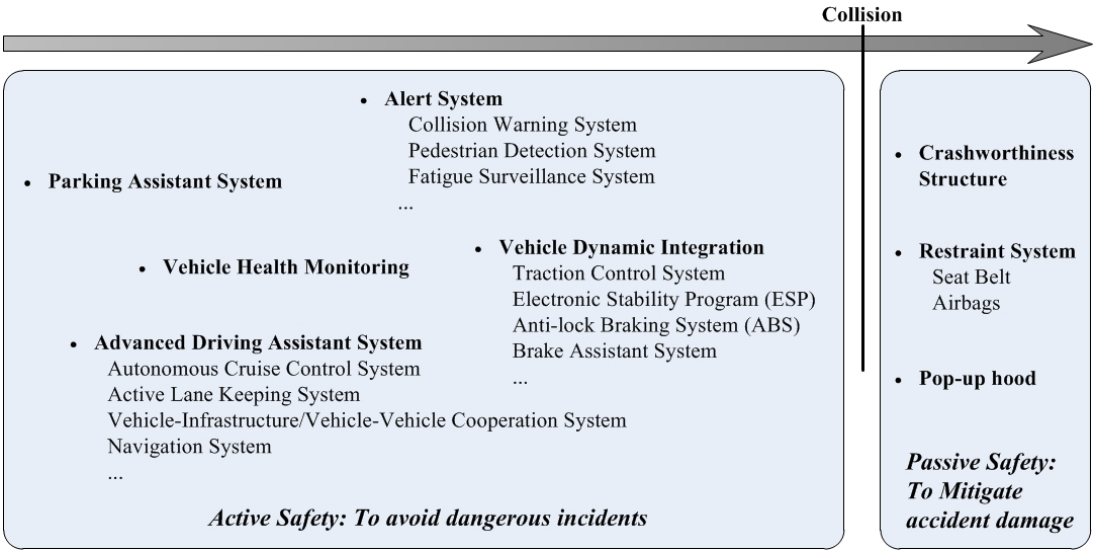

Figure 1.1: Integrated technologies for vehicle safety

At the same time, many safety features are added to vehicles, as shown in Fig. 1.1. These technologies fall into two categories: "active safety", which aims to prevent crashes and "passive safety", which can protect occupants from injuries during crash accidents. With the development of electronics, communication and computer science, the active safety technologies, such as Electronic Stability Program (ESP), Vehicle-to-Vehicle Cooperation System and Automatic Driving, are highlighted in recent years. However, although great efforts are spent on accident avoidance, human are still far from none-accident traffic. Therefore, the passive safety keeps an important design attribute of academic researchers, vehicle manufacturers and consumers.

Generally, the passive safety systems of vehicle contains crashworthiness structure and some non-structural equipments. Crashworthiness structures refer to the deformable components, which are designed to absorb the crash kinetic energy and ensure the crash deceleration pulse below the upper limit of human tolerance [4]. It should also maintain a sufficient survival space for occupants during the whole crash process.

The non-structural equipments, typically the restraint system (e.g. airbags and seat-belts), will cushion high deceleration spikes of occupants and provide additional protection for secondary injuries. As they have no significant contribution on dissipating the crash energy of the vehicle, crashworthiness structures are serving as the base of vehicle passive safety.

1.1.2 Crashworthiness Structure

The core idea of crashworthiness structure design is to preset a crumple zone, which can absorb kinetic energy of vehicles during crashes. In this research, the main work is focused on frontal crash safety and relative structures. For the sake of brevity, the term "crashworthiness" will be referring to frontal crashworthiness of vehicle in the rest of this dissertation.

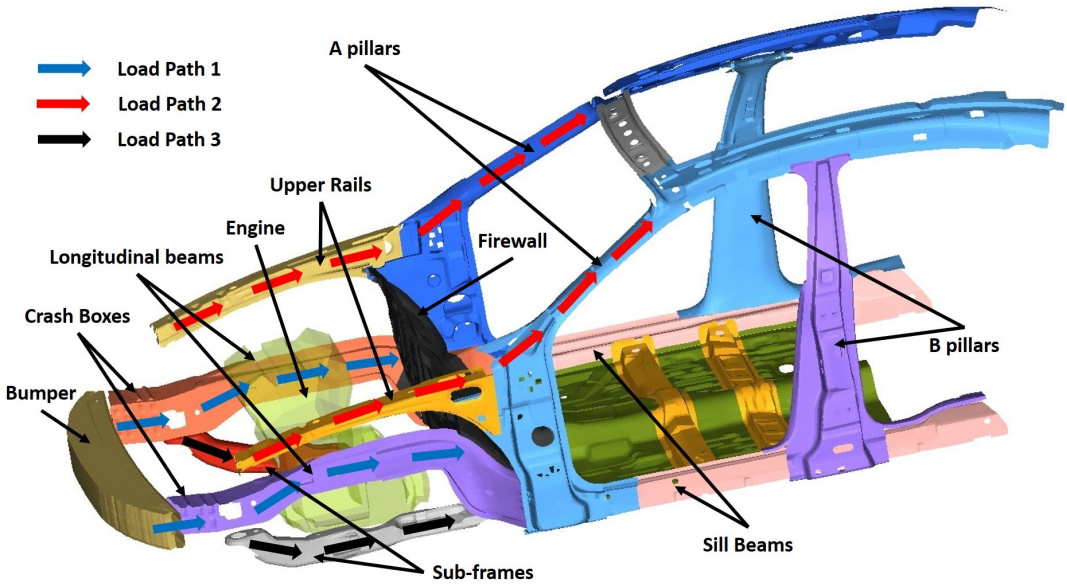

Figure 1.2: Load paths of vehicle frontal structure

The design process of crashworthiness structure is also called as crash energy management (CEM) design, which seeks to control the paths of load transformation and optimise energy absorbing. Generally, there are several load paths in the frontal structure of a modern sedan as shown in Figure 1.2.

- Path1: Accessories - Bumper - Crash boxes - Longitudinal beams
- Path2: Upper rails - A pillars
- Path3: Sub-frames - Sill beams

The components in three paths are deformable and can absorb the impact energy. Especially, the first path affords more than 50% of total crash energy in most frontal crashes [5]. For this reason, the components in the first path are highly considered by engineers in vehicle crashworthiness design. The features and functions of these components are discussed as follow:

- Bumper: the bumpers are usually reinforcement bars made by steel, aluminium, plastic or composite material and can absorb crash energy in a certain extent. The main purpose of bumper is to minimize the cost of repair after low speed crashes. It can also benefit to the protection of pedestrian.
- Crash boxes: the crash boxes are generally thin-walled tubes with well-designed cross-section shape and crumple points (e.g. ditches and crash beads). They may collapse in particular pattern to absorb energy efficiently.
- Longitudinal beams: the longitudinal beams are also thin-walled structure, but longer and stronger than crash boxes. The deformation modes of longitudinal beams include folding, tearing and bending. Some reinforcing components may be used to strengthen the beams and optimize the energy absorbing.

Besides deformable part, some components in the vehicle frontal structure should be strong enough. In most crashworthiness studies, engine and firewall are generally considered as rigid bodies. Especially, the firewall refers to the rigid wall between the engine room and passenger cabin. If a vehicle crashes, the firewall can prevent the intrusion of vehicle cabin and therefore ensure enough living space for driver and passenger.

1.2 Research Motivation

1.2.1 Analysis of Crash Tests

Crashworthiness structures are supposed to fulfil high standard requirements. However, the study of vehicle crashworthiness is a complex and important task in both academia and industry.

The full vehicle crash tests and numerical simulations are the most common ways in crashworthiness studies. There are pros and cons to both of them.

The full vehicle crash tests use vehicle prototypes to imitate the crashes in different conditions. The tests are destructive processes. And some auxiliary equipments, such as traction system and high speed cameras, are also required. For this reason, it is costly to conduct a crash test. On the contrary, numerical simulations are computer-aided and much cheaper than crash tests.

Another advantage of simulations is that they can offer all details of vehicle crash processes, according to the requirements and configuration of the users. However, the data from crash tests can only be recorded by some sensors, such as accelerometers and cameras. Only a few important data are available from the measurement in crash tests. Some information, which are partly useful for structure design or crash analysis, is missing.

However, the crash tests follow rigorous scientific and safety standards and can offer more reliable results than numerical simulations. This is because that the simulations are based on numerical models of vehicles. Modern vehicles are consisted by thousands of components, as well as different kinds of materials and connections. The modeling of vehicles can not be absolutely accurate. Moreover, although advanced numerical simulation technologies are developed, there is still none consistent accurate simulation to predict the crash performance exactly. So the crash tests are indispensable in some cases.

Given the above analysis, it is of great meaning to analyze the crash tests results effectively. In this work, the relationship between the measured signals in crash tests and vehicle structures will be investigated. The crash signals will be analysed to get more information about the vehicle crashworthiness structure, which will benefit the vehicle structure design.

1.2.2 Mathematical Modeling of Crash Process

The vehicle crash process is a complex process with non-linear large deformation. Modeling of vehicle crashes, which can be used to represent and predict the crash processes, remains an interesting topic in both academic and industrial areas. Although Finite Element (FE) models are widely used, they have limitations in three aspects. Firstly, FE models require detailed information of vehicles, including geometry, material and connection of every component in the vehicle. Therefore, the developing of FE models is very complex and costly. Secondly, FE models are not directive models of crashes. They are the models of vehicle bodies, which should be simulated to predict crash processes. The simulations are time consuming and therefore cannot be used in real-time applications. Finally, FE models are complex and contain too many parameters. The influence of each parameter can not be reflected clearly in simulation results.

Owing to these reasons, there is a huge amount of motivational force behind this work to establish a mathematical model for vehicle crashes, which can represent the vehicle crash processes with low complexity. In addition, it should predict the crashworthiness behaviour of vehicle structures in an acceptable accuracy. The derived models could be used to improve the vehicle crash safety.

1.3 State of the Art

1.3.1 Vehicle Crash Modeling

The modeling of vehicle crashes is a challenging topic in vehicle safety. Up to now, several kinds of models, as shown in Figure 1.3, are used in real applications. Similar to modeling problems in other areas, there is a huge contradiction between model complexity and accuracy. This antinomy is especially significant for vehicle safety applications. With more physical information involved in the models, the accuracy and applicability of models improve a lot. At the same time, the cost of modeling process and model implementation will increase correspondingly. The researchers and engineers should select proper models for specific purposes.

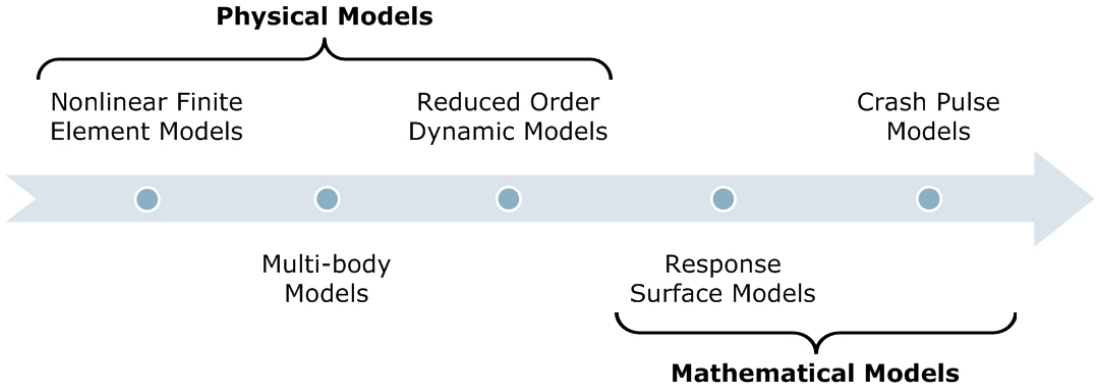

Figure 1.3: Common used models of vehicle crashes

Nonlinear Finite Element Models

Vehicle crashes are typical processes with large deformation and displacement, which contains several nonlinear factors (e.g. geometric nonlinearity and material nonlinearity). For this reason, nonlinear finite element (FE) models is the most widely used models in vehicle safety area, such as structural crashworthiness analysis.

Generally, a detailed FE model is developed by the discretization (i.e. meshing) of corresponding vehicle CAD model and specification of material properties. It can simplify a continuous problem into a discrete problems with finite degrees of freedom (DOF). With the knowledge of material, the finite element functions are built according to the minimum total potential energy principle or virtual work principle. The functions can be solved with the boundary conditions and then the nodal displacements and element stresses are acquired. For nonlinear FE models of vehicles, the explicit finite element analysis method is usually selected for the solving process.

It can be seen that both developing and implementing of FE models are time consuming work, especially for large detailed FE models. More importantly, the using of FE models requires full information of physical structures, including geometrical shapes, material properties and connection types. So it is usually used in middle and later stage of vehicle structure design, such as those shown in [6–8].

Some commercial software packages of FE method are developed and widely used. In these packages, the implementation of FE method includes the following three steps:

- Pre-processing: includes model development and configuration (includes definition of loads, constraints and boundary conditions).
- Solving: solves the finite element functions by specified solver and outputs the data files.
- Post-processing: deals the output data and visualizes the results.

In the vehicle safety area, the Hyperworks are usually used for the pre- and post-processing. The common used solvers include LS-DYNA, PAM-CRASH and RADIOSS.

Multi-body Models

Multi-body models are another kind of numerical models and used for both kinetic and dynamic analysis. The models represent structures with rigid bodies, which are connected by joints, springs and dampers. Based on different mechanical principles, system dynamic can be solved in various ways:

- Roberson-Wittenberg method (R/W method): it is developed based on the Newton-Euler equations. The R/W method can achieve concise equations with clear geometric interpretations.
- Lagrange method: it is one of analytical mechanics methods. Based on the D'Alembert's principle and virtual work principle, the Lagrange method develops dynamic functions with least number of unknown variables. However, the calculation and derivation of Lagrange functions may lead the large computation load.
- Variational method: based on the Gauss's principle of least constraint, the Variational method requires no dynamic equations of system. By comparing the constraint value of real and possible movements, the problem will be solved by searching conditional extrema of functions.

The multi-body models are mostly used in the research of pedestrian safety [9–11] and occupant safety [12, 13]. In these research, some passenger impact simulation software, developed according to the multi-body theories, are used. Now the MADYMO (MAthematical DYnamic MOdel), which is developed by the Netherlands Organization for Applied Scientific Research (TNO), is most widely used software. The MADYMO contains a model library of general crash dummies, including Hybrid iii, EuroSID, US-DOTSID, etc. In addition, MADYMO also offers some useful tools for crash simulation, such as Folder, AutoDOE and ADVISER.

Reduced Order Dynamic Models

Reduced order dynamic models mainly include lumped mass models [14–16], coarse-mesh FE models [17, 18] and fine-grained lumped models [19–21]. Although different

in modeling details, all reduced order dynamic models are based on the same idea, that is to use simplified model with reduced number of degrees of freedom to capture the gross motion of vehicle components during crashes. Comparing with the FE models, they have lower complexity and consequently less accuracy, as less structure information are involved in the models.

The lumped mass models are the most common used models, which attempt to use basic components, such as spring, damper and mass, to represent the relative structures briefly. However, this may introduce new parameters to the model. For example, the dimensions and sheet metal thickness of some structural components in an FE model are the representation of same dimensions and sheet thickness in real structures. In a reduced order dynamic model however, a nonlinear spring may represent a structural member. The spring parameters (such as stiffness) are not as easy to correlate to actual dimensions of the structural member in the real structure. Considering the nonlinear properties of vehicle structure, the identified parameter of a crash may vary a lot in other crashes, which leads the implementation of reduced order dynamic models very difficult.

Response Surface Models

Response surface models (RSMs), also called functional approximation models, are essentially general purpose meta-models and popular in many engineering applications. Especially in some complex systems, RSMs can reduce computation load of systems by efficient approximation of them. The main feature of RSMs is that they skip the description of physical system and explore the relationships between the input factors and the response mathematically [22]. In general, the response variable y depends on the factors $\xi_{1\sim i}$, $i = 1, 2, \ldots, k$, i.e.

$$y = f(\xi_1, \xi_2, \ldots, \xi_k) + \varepsilon \tag{1.1}$$

where f is the actual response function, which can be unknown and mathematically complicated. ε represents other terms not accounted for in f, such as measurement error, background noise and effect of other (possibly unknown) factors. Usually, ε is treated as a statistical error and assumed to have normal distribution with zero mean, i.e. $E(\varepsilon) = 0$. If a function $F(\xi_1, \xi_2, \ldots, \xi_k)$ satisfies

$$\begin{aligned} F(\xi_1, \xi_2, \ldots, \xi_k) &\equiv E(y) \\ &= E(f(\xi_1, \xi_2, \ldots, \xi_k)) + E(\varepsilon) \\ &= f(\xi_1, \xi_2, \ldots, \xi_k) \end{aligned} \tag{1.2}$$

$F(\xi_1, \xi_2, \ldots, \xi_k)$ is the response surface model of the system.

In practice, the response surface models are constructed via the following three steps:

- Design of Experiments (DOE): setting the factors at several proper levels for trial experiments to ensure the modeling process is carried out in a cost effective and reproducible manner. The basic method is full factorial experiment, which tests the factors in all possible level. In complex cases, other design methods, such as the Latin Square Design and Crossover Design, may be employed.

- Data Collection: acquiring sample data from designed experiments. The experiments are conducted by real crash tests or simulations, such as FE simulations.
- Data Fitting: fitting the sample data to a function of corresponding factors. The common used fitting algorithms include polynomial regression [23, 24], various types of artificial neural networks [25–27], as well as Kriging [28].

[29] provides an overview of RSM applications in the literature of crashworthiness, especially in the optimization design of vehicle structure. [30–33] are some application cases. However, there are two main shortages for RSMs. Firstly, the relationship between RSM parameters and physical structures are not clear. In other words, RSMs focus on the approximation of output value only and ignore the physical meaning of model parameters. Secondly, RSMs are difficult to work in nonlinear cases with a few input variables. The effective field may be limited due to the interacting of input variables.

Crash Pulse Models

In vehicle safety research, the crash pulses usually refer to acceleration signals of vehicle during crashes, which are basic record of crashes. The study of crash pulse is widely considered in vehicle safety area for several purposes. Firstly, crash pulses represent the dynamic response and energy change of vehicle structure during crash processes. They play an important role in the vehicle structural optimization, such as [34, 35]. Secondly, they are used in the validation of crash simulations. All existing model validation algorithms are conducted by comparing the crash pulses of full car tests and simulations, which will be discussed in the subsection 1.3.2. Finally, they help to evaluate the injury severity of crashes as well. Some works are given as [36–38].

The modeling of crash pulse is a challenging work. Generally, the model of crash pulse uses a mathematical function to represent the vehicle acceleration and consequently the crash process. Given an acceleration signal $x(t)$, the crash pulse model $F_\theta(t)$ should ensure

$$\begin{cases} r_a(t_0) = x(t_0) - F_\theta(t_0) \approx 0 \\ r_v(t_0) = \int_0^{t_0} r_a(t)\,dt \approx 0 \\ r_d(t_0) = \int_0^{t_0} r_v(t)\,dt = \int_0^{t_0}\int_0^{t_0} r_a(t)\,dtdt \approx 0 \end{cases} \tag{1.3}$$

at all the time $t_0 \geqslant 0$, where $r_a(t)$, $r_v(t)$ and $r_d(t)$ are the residual signals of acceleration, velocity and displacement respectively. The used functions may vary according to the pulse shape. [39] modelled crash pulses by the square, triangular and half sine functions roughly. Recently, some work are also done to develop more accurate crash pulse models to represent vehicle crash details [40–42].

Unfortunately, the crash pulse model, $F_\theta(t)$, is usually only valid for a specified condition θ. Crash pulses may be influenced by numerous factors, such as impact velocity, collision partner and crash mode. [43] gave a qualitative discussion of model

parameter variance in difference crashes. To the best of author's knowledge, there is still no proposed crash pulse model, which is suitable for difference crashes.

To overcome this limitation, a novel scheme is proposed for the modeling of vehicle crash pulse in this PhD work. The proposed model is highly related to vehicle crashworthiness structure and the corresponding deformations in the crash process. The model variance in crashes with different velocities are also studied.

1.3.2 CAE Model Validation

The CAE simulations are widely used in vehicle engineering for various purposes. For this reason, the validation of CAE models is highly considered by relative engineers and researchers. In the context of vehicle safety, the validation is normally conducted by comparisons between crash response signals from CAE simulations and those recorded in real car crash tests [44]. The core topic of model validation is to define comparison metrics, which can quantitative measure the discrepancy of these time histories.

Generally, the comparison metrics can be grouped into two categories: deterministic metrics and stochastic metrics. Deterministic metrics focus on the collected data and ignore the uncertainties in both measurement and simulations. On the contrary, stochastic metrics consider the uncertainties of data, such as random experimental error and parameter variations. Up to now, various comparison metrics of both categories have been proposed and employed for vehicle safety applications. Some software, such as Curve Analyzer created by University of Chalmers [45] and Roadside Safety Verification and Validation Program (RSVVP) created by Worcester Polytechnic Institute [46], are also developed. Especially, the RSVVP is a model validation program developed in Matlab environment, which offers common used pre-processing functions. The diagram in Figure 1.4 lists some typical comparison metrics in the literature. Their mathematical formulations and features will be introduced in the following subsections.

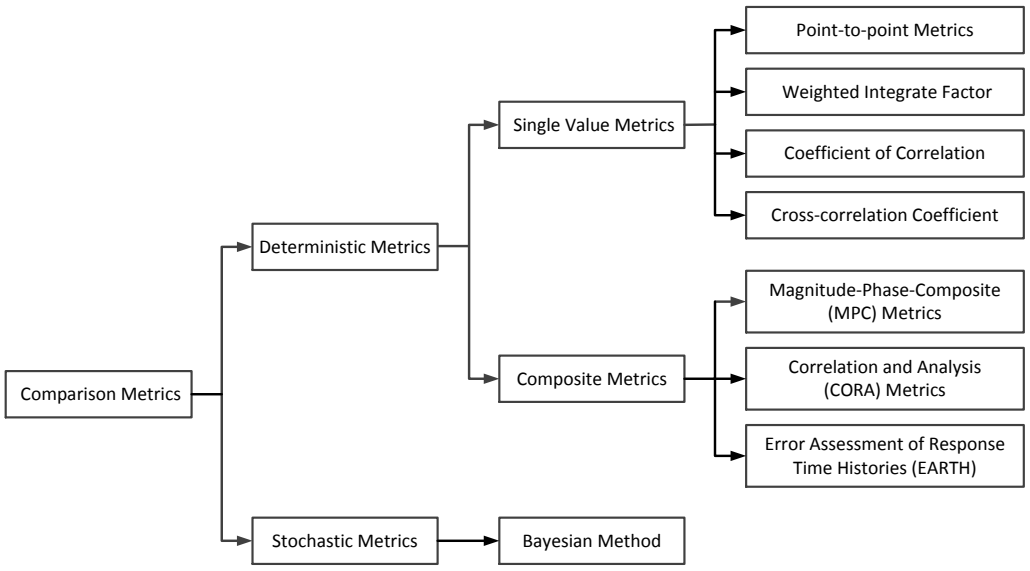

Figure 1.4: Typical comparison metrics for vehicle safety applications

Single Value Metrics

The single value metrics involve only one error measure in the comparison, which are the base of composite metrics. The first think of time histories comparison is to compare the signals point-to-point. L_1 and L_2 norms are used to measure the value errors. Considering the facts that norms are not normalized and highly depended on the number of time points, some uniformed metrics are proposed, as listed in Tab. 1.1 [47]. r_i is the i-th value of reference signal and t_i is that of test signal, n is the length of compared time histories.

Table 1.1: Point-to-point comparison metrics

Name of Metric	Formulations
Zilliacus error	$\frac{\sum \lvert t_i - r_i \rvert}{\sum \lvert r_i \rvert}$
RMS error	$\frac{\sqrt{\sum (t_i - r_i)^2}}{\sqrt{\sum t_i^2}}$
Theil's inequality	$\frac{\sqrt{\sum (t_i - r_i)^2}}{\sqrt{\sum t_i^2} + \sqrt{\sum r_i^2}}$
Whang's inequality	$\frac{\sum \lvert t_i - r_i \rvert}{\sum \lvert t_i \rvert + \sum \lvert r_i \rvert}$
Regression efficient	$\sqrt{1 - \frac{(n-1)\sum (t_i - r_i)^2}{n \sum (r_i - \bar{r})^2}}$

Different with point-to-point comparisons, the weighted integrate factor measures global magnitude difference directly [48]. Its formulation is defined as follows:

$$Err = \sqrt{\frac{\sum \max\left(r_i^2, t_i^2\right)\left(1 - \frac{\max(0, r_i t_i)}{\max\left(r_i^2, t_i^2\right)}\right)^2}{\sum \max\left(r_i^2, t_n^2\right)}} \tag{1.4}$$

The coefficient of correlation ρ reflects on how much degrees a signal can be determined by the other one, which is also used for signal comparison.

$$\rho = \frac{n \sum_{i=1}^{n} t_i r_i - \sum_{i=1}^{n} t_i \sum_{i=1}^{n} r_i}{\sqrt{n \sum_{i=1}^{n} t_i^2 - \left(\sum_{i=1}^{n} t_i\right)^2} \sqrt{n \sum_{i=1}^{n} r_i^2 - \left(\sum_{i=1}^{n} r_i\right)^2}} \tag{1.5}$$

The coefficient of correlation is sensitive with the time error. So the cross-correlation coefficient, also called sliding dot product, is modified from the coefficient of correlation.

$$\rho(n_0) = \frac{(n - n_0) \sum_{i=1}^{n-n_0} t_i r_{i+n_0} - \sum_{i=1}^{n-n_0} t_i \sum_{i=1}^{n-n_0} r_{i+n_0}}{\sqrt{(n - n_0) \sum_{i=1}^{n-n_0} t_i^2 - \left(\sum_{i=1}^{n-n_0} t_i\right)^2} \sqrt{(n - n_0) \sum_{i=1}^{n-n_0} r_{i+n_0}^2 - \left(\sum_{i=1}^{n-n_0} r_{i+n_0}\right)^2}} \tag{1.6}$$

where n_0 is the shifting step of test signal. When $\rho(n_0)$ achieves maximum, the shifted signals is correlated to the reference signal in the highest degree. n_0 is a measurement of the phase error between compared signals [49, 50].

Composite Metrics

To make a better comparison, discrepancies on more aspects, such as magnitude, phase or time-of-arrival (TOA), frequency or slope and shape, are involved and the composite metrics are then proposed. In composite metrics, different measures are designed specifically for each discrepancy and combined into a comprehensive assessment.

Magnitude-Phase-Composite (MPC) metrics measure the discrepancies of both amplitude and time and combined together to a comprehensive metric. Tab. 1.2 lists four typical MPC metrics, where $\vartheta_{rr} = \sum r_i^2$, $\vartheta_{tt} = \sum t_i^2$, $\vartheta_{rt} = \sum r_i t_i$, $m = \frac{\vartheta_{tt} - \vartheta_{rr}}{\sqrt{\vartheta_{tt}\vartheta_{rr}}}$ and $a_1 = sign(\vartheta_{rt})$, $a_2 = sign(m)$.

Table 1.2: Typical Magnitude-Phase-Composite (MPC) metrics

	Magnitude	Phase	Comprehensive
Geers [51]	$M_G = \sqrt{\frac{\vartheta_{tt}}{\vartheta_{tt}}} - 1$	$P_G = 1 - \frac{\vartheta_{rt}}{\sqrt{\vartheta_{tt}\vartheta_{rr}}}$	$\sqrt{M_G^2 + P_G^2}$
Geers CSA [52]	$M_{GC} = M_G$	$P_{GC} = 1 - \frac{\lvert\vartheta_{rt}\rvert}{\sqrt{\vartheta_{tt}\vartheta_{rr}}}$	$a_1\sqrt{M_{GC}^2 + P_{GC}^2}$
Sprague & Geers [53]	$M_{SG} = M_G$	$P_{SG} = \frac{1}{\pi}\cos^{-1}\frac{\vartheta_{rt}}{\sqrt{\vartheta_{tt}\vartheta_{rr}}}$	$\sqrt{M_{SG}^2 + P_{SG}^2}$
Russell [47]	$M_R = a_2 \log_{10}(1 + \lvert m\rvert)$	$P_R = P_{SG}$	$\sqrt{\frac{\pi}{4}(M_R^2 + P_R^2)}$

Comparing with first three metrics, the Russell measure of magnitude discrepancy is symmetric, i.e. the measure value is no matter to the selection of reference signal. For the phase discrepancy, the measure in Sprague & Geers (S&G) and Russell results an phase error in angle, which has a more clear meaning than the first two. Except these difference, all these metrics use the root-sum square of magnitude and phase as the composite measure. Especially, the S&G metric is recommended to assess the similarity of magnitude and phase by [54].

The Correlation and Analysis (CORA) is another composite metric, recommended by ISO/TR 16250. It consists of two measures: 1) a corridor rating, which considers the fitting degree between the test signal and the corridor and 2) a cross correlation rating, which evaluates the level of correlation analytically [55]. In addition, a composite measure, called global rating, are combined by linear weighted of all measures. The CORA use corridor method to remove the influence of noisy signals and improve the robust of comparison. The shortages of CORA is that it contains many parameters to be adjusted manually.

Error Assessment of Response Time Histories (EARTH) is a comprehensive scheme to compare time histories on three aspects: magnitude, phase and slope [44, 56]. Comparing with MPC metrics, the slope is involved in the EARTH comparison and therefore improves the assessment. In addition, each measure of EARTH is calculated without the influence from other two features and therefore keep independence. The Enhanced Error Assessment of Response Time Histories (EEARTH) scheme, proposed

in [57], is improved from EARTH. The main improvement is that EEARTH translates the original measures into intuitive scores between 0 and 100% and involves an integrated calibration process which incorporates physical-based thresholds and knowledge of subject matter experts (SMEs). The EEARTH is also selected into ISO standard ISO/TR16250.

Stochastic Metrics

In the view of stochastic method, the data used for model validation are influenced by various factors. For one respect, the result of full scale tests are probabilistic as the existing of random experiment error. And the measurement of tests will be noised. For another respect, the CAE result are also not to be deterministic. The parameters of CAE simulation are set as nominal value, which can experience random variation in physical world.

The brute-force way of performing stochastic analysis is running trial simulations for adequately times and then analyze the results with random variance like real word. The stochastic metrics, such as Smirnov distance [58] and Kullback-Leibler [59] divergence, are used to measure the difference of the distributions. Obviously, this method can only be used for small problems with few parameters.

The Bayesian hypothesis testing is the most common used stochastic method of model validation. It has been widely studied by researchers and engineers, see for instance [60–62]. Generally, the Bayes factor, which refers to the ratio of posterior and prior density values, is used as metric [63]. In the vehicle safety area, some examples are given in [64–66].

2 Research Methodology

2.1 CAE Simulations

In this thesis, the research is based on the crashes in different scenarios. Besides physical crash tests, Finite Element (FE) simulations are involved as well. The used vehicle is 2010 Toyota Yaris four-door passenger sedan. The corresponding FE model, as shown in Figure 2.1, is developed by the National Crash Analysis Center (NCAC) through the reverse engineering process. Table 2.1 lists the summary of this FE model. The physical features (include weight; pitch, roll, and yaw inertias; and coordinates for the gravity center) of FE model and physical car are found to be similar and within acceptable limits [67].

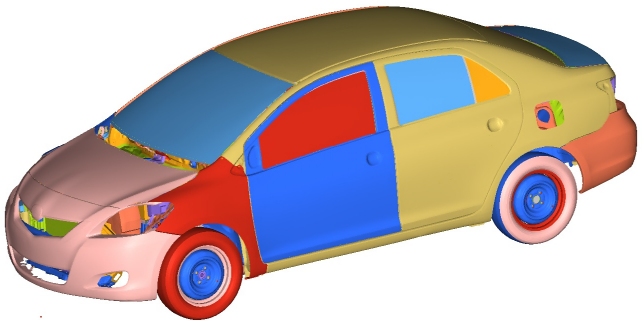

Figure 2.1: Detailed FE model of 2010 Toyota Yaris four-door passenger sedan

In the FE simulations, the accelerations of some nodes on the vehicle body are recorded to measure the crash details, as list in Table 2.2. In these sensors, S1 locates on the vehicle gravity center and S2∼S5 are corresponded to the accelerometers in NCAP frontal crash tests. The others are used to measure the deformations of energy absorbing components.

The developed FE model was validated against the relative frontal NCAP tests of National Highway Traffic Safety Administration (NHTSA), i.e. Test 5677, Test 6221 and Test 6069. The validation metrics of S2∼S5 are calculated by the RSVVP program. More information of validation can be found in [67].

The FE model was used for frontal crash simulations of Toyota Yaris. Hypermesh is used for pre-processing of simulations and Radioss is employed as solver. In this PhD project, nine frontal crash simulations were conducted with the initial velocities of

Table 2.1: Toyota Yaris FE model summary

Item	Number
Number of Parts	917
Number of Nodes	1,480,422
Number of Solid Elements	258,887
Number of Shell Elements	1,250,424
Number of Beam Elements	4,738
Number of Mass Elements	159
Number of Extra Node Set Connections	20
Number of Joint Connections	39
Number of Nodal Rigid Body Connections	727
Number of Rigid Body Connections	2
Number of Spotweld Connections	4,107
Number of Beam Element Connections	4,425

Table 2.2: Locations of accelerometers in FE simulations

No.	Symbol	Description
1	S1	Vehicle Gravity Center
2	S2	Engine Top
3	S3	Engine Bottom
4	S4	Left Rear Seat
5	S5	Right Rear Seat
6	S6	Center of Bumper Front Surface
7	S7	Connection of Bumper and Left Crash box
8	S8	Connection of Bumper and Right Crash box
9	S9	Connection of Left Crash box and Left Beam
10	S10	Connection of Right Crash box and Right Beam
11	S11	End Point of Left Beam
12	S12	End Point of Right Beam

10km/h, 12km/h, 16km/h, 20km/h, 25km/h, 32km/h, 40km/h, 48km/h and 56km/h. An 56km/h frontal crash with 10 degree oblique angle was also simulated. The recorded accelerations will be pre-processed firstly, as introduced in Section 2.2. Then they will served as the data source and used in this PhD project.

2.2 Signal Pre-processing

The crash signals mainly refer to the accelerations of vehicle components. They can reflect the performance of vehicle structure and therefore be used for crash analysis. In physical crash tests, a few accelerometers are located on the vehicle body or dummy to record the accelerations of concerned points. For example, the acceleration of

left/right brake caliper, engine top/bottom, instrument panel and left/right rear seat will be recorded in most NCAP crash frontal tests. And in numerical simulations, the researcher can get the acceleration of any concerned point, which are pre-setted in the configuration. As the crash signals may come from different sources, the raw signals cannot be used for analysis and the pre-processing procedure is usually required. The common used pre-processing technologies in vehicle safety includes trimming, filtering, re-sampling and synchronizing.

In addition, most common used programs in vehicle crash analysis offer the functions of pre-processing, such as Test Risk Assessment Program (TRAP) and Roadside Safety Verification and Validation Program (RSVVP). In this PhD project, the RSVVP is used for the pre-processing of crash signals.

2.2.1 Filtering

Filtering is the first and most important pre-processing step before crash signals analysis. The measured crash signals are characterized by high-frequency noise in some extent. These noises cannot reflect the overall dynamics of the crash and therefore should be filtered out. To uniform the filtering process, some standards and rules are proposed. The SAE J211-1 specifications [68] provide the guidelines for the techniques of measurement used in crash tests, which is also recommended in Report 350 of National Cooperative Highway Research Program (NCHRP) [69] and European standard EN 1317 [70].

The filters used in processing vehicle crash test data are Chebyshev or Butterworth filters. Generally, these filters are described by their frequency response characteristics and categorised into different Channel Frequency Classes (CFCs). For filters in a specified CFC, their channel frequency responses should lie within the corresponding limits. Some recommended CFCs for vehicle structural accelerations and forces and their limits, proposed in SAE J211-1, are listed in Table 2.3.

Table 2.3: Recommended CFCs for vehicle structural accelerations and forces

Measured signals	CFC	3dB limit	Stop damping
Accelerations for total vehicle comparison	60	100Hz	-30dB
Accelerations for collision simulation input	60	100Hz	-30dB
Accelerations for component analysis	600	1000Hz	-40dB
Accelerations for integration	180	300Hz	-30dB
Barrier face force	60	100Hz	-30dB

According to [68], the filter function of RSVVP is a 4-pole Butterworth low-pass filter [71]. The algorithm is to filter the signal twice, once forward and once backward, using the following equations:

$$y(t) = a_0 x(t) + a_1 x(t-1) + a_2 x(t-2) + b_1 y(t-1) + b_2 y(t-2) \qquad (2.1)$$

where, t is the sampling instant, $x(t)$ is the input signal (i.e. original signal) and $y(t)$ is the filtered output. For the particular CFC value, the parameters in Equation 2.1 are

defined as:

$$a_0 = \frac{{\omega_a}^2}{1 + \sqrt{2}\omega_a + {\omega_a}^2} \tag{2.2}$$

$$a_1 = 2a_0 \tag{2.3}$$

$$a_2 = a_0 \tag{2.4}$$

$$b_1 = \frac{-2\left({\omega_a}^2 - 1\right)}{1 + \sqrt{2}\omega_a + {\omega_a}^2} \tag{2.5}$$

$$b_2 = \frac{-1 + \sqrt{2}\omega_a - {\omega_a}^2}{1 + \sqrt{2}\omega_a + {\omega_a}^2} \tag{2.6}$$

where

$$\omega_a = \frac{\sin\left(\omega_d \cdot T/2\right)}{\cos\left(\omega_d \cdot T/2\right)} \tag{2.7}$$

$$\omega_d = 2\pi \cdot CFC \cdot 2.0775 \tag{2.8}$$

and T is the sample period in second.

2.2.2 Re-sampling

The re-sampling and synchronizing are mostly used for model validation, where signals are compared with each other. As the crash signals are measured in different tests or simulations, the sampling frequency may be different. To make signals comparable point-to-point, the re-sampling operation is conducted to the signals which have lower sampling frequency at the highest sampling frequency of other signals. The re-sampling is usually achieved by interpolation methods, such as linear interpolation and cubic interpolation. [71] checked the performance of different interpolation methods and proved the linear interpolation is optimal for vehicle crash applications.

2.2.3 Synchronizing

If the original signals from different sources are not acquired at the exactly same starting instant, the additional phase error will exist in the model validation. So synchronizing is employed to ensure the compared signals have same start time by shifting the signals along the abscissa direction, i.e. the time axis. In the synchronizing, a signal is set as reference and other signals will be trial shifted by k steps. k can be either positive or negative, which refers to the moving forward or backward correspondingly. The accumulated errors between trial shifted signal and reference signal are the target function, which is to be minimized by synchronizing. The errors can be calculated in two manners: absolute area of residuals or the sum of squared residuals. The trial shifting with least error will be selected as the best synchronizing result.

2.2.4 Trimming

The trimming of signals is an important step before analysis with two purposes. Firstly, it ensures only the accelerations in crash duration will be used for further investigation

and the rest parts, such as the acceleration before the initial impact, are cut out. Secondly, the trimming ensures signals have same length in signal comparison.

2.3 Signal Processing Tools

2.3.1 Hilbert-Huang Transform

The Hilbert-Huang transform (HHT) is an adaptive data analysis method proposed by Huang et al. in NASA [72]. It is specifically suitable for time-history signals from nonlinear and non-stationary processes. It has been widely used in many disciplinary areas and applications, including Finance, Biomedicine, Meteorology and so on. HHT contains the combination of the empirical mode decomposition (EMD), which decomposes a signal into a series of components and the Hilbert spectral analysis (HSA), which calculates the instantaneous frequency.

Empirical Mode Decomposition

According to [73], the signals are consisting of several coexisting oscillations with different frequencies. In other words, signals can be treated as fast oscillations superimposed to slow oscillations. These oscillations reflect the inherent features of original signals and are defined as intrinsic mode functions (IMFs), which satisfy the following conditions:

- In the whole data set, the number of extrema and the number of zero crossings must either equal or differ at most by one.
- At any data point, the mean value of the envelope defined using the local maxima and the envelope defined using the local minima is zero.

It can be mathematically formulated as

$$x(t) = \sum_{i=1}^{k} s_i(t) = \sum_{i=1}^{k} A_i(t) \cos(\phi_i(t)), A_i(t), \phi_i'(t) > 0 \tag{2.9}$$

where $x(t)$ is the original signals and $s_i(t)$ is an amplitude modulated-frequency modulated (AM-FM) signal, which oscillates around 0.

The core methodology of EMD is the shifting process, which can obtain the IMFs of the given signal $x(t)$. Figure 2.2 shows the shifting process of a signal.

- Step 1: Set initial $i = 1$, $j = 1$ and $x_{1,1}(t) = x(t)$.
- Step 2: Extract the local maxima and minima of signal $x_{i,j}(t)$ and construct the upper and lower envelops of $x_{i,j}(t)$ by interpolation of the maxima and minima, i.e. $u_{i,j}(t)$ and $l_{i,j}(t)$.

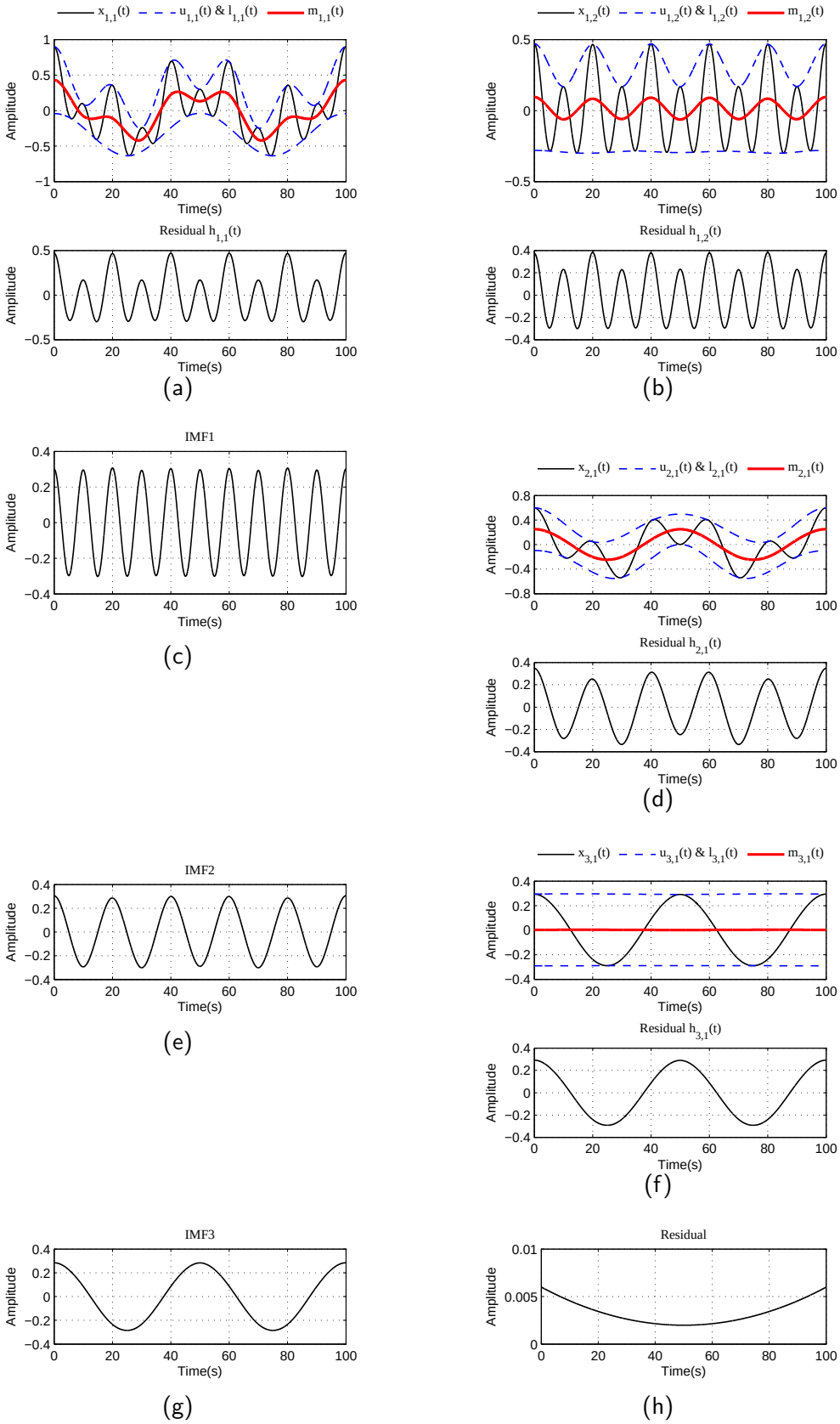

Figure 2.2: EMD process illustration

- Step 3: Calculate the mean of the upper and lower envelops, recorded as $m_{i,j}(t) = \frac{1}{2}(u_{i,j}(t) + l_{i,j}(t))$. Define $h_{i,j}(t) = x_{i,j}(t) - m_{i,j}(t)$. Step 2 and 3 are shown in Figure 2.2(a).

- Step 4: As shown in Figure 2.2(b), Steps 2 and 3 are repeated for signal $x_{i,j+1}(t) = h_{i,j}(t)$, until $h_{i,j}(t)$ fulfills the definition of IMF. The i-th IMF is recorded as $s_i(t) = h_{i,j}(t)$.

- Step 5: Calculate residual $x_{i+1,1}(t) = x_{i,1}(t) - s_i(t)$. Stop the shifting process until $x_{i+1,1}(t)$ has only one or no extremum. Otherwise, repeat Steps 2 to 4 for signal $x_{i+1,1}(t)$ to get other IMFs.

Ensemble Empirical Mode Decomposition

If the original signal is noised, the performance of EMD may be significantly deteriorated. One of the problems is the mode mixing, which is caused by intermittence in noised signals. The Ensemble Empirical Mode Decomposition (EEMD) is a noised aided method to improve the decomposition of noised signals.

In EEMD, the white noises of finite variance is added to original signal to get the trails. And the "true" IMF component is the mean of corresponding IMFs obtained through EMD of an ensemble of trials. The EEMD algorithm can be described as:

- Step 1: Set initial $j = 1$. Create white noise $n_j(t)$ with the given amplitude and add it to the original signals, i.e. $x_j(t) = x(t) + n_j(t)$.

- Step 2: Decompose the noisy signal $x_j(t)$ by the EMD method and get $x_j(t) = \sum_{i=1}^{n} s_{i,j}(t)$. $s_{i,j}(t)$ is the j-th trial of the i-th IMF.

- Step 3: Repeat Step 1 and Step 2 for N times with $j = j + 1$.

- Step 4: Compute the ensemble mean of the N trials for each IMF as the final result, i.e. $s_i(t) = \frac{1}{N}\sum_{j=1}^{N} s_{i,j}(t)$.

In vehicle safety applications, the residual and some low frequency IMFs can be summed as a trend component of original signal. That is

$$x(t) = \sum_{i=1}^{I} s_i(t) + Tr \tag{2.10}$$

where I is the number of high frequency IMFs with zero mean. Tr are the trend component, which shows global variance of original signal. In this thesis, the trends of vehicle crash responses in different velocity crashes are shown in Figure 2.3.

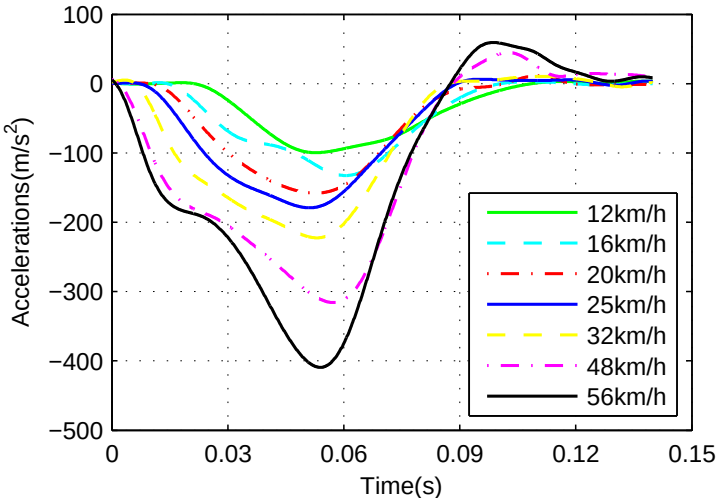

Figure 2.3: Trends of vehicle crash responses in different velocity crashes

Hilbert Spectral Analysis

The HSA uses the Hilbert transform to compute the instantaneous frequency of signals. For an arbitrary time series $x(t)$, its Hilbert Transform $y(t) = \mathcal{H}(x(t))$ is defined as

$$y(t) = \mathcal{H}(x(t)) = \frac{1}{\pi} P \int_{-\infty}^{\infty} \frac{x(\tau)}{t-\tau} d\tau \tag{2.11}$$

where "P" indicates the Cauchy Principal Value of the integral, which is to handle the singularity at $\tau = t$. In this context, "P" is utilized in the manner as follows

$$\frac{1}{\pi} P \int_{-\infty}^{\infty} \frac{x(\tau)}{t-\tau} d\tau = \lim_{\varepsilon \to 0^+} \frac{1}{\pi} \int_{|t-\tau| \geqslant \varepsilon} \frac{x(\tau)}{t-\tau} d\tau \tag{2.12}$$

With this definition, $x(t)$ and $y(t)$ form the complex conjugate pair. An analytic signal, $z(t)$, are consequently combined as

$$z(t) = x(t) + iy(t) = a(t) e^{i\theta(t)} \tag{2.13}$$

where $i = \sqrt{-1}$, $a(t)$ and $\theta(t)$ are the corresponding amplitude and phase, defined as

$$a(t) = \left[x^2(t) + y^2(t)\right]^{1/2} \tag{2.14}$$

$$\theta(t) = \arctan\left(\frac{y(t)}{x(t)}\right) \tag{2.15}$$

Then the instantaneous frequency are calculated as

$$\omega(t) = \frac{d\theta(t)}{dt} \tag{2.16}$$

In the HHT, the HSA will be conducted to each IMF, which is decomposed by EEMD process. The corresponding instantaneous amplitude and frequency are consequently calculated and the time-frequency spectrum of crash signals can then be obtained.

HHT in Vehicle Safety

Due to the complex structure of vehicle, the crash responses are generally nonlinear and non-stationary. Compared with other time-frequency analysis technologies, HHT is an adaptive method and more suitable for the analysis of vehicle crash responses.

In this PhD work, the crash responses are decomposed by EEMD algorithm. The extracted trend describes the global variance of vehicle acceleration clearly. Without local oscillations, the trend helps to illustrate the corresponding relationship between energy absorbing components and crash stages. A piecewise model, which fits the trend well, can be proposed to represent vehicle crash process. Moreover, the IMFs, which contain the frequency features of original crash responses, are also highly related to the deformations of energy absorbing components. The HSA of these IMFs will indicate the deformation periods of each energy absorbing component. For this reason, IMFs will be utilized to identify the detailed crash process from measured crash responses. In CAE model validation, both trend and IMFs will be compared to check the global and local errors respectively. In conclusion, HHT is an effective method to investigate crash responses and can be used in the analysis, modeling and CAE validation of vehicle crashes.

2.3.2 Dynamic Time Warping

Dynamic time warping (DTW) is an algorithm to rematch two time histories as much as possible by expanding or compressing time axis. For two time histories, $X = \{x(1), x(2), \cdots, x(i), \cdots, x(m)\}$ and $Y = \{y(1), y(2), \cdots, y(i), \cdots, y(n)\}$, a cost function $d(i,j)$ is defined to measure the distance and local shape difference between $x(i)$ and $y(j)$. In the research of this thesis, $d(i,j)$ is defined as

$$d(i,j) = \left((i-j)^2 + (x(i) - y(j))^2\right) |dx(i) - dy(j)|^{\alpha} \tag{2.17}$$

where $dx(i) = x(i) - x(i-1)$, $dy(j) = y(j) - y(j-1)$ and α is an adjustable parameter for shape factor.

A set of coordinate pairs $W = \{w(1), w(2), \cdots, w(k) = (i,j), \cdots, w(l)\}$, where $\max(m,n) \leqslant l \leqslant m+n-1$, is used to represent the rematch result. The coordinate pairs should fulfil three constrains:

- Boundary condition: the two time histories should start and end at the same time. In other words, the path should start from the $w(1) = (1,1)$ and end with $w(l) = (m,n)$.
- Continuity: given $w(k) = (i,j)$, the next coordinate pair $w(k+1) = (i',j')$ should be neighboring elements, i.e. $i' \leq i+1$ and $j' \leq j+1$. For the sake of brevity, it can be wrote as $w(k+1) \leq w(k) + 1$.
- Monotonicity: the matching should retain the original order. That is $w(k) \leq w(k+1)$, i.e. $i \leq i'$ and $j \leq j'$.

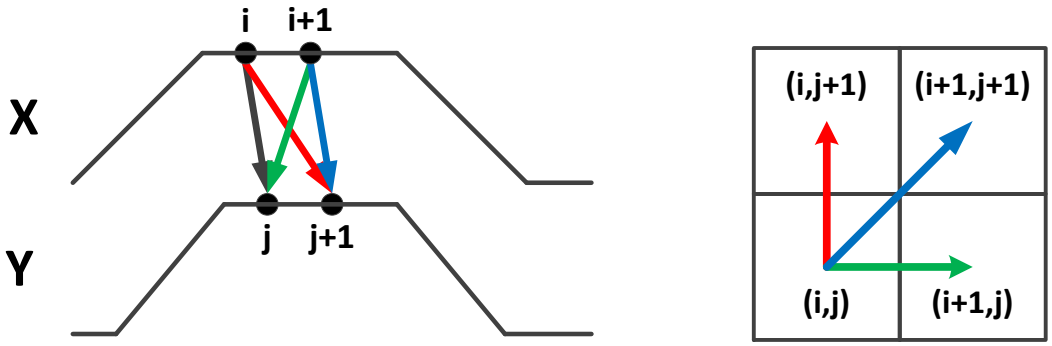

(a) Signal Representation (b) Matrix Representation

Figure 2.4: Rematch step under the constrains of continuity and monotonicity

According to the constrains of continuity and monotonicity, $w(k+1)$ has only three choices after $w(k)$ is decided, as shown by three coloured arrows in Figure 2.4.

An m-by-n order matrix D is constructed with the element $D_{i,j} = d(i,j)$. DTW is an optimization problem, which minimizes the total warping cost, i.e.

$$\begin{aligned} \min \quad & DTW(X,Y) = \sum_{k=1}^{l} D_{w(k)} \\ \text{s.t.} \quad & w(1) = (1,1) \\ & w(l) = (m,n) \\ & w(k) \leq w(k+1) \leq w(k)+1 \end{aligned} \tag{2.18}$$

To solve the problem, an m-by-n order cumulative cost matrix Γ is calculated as

$$\Gamma_{i+1,j+1} = \min \begin{cases} \Gamma_{i,j+1} + D_{i+1,j+1} \\ \Gamma_{i,j} + \rho D_{i+1,j+1} \\ \Gamma_{i+1,j} + D_{i+1,j+1} \end{cases} \tag{2.19}$$

where $i \geq 1$, , $j \geq 1$, $\Gamma_{1,1} = D_{1,1}$ and ρ is the compensation factor. The minimized total warping cost is $\Gamma_{m,n}$ and the corresponding element coordinates is retrieved as W.

An example is given to illustrate the retrieve process, as shown in Figure 2.5. The black bold values combine the cost matrix D. The cumulative cost matrix Γ is calculated with $\rho = 1$ and shown as the coloured value. $\Gamma_{m,n} = 18$ is the minimized $DTW(X,Y)$. The warping result W is shown by the red arrows.

A traditional application of DTW is the automatic speech recognition, to cope with different speaking speeds [74, 75]. Recently, it is also used in some new areas, such as data mining [76, 77], gesture recognition [78, 79]. In vehicle safety area, the comparison of two signals are often made for model validation. DTW algorithm are introduced into the signal comparison in some work, such as [44, 56, 57]. As DTW can decompose the discrepancy orthogonally by warping the compared signals, the measured magnitude error and phase error are independent with each other. However, the rematch process is likely to be influenced by local oscillations of original signals. In this PhD work, the

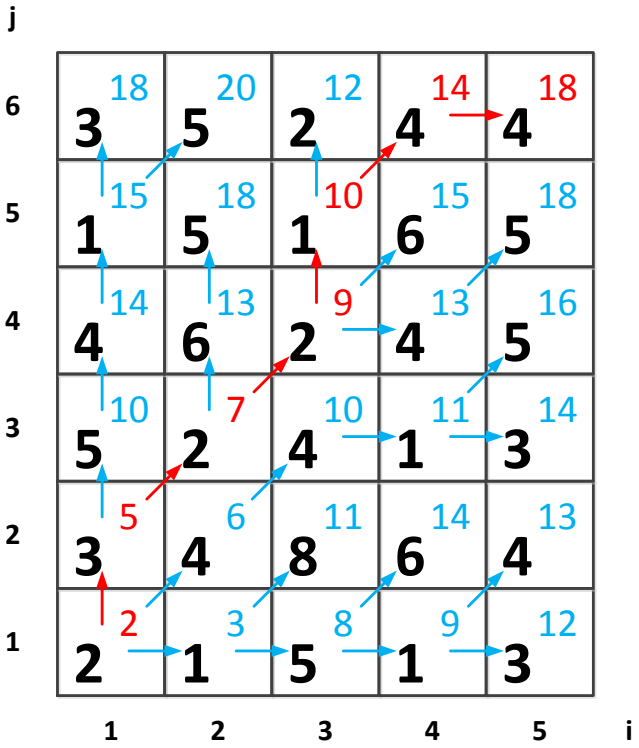

Figure 2.5: Example of dynamic time warping

global trend of compared signals are proposed in the DTW process, which helps to achieve more reasonable comparison.

2.4 Crashes Stages and Piecewise Model

To offer stable deformation performance in crashes, the crashworthiness structure is designed meticulously. Some work has studied the relationship between structure deformation and energy loss at the end of accidents [80, 81]. Generally, the deformation of components in load paths may occur in a specific order. Figure 2.6 shows the deformation process of main energy absorbing components, i.e. bumper, crash boxes and frontal longitudinal beams, in Yaris 56km/h frontal crash. It can be seen that, the periods, when these components collapse, occur in sequence without overlap. More importantly, the trend of crash response has different slopes in the periods.

Consequently, the crash process contains different stages and can be presented by a piecewise model, as shown in Figure 2.7. In this model, each segment refers to a crash stage, which is corresponded to an energy absorbing component:

- O-A: some accessories, such as front-cove, are crushed in a very short period. The deceleration keeps zero in this stage.
- A-B: it refers to the deformation of bumper. Typically, the deceleration in this stage increases significantly.

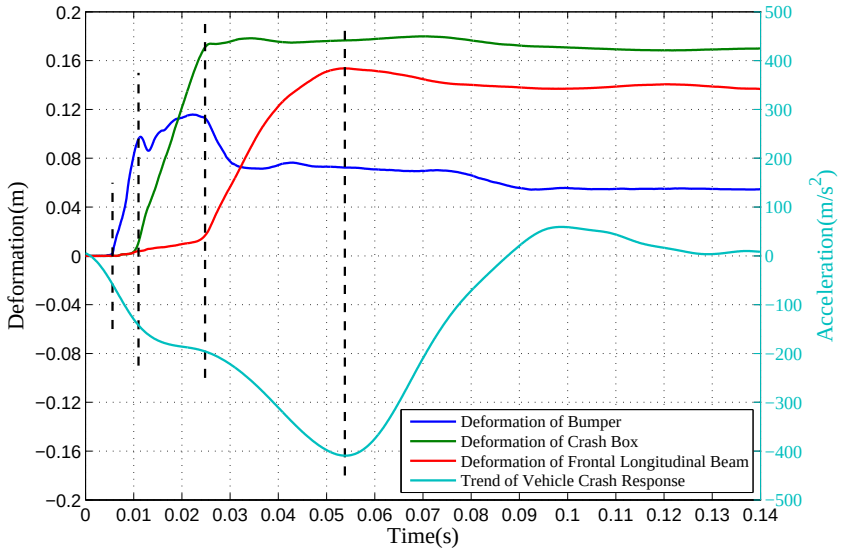

Figure 2.6: The relationship between energy absorbing components and vehicle crash response

- B-C: in this stage, the crash boxes are compressed to absorb energy. As the deformation mode is folding, the deceleration in this stage varies slowly.
- C-D-Eb-E: the deformation of longitudinal beams and movement of engine happen in this stage. The deceleration will achieve the peak firstly and then go down. At the time of Eb, the crash process is finished and vehicle is separated from barrier. Overshoot, shown as point E, maybe caused the inner force of vehicle.
- E-F: the deceleration turns to zero as there is no significant external force working on the vehicle.

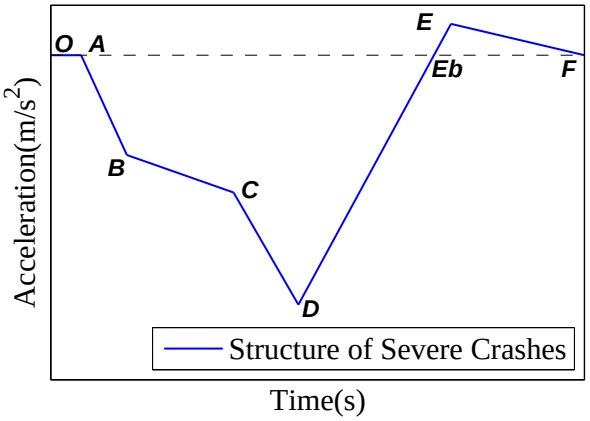

Figure 2.7: Piecewise model of vehicle frontal crashes

This model refers to a crash with high crash velocity, as it contains the deformation of all energy absorbing components. However, the impact velocity varies a lot in different crashes and lead deformation of different components. Considering the initial velocity

of vehicle and energy absorbing abilities of crashworthiness components, the crashes can be categorised as light, moderate and sever crashes.

More clearly, given the condition that initial kinetic energy of vehicle is less than ΔJ_1, which is the maximum absorbed energy of bumper, only the bumper will be crushed in the crash and other components will not be deformed. In the case that the initial kinetic energy is less than energy absorbing ability of both bumper and crash boxes, defined as ΔJ_2, the bumper and crash boxes will be deformed together and the longitudinal beams will remain the same. Finally, if the initial kinetic energy is even higher, all of these components will be deformed.

Figure 2.7 shows the model of severe cases. For the light and moderate crashes, the shapes of vehicle accelerations in the crashes are shown in Figures 2.8(a) and Figures 2.8(b) correspondingly.

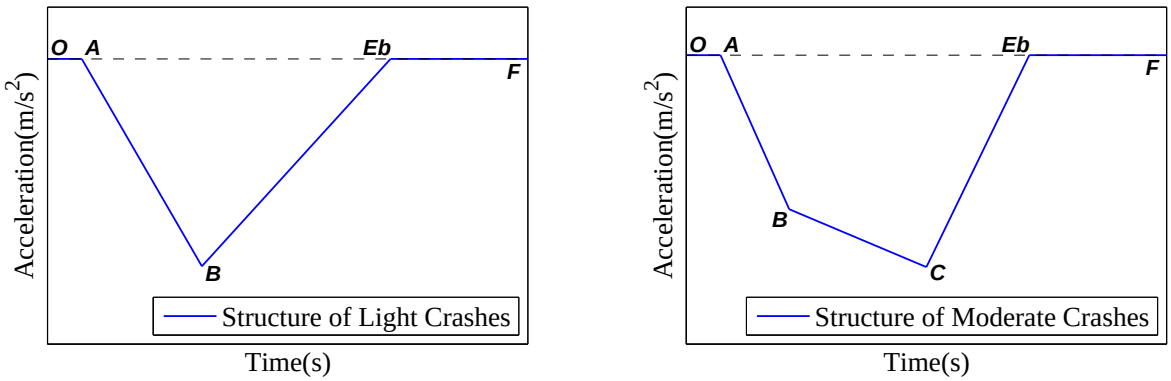

(a) Light Crashes

(b) Moderate Crashes

Figure 2.8: Models of light and moderate crashes

3 Concluding Remarks

3.1 Dissertation Conclusions

This PhD project investigates the vehicle frontal crash process using various signal processing tools. The main work of this project, as shown in Figure 3.1 and can be summarised as follows:

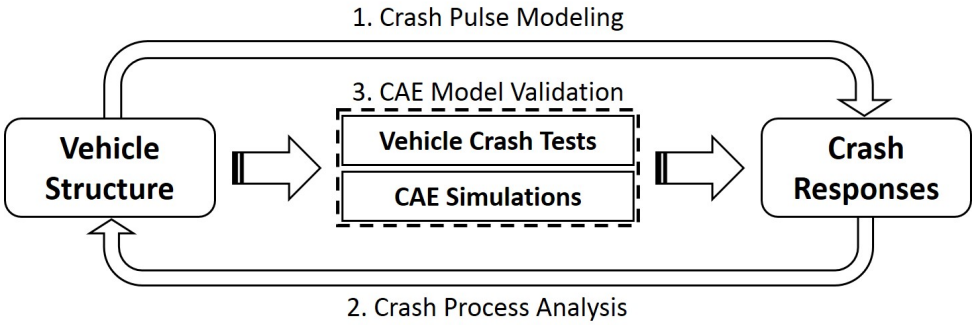

Figure 3.1: Main work of the PhD project

- The relationship between the crash response and crashworthiness structure is investigated firstly. The impact loads are transmitted through the designed paths and the energy absorbing components (i.e. bumper, crash boxes and longitude beams) combine the most important one of them. Each component has unique deformation mode and deformation period. For one respect, the features of energy absorbing components decided the crash process to a great extent. For the another hand, the features of each components can be extracted from the crash response signal with proper signal processing tools.
- The crash signals, especially the deceleration of vehicle passenger cabin, is used to analysis the vehicle crash process with the help of EEMD algorithm. EEMD is a time-frequency analysis algorithm suitable for the nonlinear and non-stationary signals. In the vehicle crash analysis, the EEMD decomposes the crash response signal into a low frequency trend and some high frequency oscillations. The trend shows the global variance of vehicle acceleration. For some sever frontal crashes, the trend can be divided into several stages according to the local slopes, which are corresponded to the deformation periods of energy absorbing components. At the same time, the time-frequency spectrum of IMFs can illustrate the deformation details of each component, as well as the movement of engine. In the other

cases, such as low speed or oblique crashes, the analysis of IMFs keeps working effectively, while the trend cannot. The proposed scheme enables engineers to identify the crash details through the acceleration signal of vehicle cabin only.

- A piecewise model of frontal crashes is proposed to describe the variance of vehicle acceleration. The model uses several segments to represent the deformations of bumper, crash boxes and frontal beams. Especially, the crashes are classified into three catalogues according to the impact energy: light, moderate and sever crashes. As more components are involved in the crashes with higher energy, crashes in different types have specific model structures. For a specific vehicle, the model parameters of 56km/h frontal crash are identified firstly from the data of corresponding NCAP frontal crash test, as it is available for most vehicle designs. The model parameters of frontal crashes in other velocities can be derived from previous identification result and the crash processes are predicted consequently.

- The model validation scheme in vehicle safety research is discussed and time-frequency decomposition is involved in the comparison of vehicle crash time histories. Different with the existing methods, the proposed scheme compares the trend and IMFs separately. By involving the DTW process, the comparison of trend signals provides the global errors on magnitude and time, which are orthogonal and independent. This is a robust way to measure the overall difference between test and reference signal, as it is free of the influence of high frequency components. At the same time, the IMFs offer the local information of original signal for further comparison. For one respect, each IMF has a high energy duration, which refers to the "working period" of relative structural components. The time durations are compared in pair firstly. For the other respect, the amplitude and frequency errors are also measured for each pair of IMFs. So the comparison of IMFs is related to the crash details, especially the deformation of vehicle components. The comparison results of trend and IMFs are combined to a general measure of time history difference, which suitable for vehicle safety application.

3.2 Contributions to Knowledge

The main contributions of this PhD project are fourfold:

- This work illustrates the relationship between the vehicle structure and crash response. Especially, the main energy absorbing components, includes the bumper, crash boxes and frontal longitude beam, are corresponded with different parts of the deceleration of vehicle cabin. In other words, vehicle decelerations are mainly decided by the performance of these components, albeit there existing local variances influenced by other parts of vehicle. The relationship can be used for various aspects of vehicle safety, includes crash signal analysis, crash modeling and prediction, as well as model validation.

- An EEMD based scheme is proposed to analysis the vehicle crash responses. Especially, a crash response signal is decomposed into a trend signal and a series of high frequency oscillations, which contains the information of vehicle structure deformation. Through the Hilbert transformation of oscillations, the deformation period of each energy absorbing components are identified. The trend signal can then be divided into several stages correspondingly. The proposed scheme is suitable for different crash condition, including frontal and oblique crashes in different velocities. The analysis result is helpful for the engineers to analyse vehicle crash tests effectively and therefore improve the crashworthiness design.

- The full vehicle crash process are modelled by a piecewise structure. The proposed model represents the vehicle acceleration directly and therefore has low complicity. It involves the vehicle structure information at the same time by using the segments to describe the deformation of energy absorbing components. This ensures that the proposed model have superior prediction accuracy than other crash pulse models. In addition, the proposed model is easy to be built based on the NCAP frontal crash test data. The model parameters of other frontal crashes can be derived functionally with the impact velocity as the only input variable.

- A comprehensive comparison scheme for time histories is proposed for vehicle safety model validation. In the proposed scheme, the trend of time history is compared firstly to provide a robust measure of global difference. The DTW algorithm is used to rematch the compared trends. The discrepancy is then decomposed orthogonally and measured by two metrics: time metric and magnitude metric. Moreover, the comparison of high frequency oscillations contains three aspects: working period, average frequency and average magnitude, which reflect the different performances of structure components. The advantages of the proposed scheme is that it offers more features for comparison and each metric has clear physical meaning. Therefore the proposed scheme is closed to the comparison of SMEs.

3.3 Future Work

In the future, the following work are expected to be continued:

- The deformation features of each energy absorbing components should be further investigated. More specifically, each energy absorbing component is supposed to be crushed separately. And the responses should be measured and compared with their performance in full vehicle crashes. The variance on deformation period, deceleration magnitude and frequency will be discussed.

- Although the prediction scheme of frontal crashes is given in the current work, more work is still to be done to predict the crashes with complex condition, such as offset crashes and vehicle to vehicle crashes. In these cases, only a few components are involved in the crashes and deform in a specific order. So the

parameters of piecewise structure, i.e. the start time, end time and slopes of each segment, should be further studied.

- The proposed comparison scheme measures the difference of crash time histories on several aspects. Especially, the error of trend and oscillations are calculated separately. So it is meaningful to make a reasonable combination of them to make a general measurement of signals' difference. In addition, only a few comparisons are done in the current work because of the limitation of crash data. In the further, more cases are supposed to be involved to check the performance of the proposed comparison scheme.

References

[1] L. J. K. Setright, *Drive on!: a social history of the motor car*. London: Granta Books, 2002.

[2] J. A. Jakle and K. A. Sculle, *Lots of parking: Land use in a car culture*. Santa Fe, New Mexico, and Staunton, London: University of Virginia Press, 2004.

[3] *Global status report on road safety 2015*. World Health Organization, 2015.

[4] P. Du Bois, C. C. Chou, B. B. Fileta, T. B. Khalil, A. I. King, H. F. Mahmood, H. J. Mertz, J. Wismans, P. Prasad, and J. E. Belwafa, *Vehicle crashworthiness and occupant protection*. Southfield, Michigan: American Iron and Steel Institute, 2004.

[5] P. Griškevičius and A. Žiliukas, "The absorption of the vehicles front structures," *Transport*, vol. 18, no. 2, pp. 97–101, 2003.

[6] K. Hamza and K. Saitou, "Design optimization of vehicle structures for crashworthiness using equivalent mechanism approximations," in *ASME 2003 International Design Engineering Technical Conferences and Computers and Information in Engineering Conference*, no. DETC2003/DAC-48751, (Chicago, Illinois, USA), pp. 459–472, American Society of Mechanical Engineers, September 2003.

[7] D. Y. Chen, L. M. Wang, C. Z. Wang, L. K. Yuan, T. Y. Zhang, and Z. Z. Zhang, "Finite element based improvement of a light truck design to optimize crashworthiness," *International Journal of Automotive Technology*, vol. 16, no. 1, pp. 39–49, 2015.

[8] H. Mozafari, S. Khatami, H. Molatefi, V. Crupi, G. Epasto, and E. Guglielmino, "Finite element analysis of foam-filled honeycomb structures under impact loading and crashworthiness design," *International Journal of Crashworthiness*, vol. 21, no. 2, pp. 148–160, 2016.

[9] L. Van Rooij, K. Bhalla, M. Meissner, J. Ivarsson, J. Crandall, D. Longhitano, Y. Takahashi, Y. Dokko, and Y. Kikuchi, "Pedestrian crash reconstruction using multi-body modeling with geometrically detailed, validated vehicle models and advanced pedestrian injury criteria," in *Proceedings of 18th International Technical Conference on the Enhanced Safety of Vehicles (ESV)*, no. 468, (Nagoya, Japan), National Highway Traffic Safety Administration, May 2003.

[10] J. Elliott, M. Lyons, J. Kerrigan, D. Wood, and C. Simms, "Predictive capabilities of the MADYMO multibody pedestrian model: Three-dimensional head translation and rotation, head impact time and head impact velocity," *Proceedings of the Institution of Mechanical Engineers, Part K: Journal of Multi-body Dynamics*, vol. 226, pp. 266–277, September 2012.

[11] H. Sankarasubramanian, A. Chawla, S. Mukherjee, and D. Goehlich, "Optimisation study on multibody vehicle-front model for pedestrian safety," *International Journal of Crashworthiness*, vol. 21, no. 1, pp. 63–78, 2016.

[12] M. ElKady, A. Elmarakbi, J. MacIntyre, and M. Alhariri, "Multi-body integrated vehicle-occupant models for collision mitigation and vehicle safety using dynamics control systems," *International Journal of System Dynamics Applications (IJSDA)*, vol. 5, no. 2, pp. 80–122, 2016.

[13] G. Amato, F. O'Brien, B. Ghosh, and C. K. Simms, "Multibody modelling of a TB31 and a TB32 crash test with vertical portable concrete barriers: Model verification and sensitivity analysis," *Proceedings of the Institution of Mechanical Engineers, Part K: Journal of Multi-body Dynamics*, vol. 227, no. 3, pp. 245–260, 2013.

[14] P. Jonsén, E. Isaksson, K. Sundin, and M. Oldenburg, "Identification of lumped parameter automotive crash models for bumper system development," *International Journal of Crashworthiness*, vol. 14, no. 6, pp. 533–541, 2009.

[15] W. Pawlus, H. R. Karimi, and K. G. Robbersmyr, "Development of lumped-parameter mathematical models for a vehicle localized impact," *Journal of Mechanical Science and Technology*, vol. 25, no. 7, pp. 1737–1747, 2011.

[16] S. M. Ofochebe, C. G. Ozoegwu, and S. O. Enibe, "Performance evaluation of vehicle front structure in crash energy management using lumped mass spring system," *Advanced Modeling and Simulation in Engineering Sciences*, vol. 2, no. 1, p. 1, 2015.

[17] Z. Li, M. W. Kindig, D. Subit, and R. W. Kent, "Influence of mesh density, cortical thickness and material properties on human rib fracture prediction," *Medical engineering & physics*, vol. 32, no. 9, pp. 998–1008, 2010.

[18] S. Engel, C. Bögle, and D. Lukaszewicz, "Modelling of composite failure during vehicle crash using cohesive elements," *International Journal of Automotive Composites*, vol. 1, no. 4, pp. 333–348, 2015.

[19] W. Abramowicz, "Thin-walled structures as impact energy absorbers," *Thin-Walled Structures*, vol. 41, no. 2-3, pp. 91–107, 2003.

[20] W. Abramowicz, "An alternative formulation of the FE method for arbitrary discrete/continuous models," *International Journal of Impact Engineering*, vol. 30, no. 8-9, pp. 1081–1098, 2004.

[21] K. Takada and W. Abramowicz, "Fast crash analysis of 3D beam structures based on object oriented formulation," *SAE Technical Paper 2004-01-1728*, 2004.

[22] R. H. Myers, D. C. Montgomery, and C. M. Anderson-Cook, *Response surface methodology: process and product optimization using designed experiments*. Hoboken, New Jersey, USA: John Wiley & Sons, 4th edition ed., 2016.

[23] G. E. Box, J. S. Hunter, and W. G. Hunter, *Statistics for experimenters: design, innovation, and discovery*. New Jersey, USA: John Wiley & Sons, 2nd ed., 2005.

[24] R. J. Yang, N. Wang, C. H. Tho, J. P. Bobineau, and B. P. Wang, "Metamodeling development for vehicle frontal impact simulation," *Journal of Mechanical Design*, vol. 127, no. 5, pp. 1014–1020, 2005.

[25] N. Dyn, D. Levin, and S. Rippa, "Numerical procedures for surface fitting of scattered data by radial functions," *SIAM Journal on Scientific and Statistical Computing*, vol. 7, pp. 639–659, April 1986.

[26] S. Haykin, *Neural Networks: A comprehensive foundation*. Prentice-Hall, 2nd edition ed., 1999.

[27] L. K. Hansen and P. Salamon, "Neural network ensembles," *IEEE Transactions on Pattern Analysis and Machine Intelligence*, vol. 12, no. 10, pp. 993–1001, 1990.

[28] M. J. Sasena, P. Papalambros, and P. Goovaerts, "Exploration of metamodeling sampling criteria for constrained global optimization," *Engineering Optimization*, vol. 34, no. 3, pp. 263–278, 2002.

[29] T. W. Simpson, A. J. Booker, D. Ghosh, A. A. Giunta, P. N. Koch, and R.-J. Yang, "Approximation methods in multidisciplinary analysis and optimization: a panel discussion," *Structural and Multidisciplinary Optimization*, vol. 27, no. 5, pp. 302–313, 2004.

[30] Y. Shi, J. Wu, and G. S. Nusholtz, "Optimal frontal vehicle crash pulses - a numerical method for design," in *Proceedings of 18th International Technical Conference on the Enhanced Safety of Vehicles (ESV)*, no. 514, (Nagoya, Japan), National Highway Traffic Safety Administration, May 2003.

[31] L. Shi, R.-J. Yang, and P. Zhu, "An adaptive response surface method for crashworthiness optimization," *Engineering Optimization*, vol. 45, no. 11, pp. 1365–1377, 2013.

[32] A. Deb, R. S. Gunti, C. Chou, and U. Dutta, "Use of truncated finite element modeling for efficient design optimization of an automotive front end structure," *SAE Technical Paper 2015-01-0496*, 2015.

[33] B. Liu, J. Yang, Z. Zhan, L. Zheng, B. Lu, K. Wang, Z. Zhu, and Z. Qiu, "An enhanced input uncertainty representation method for response surface models in automotive weight reduction applications," *SAE International Journal of Materials and Manufacturing*, vol. 8, pp. 616–622, 04 2015.

[34] L. Gu, R.-J. Yang, G. Li, and T. Tyan, "Structural optimization for crash pulse," *SAE Technical Paper 2005-01-0748*, 2005.

[35] D. Ito, Y. Yokoi, and K. Mizuno, "Crash pulse optimization for occupant protection at various impact velocities," *Traffic Injury Prevention*, vol. 16, no. 3, pp. 260–267, 2015.

[36] J. Hu, K. Fischer, P. Lange, and A. Adler, "Effects of crash pulse, impact angle, occupant size, front seat location, and restraint system on rear seat occupant protection," *SAE Technical Paper 2015-01-1453*, 2015.

[37] C.-K. Park and C.-D. S. Kan, "Objective evaluation method of vehicle crash pulse severity in frontal new car assessment program (NCAP) tests," in *Proceedings of 24th International Technical Conference on the Enhanced Safety of Vehicles (ESV)*, no. 15-0055, (Gothenburg, Sweden), National Highway Traffic Safety Administration, June 2015.

[38] M. Mendoza-Vazquez, L. Jakobsson, J. Davidsson, K. Brolin, and M. Östmann, "Evaluation of thoracic injury criteria for THUMS finite element human body model using real-world crash data," in *Proceedings-International Research Council on the Biomechanics of Injury (IRCOBI)*, no. IRC-14-62, (Berlin, Germany), pp. 528–541, September 2014.

[39] V. Agaram, L. Xu, J. Wu, G. Kostyniuk, and G. Nusholtz, "Comparison of frontal crashes in terms of average acceleration," *SAE Technical Paper 2000-01-0880*, 2000.

[40] W. Pawlus, H. R. Karimi, and K. G. Robbersmyr, "Data-based modeling of vehicle collisions by nonlinear autoregressive model and feedforward neural network," *Information Sciences*, vol. 235, pp. 65–79, 2013.

[41] L. Zhao, W. Pawlus, H. R. Karimi, and K. G. Robbersmyr, "Data-based modeling of vehicle crash using adaptive neural-fuzzy inference system," *IEEE/ASME Transactions on Mechatronics*, vol. 19, pp. 684–696, April 2014.

[42] A. Klausen, S. S. Tørdal, H. R. Karimi, K. G. Robbersmyr, M. Ječmenica, and O. Melteig, "Mathematical modeling and numerical optimizition of three vehicle crashes using a single-mass lumped parameter model," in *Proceedings of 24th International Technical Conference on the Enhanced Safety of Vehicles (ESV)*, no. 15-0168, (Gothenburg, Sweden), National Highway Traffic Safety Administration, June 2015.

[43] M. Varat and S. E. Husher, "Crash pulse modeling for vehicle safety research," in *Proceedings of 18th International Technical Conference on the Enhanced Safety of Vehicles (ESV)*, no. 501, (Nagoya, Japan), National Highway Traffic Safety Administration, May 2003.

[44] H. Sarin, M. Kokkolaras, G. Hulbert, P. Papalambros, S. Barbat, and R.-J. Yang, "Comparing time histories for validation of simulation models: error measures and metrics," *Journal of Dynamic Systems, Measurement, and Control*, vol. 132, no. 6, pp. 061401:1–10, 2010.

[45] A. Larsson, M. Pettersson, and H. Svensson, *CurveAnalyzer v1.0 - User Manual*. Chalmers University of Technology, 2003.

[46] M. H. Ray and M. Mongiardini, *Roadside Safety Verification and Validation Program (RSVVP) User's Manual*. Worcester Polytechnic Institute (WPI), 2009.

[47] D. M. Russell, "Error measures for comparing transient data: part I: development of a comprehensive error measure," in *Proceedings of the 68th Shock and Vibration Symposium*, (Hunt Valley, MD), pp. 175–184, November 1997.

[48] D. Twisk and P. Ritmeijer, "A software method for demonstrating validation of computer dummy models used in the evaluation of aircraft seating systems," *SAE Technical Paper 2007-01-3925*, 2007.

[49] L. Gu and R. Yang, "CAE model validation in vehicle safety design," *SAE Technical Paper 2004-01-0455*, 2004.

[50] X. Liu, W. Chen, and M. Paas, "Automated occupant model evaluation and correlation," in *ASME 2005 International Mechanical Engineering Congress and Exposition*, no. IMECE2005-81258, (Orlando, Florida, USA), pp. 353–358, American Society of Mechanical Engineers, November 2005.

[51] T. L. Geers, "An objective error measure for the comparison of calculated and measured transient response histories," *The Shock and Vibration Bulletin 54*, pp. 99–107, 1984.

[52] *Comparative Shock Analysis (CSA) of Main Propulsion Unit (MPU)*. 1994. Validation and Shock Approval Plan, SEAWOLF Program: Contract No.N00024-90-C-2901, 9200/SER: 03/039.

[53] M. Sprague and T. Geers, "A spectral-element method for modelling cavitation in transient fluid-structure interaction," *International Journal for Numerical Methods in Engineering*, vol. 60, no. 15, pp. 2467–2499, 2004.

[54] M. H. Ray, M. Mongiardini, and M. Anghileri, "Development of the roadside safety verification and validation program," *Roadside Safety Verification and Validation Program (Draft)*, 2008.

[55] C. Gehre, H. Gades, and P. Wernicke, "Objective rating of signals using test and simulation responses," in *Proceedings of 21st International Technical Conference on the Enhanced Safety of Vehicles (ESV)*, no. 09-0407, (Stuttgart, Germany), National Highway Traffic Safety Administration, June 2009.

[56] H. Sarin, M. Kokkolaras, G. Hulbert, P. Papalambros, S. Barbat, and R.-J. Yang, "A comprehensive metric for comparing time histories in validation of simulation models with emphasis on vehicle safety applications," in *ASME 2008 International Design Engineering Technical Conferences and Computers and Information in Engineering Conference*, (New York), American Society of Mechanical Engineers, August 2008.

[57] Z. Zhan, Y. Fu, and R.-J. Yang, "Enhanced error assessment of response time histories (EEARTH) metric and calibration process," *SAE Technical Paper 2011-01-0245*, 2011.

[58] W. Feller, "On the Kolmogorov-Smirnov limit theorems for empirical distributions," *The Annals of Mathematical Statistics*, vol. 19, no. 2, pp. 177–189, 1948.

[59] K. P. Burnham and D. R. Anderson, *Model Selection and Multimodel Inference: A Practical Information-Theoretic Approach*. New York: Springer, 2ed edition ed., 2002.

[60] X. Jiang and S. Mahadevan, "Bayesian validation assessment of multivariate computational models," *Journal of Applied Statistics*, vol. 35, no. 1, pp. 49–65, 2008.

[61] Y. Liu, W. Chen, P. Arendt, and H.-Z. Huang, "Toward a better understanding of model validation metrics," *Journal of Mechanical Design*, vol. 133, pp. 071005–1:071005–13, July 2011.

[62] S. Wang, W. Chen, and K.-L. Tsui, "Bayesian validation of computer models," *Technometrics*, vol. 51, pp. 439–451, November 2012.

[63] S. Mahadevan and R. Rebba, "Validation of reliability computational models using bayes networks," *Reliability Engineering & System Safety*, vol. 87, no. 2, pp. 223–232, 2005.

[64] M. J. Bayarri, J. O. Berger, M. C. Kennedy, A. Kottas, R. Paulo, J. Sacks, J. A. Cafeo, C.-H. Lin, and J. Tu, "Bayesian validation of a computer model for vehicle crashworthiness," technical report 163, National Institute of Statistical Sciences, RTP, NC, USA, 2005.

[65] X. Jiang, R.-J. Yang, S. Barbat, and P. Weerappuli, "Bayesian probabilistic PCA approach for model validation of dynamic systems," *SAE International Journal of Materials and Manufacturing*, vol. 2, pp. 555–563, 04 2009.

[66] M. J. Bayarri, J. O. Berger, M. C. Kennedy, A. Kottas, R. Paulo, J. Sacks, J. A. Cafeo, C.-H. Lin, and J. Tu, "Predicting vehicle crashworthiness: Validation of computer models for functional and hierarchical data," *Journal of the American Statistical Association*, vol. 104, no. 487, pp. 929–943, 2012.

[67] D. Marzougui, R. R. Samaha, C. Cui, C. Kan, and K. S. Opiela, "Extended validation of the finite element model for the 2010 toyota yaris passenger sedan," Working Paper NCAC 2012-W-005, The National Crash Analysis Center (NCAC), July 2012.

[68] "J211-1 Instrumentation for impact test - Part 1: Electronic instrumentation," Standard, SAE International, May 2014.

[69] H. E. Ross, D. L. Sicking, R. A. Zimmer, and J. D. Michie, *NCHRP report 350: Recommended procedures for the safety performance evaluation of highway features*. Transportation Research Board (TRB), National Research Council, Washington, DC, 1993.

[70] "European standard EN 1317-1 and EN 1317-2: Road restraint system," Standard, European Committee of Standardization (CEN), July 2010.

[71] M. Mongiardini, M. Ray, and C. Plaxico, "Development of a programme for the quantitative comparison of a pair of curves," *International Journal of Computer Applications in Technology*, vol. 46, pp. 128–141, February 2013.

[72] N. E. Huang and Z. Wu, "A review on Hilbert-Huang transform: Method and its applications to geophysical studies," *Reviews of Geophysics*, vol. 46, no. 2, 2008.

[73] N. E. Huang, Z. Shen, S. R. Long, M. C. Wu, H. H. Shih, Q. Zheng, N.-C. Yen, C. C. Tung, and H. H. Liu, "The empirical mode decomposition and the Hilbert spectrum for nonlinear and non-stationary time series analysis," *Proceedings of the Royal Society of London A: Mathematical, Physical and Engineering Sciences*, vol. 454, no. 1971, pp. 903–995, 1998.

[74] S. Davis and P. Mermelstein, "Comparison of parametric representations for monosyllabic word recognition in continuously spoken sentences," *IEEE Transactions on Acoustics, Speech, and Signal Processing*, vol. 28, pp. 357–366, August 1980.

[75] J. A. Kogan and D. Margoliash, "Automated recognition of bird song elements from continuous recordings using dynamic time warping and hidden Markov models: A comparative study," *Journal of the Acoustical Society of America*, vol. 103, no. 4, pp. 2185–2196, 1998.

[76] T. Rakthanmanon, B. Campana, A. Mueen, G. Batista, B. Westover, Q. Zhu, J. Zakaria, and E. Keogh, "Addressing big data time series: mining trillions of time series subsequences under dynamic time warping," *ACM Transactions on Knowledge Discovery from Data (TKDD)*, vol. 7, no. 3, pp. 10:1–10:31, 2013.

[77] F. Petitjean, G. Forestier, G. I. Webb, A. E. Nicholson, Y. Chen, and E. Keogh, "Dynamic time warping averaging of time series allows faster and more accurate classification," in *2014 IEEE International Conference on Data Mining*, pp. 470–479, IEEE, December 2014.

[78] A. Hernández-Vela, M. Á. Bautista, X. Perez-Sala, V. Ponce-López, S. Escalera, X. Baró, O. Pujol, and C. Angulo, "Probability-based dynamic time warping and bag-of-visual-and-depth-words for human gesture recognition in rgb-d," *Pattern Recognition Letters*, vol. 50, pp. 112–121, 2014.

[79] S. S. Rautaray and A. Agrawal, "Vision based hand gesture recognition for human computer interaction: a survey," *Artificial Intelligence Review*, vol. 43, no. 1, pp. 1–54, 2015.

[80] D. Vangi and F. Begani, "Performance of triangle method for evaluating energy loss in vehicle collisions," *Proceedings of the Institution of Mechanical Engineers, Part D: Journal of Automobile Engineering*, vol. 226, no. 3, pp. 338–347, 2012.

[81] D. Vangi and F. Begani, "Energy loss in vehicle collisions from permanent deformation: an extension of the 'Triangle Method'," *Vehicle System Dynamics*, vol. 51, no. 6, pp. 857–876, 2013.

Part II

Publications

Paper A

A Model of Vehicle-Fixed Barrier Frontal Crash and Its Application in the Estimation of Crash Kinematics

Zuolong Wei[1], Hamid R. Karimi[1], Kjell G. Robbersmyr[1]

1. Department of Engineering Sciences, University of Agder, PO Box 509, N-4898 Grimstad, Norway

The paper has been published as:

Z. Wei, H. R. Karimi, and K. G. Robbersmyr, "A model of vehicle-fixed barrier frontal crash and its application in the estimation of crash kinematics," *24th Enhanced Safety of Vehicles Conference (ESV2015)*, Paper Number 15-0161, 2015.

The layout has been revised.

Abstract

The study of vehicle crash process is of great importance in transportation safety. The crash pulses of vehicles during the fixed barrier impacts can reflect the crashworthiness of the vehicle structure. In this paper, a mathematical model of vehicle kinematics during the frontal crash is investigated. This work is based on the analysis of crash response signals and vehicle structure. The proposed model uses piecewise linear functions to describe the trend of crash impulse and ignores the residual oscillations. To study the model variance, the crashes in various speeds and a full car crash in complex condition are compared. At the end of paper, the crash performance of a vehicle crash is predicted according to the proposed model and therefore demonstrates its effectiveness and usability.

A.1 Introduction

Crashworthiness is one of the core topics in the passive safety of vehicles and plays an important role in the condition that the impact cannot be avoided. Generally, the analysis of crashworthiness is based on the related crash responses, i.e. the displacement, velocity and acceleration, of critical parts of a vehicle in full car crash tests. However, these tests are required appropriate facilities, one or more cars with measuring devices, experienced staff and a long time to prepare. It means they are complicated, expensive, long-lasting and therefore not easy to realize [1]. This is especially true in the early stage of vehicle design. Therefore, vehicle designers and researchers made a lot of effort to build numerical models to describe the crash processes. Up to now, various technologies are used to model the vehicle crash. Typical crash models may be classified into three broad categories [2]: 1) Detailed nonlinear finite element models. These models have excellent performance in the estimation of structural crashworthiness. However, before these crash models could be used, they usually require the details of the vehicle structure and materials. This limits the use of FE models in the design process. 2) Multibody models and multibody based lumped parameter models. As FE models, the multibody models also suffer the complexity. Consequently, the multibody based lumped parameter models make a compromise between the accuracy and complexity. Most of these models consist of energy absorbing (EA) elements with masses connected to both ends [3]. Reference [4, 5] are typical studies on the lumped parameter models. 3) Functional approximation or response surface models. The functional approximation method is widely used in academia and industry. And reference [6] provides an overview of its use in the research of crashworthiness. To achieve better approximation, some advanced technologies are also introduced in this area, such as wavelet [7] and neural network [8]. Most of these models focus on the crash response signals themselves and can hardly be related to the vehicle structure. So the physical meaning of these modes is not clear.

In the proceeding of the study, a piecewise linear model is proposed to represent the vehicle-rigid wall frontal crash. Compared to existing models, this model is developed based on the analysis of crash responses and therefore can reflect the performance

of vehicle structures in crashes. The rest part of this paper is organized as follows: In the next section, the crashworthiness structure is introduced firstly. Afterwards, the proposed model is proposed. In this section, the modelling procedures will be presented in detail and the influences of crash condition are also discussed. After that, an estimation of vehicle kinematics is given as an application of the proposed model. The conclusion goes finally.

A.2 Vehicle Structure

Most of modern commercial cars have unibody construction, i.e. a single entity forms a car's body and frame. The vehicle body is usually made of steel or aluminum that is stamped with the appropriate cross members and everything is mounted directly to it. In this paper, only the frontal crash of unibody construction is studied.

To improve the crashworthiness, the vehicles are meticulously designed. As an integration, the vehicle structure would transmit the impact load in a proper way, i.e. load-carrying path. In addition, there are some weak components arranged as crumple zone. During the crash, the crumple zone will deform and absorb energy and ensure the rest parts of the vehicle are safe. In the local design, the material and shape of beams, shells and connectors are also considered to achieve better energy-absorbing performance.

A.2.1 Load-carrying Path and Crash Process

Generally, vehicles have a high relative velocity in the crashes. For this reason, the frontal structures always have enough space for the crashworthiness design. In many vehicles, there are three paths to transmit the impact load:

1) Path1: Accessories-Front bumper and Crash box-Front longitudinal beam-Engine-Firewall

2) Path2: Upper wing beam-A pillar-Guard beams of door;

3) Path3: Sub-frame-Sill beam

For most cases, the first path affords more than half of the total energy in crashes. Accordingly, the ideal crash process contains several stages:

1) Accessory crush. This is designed to protect the pedestrian. This stage is very short and nearly has no influence on the energy and velocity of vehicles.

2) Bumper crash and Crash box. The bumper is helpful in the low-speed crashes. Its ability for the energy absorbing is limited.

3) Longitudinal beam collapse. This part is responsible for crash compatibility, i.e. to protect the opposing vehicle in some extent and make the total lost lower in crashes.

4) Engine compression. Engine should be seen as a mass with limited deformation in crashes. In some high speed crashes, it will crush into the firewall and be compressed a little.

5) Firewall deformation. Firewall is much stronger than other components to protect the passenger cabin.

A.2.2 Crashworthy Structures

In most vehicles, longitudinal beams are designed as the crashworthy structures and employed for the energy absorbing. Although, the longitudinal beams can be various in terms of the material, section shape and processing technology, they follow the same requirement in design to optimise its performance:

1) No deformation in low speed crashes; Collapse progressively and absorbing the energy effectively in high speed crashes.

2) Having repeatable and reliable failure mode to ensure its performance in different crashes.

For this reason, the crashworthy structures of vehicles always experience a stables process of collapse during different crashes. In this process, the deformation follows a linear trend and have a series of oscillations. To sum up, the crash processes of vehicles yield to an internal pattern, which is controlled by the load-carrying path and beam collapse mode. For this reason, a functional model is proposed to present the vehicle crash process.

A.3 Crash Model

During a crash, the response signals contain several parts, which are corresponding to the crash stages. A piecewise model can be therefore identified by the accelerations and external force.

A.3.1 Piecewise Linear Model

There are some mathematical models of crash response in the literature, such as sine, triangular, and haversine [9]. However, none of them consider the vehicle structure and consequently are neither precise enough nor adjustable for different crash scenarios. To illustrate the proposed modelling process, NHTSA Test 5677, in which Yaris is crashing to a rigid wall in 56km/h, is employed for example.

Model Structure

The response of vehicle crashes can be recorded by the acceleration signals (crash impulses). Figure A.1 shows the acceleration signal of the left rear seat during the crash and the proposed model structure.

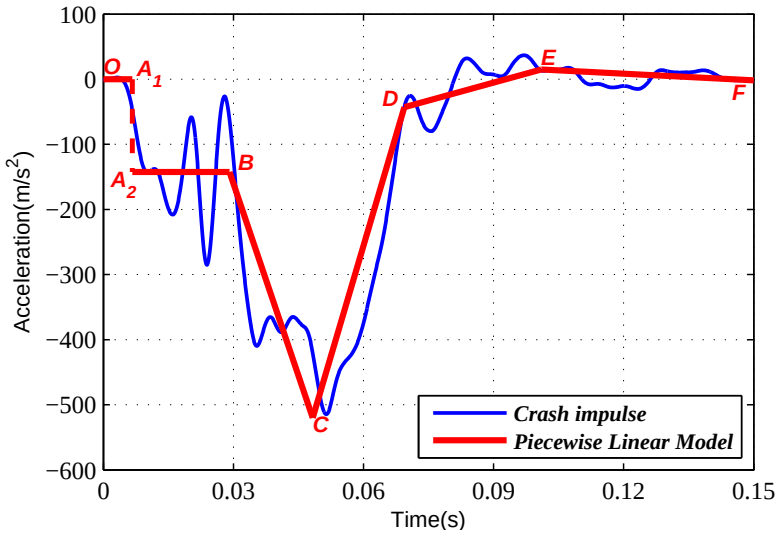

Figure A.1: Piecewise linear model structure for front crash of sedans

Comparing with load-carrying path and crash stages presented above, the physical meaning of the model structure is as follows:

1) Original-A1 segment: The accessory are crushed and bumper deform. In this stage, there is no significant acceleration.

2) A2-B segment: The crash box and longitudinal beam are working. During this time, the acceleration is stable around a level.

3) B-C-D segment: The longitudinal beam keeps working and the engine is crashing to the firewall. The force worked on the firewall makes the sharp slowdown of the cabin.

4) D-E-End segment: Restitution process. The crumple area is fully compressed and most energy are absorbed. Some internal energy is released and leads the oscillation of velocity.

Although some local oscillations (the high frequency component of acceleration signals) are lost in this model structure, it reflects the trend (base mode) of acceleration in a full crash. Because the integration of the oscillations approaches zero [10], this model can keep a good performance in the estimation of velocity and displacement.

Time of Model Nodes

In the presented model structure, the time and value of each node (i.e. A1, A2 and B∼F) are to be decided. For O-A1 stage, the acceleration is small and the variation of velocity is tiny. The end of this stage T_A satisfies:

$$\Delta v_A = \int_0^{T_A} a(t)\,dt = -1\% \times v_{init} \tag{A.1}$$

and

$$Acc_{A1} = 0 \tag{A.2}$$

where Δv_A is the velocity change during $0 \sim T_A$, signal $a(t)$ is the vehicle crash response and v_{init} is the initial velocity of vehicle.

For node F, T_F is the end time of signals and the acceleration Acc_F is the value of end time. The times of other nodes are discussed in this part and the accelerations will be studied in the next part.

Comparing to A2-B, the main feature of B-C-D process is that the engine is compressed by the firewall. The contact force slowdowns the cabin drastically. Correspondingly, the reacting force makes the deceleration of engine turn smaller (See Figure A.2). So the time of B, T_B, is the time of minimum engine deceleration.

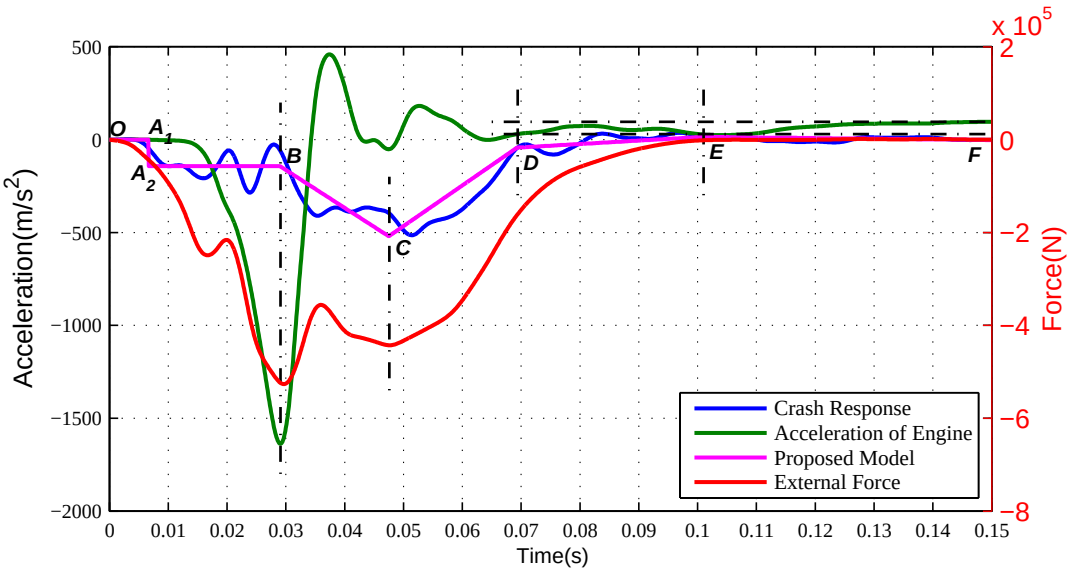

Figure A.2: Time identification of proposed model structure

After T_B, the engine experiences a "step response" like process with the input of the reacting force from firewall and finally arrives the stable value when the time finished. So T_D can be set as the time when engine acceleration arrives the steady area. A recommended steady area can be seen from the maximum to the minimum value of engine acceleration after the T_E (will be given later).

Node C refers to the maximum deceleration in the crash process. Of course, it can be decided directly by the minimum point of crash response. However, in some cases, Acc_C is not significantly lower than the neighborhood and therefore T_C suffers a great uncertainty. This is because of the combined effect of the oscillations from engine and rest part of the vehicle. And neither of them plays a leading role. For these cases, an alternated method is given as below.

It should be noted that the crash response signal is measured from one point of the vehicle body. That means it cannot reflect the general response exactly perfect. To solve this problem, the external force, which works on the vehicle is to be studied (See Figure A.2).

As shown, the first maximum force is corresponding to the node B and contributes

to the maximum deceleration of the engine. The second maximum force is related to the Node C, as the engine acceleration is not significant at that period. So, T_C equals to the time of the second maximum force. For the restitution stage, T_E is the time when external force falls to 1% of the maximum value.

Accelerations of Model Nodes

The proposed model is hoped to make the error of acceleration and velocity small. For convenience in computation, the accelerations of B∼E should ensure: 1) $Acc_B \sim Acc_E$ locate near the real crash response; 2) the interaction of the proposed model, i.e. the velocity of model, is same with the real crash response at times T_B, T_D and T_F. Setting $Acc_D = a(T_D)$ arbitrarily and the rest accelerations are decided as follows:

1) To ensure

$$\int_0^{T_B} Acc(t)\,dt = Acc_B \cdot T_{AB} = \Delta v_{AB} = \int_0^{T_B} a(t)\,dt \tag{A.3}$$

where $T_{AB} = (T_B - T_A)$, Acc_B is set as

$$Acc_B = \frac{\int_0^{T_B} a(t)\,dt}{T_B - T_A} \tag{A.4}$$

2) To ensure

$$\begin{aligned}\int_{T_B}^{T_D} Acc(t)\,dt &= \frac{1}{2}\left(Acc_B \cdot T_{BC} + Acc_C \cdot T_{BD} + Acc_D \cdot T_{CD}\right)\\ &= \Delta v_{BD} = \int_{T_B}^{T_D} a(t)\,dt\end{aligned} \tag{A.5}$$

and

$$\begin{aligned}\int_{T_D}^{T_F} Acc(t)\,dt &= \frac{1}{2}\left(Acc_D \cdot T_{DE} + Acc_E \cdot T_{DF} + Acc_F \cdot T_{EF}\right)\\ &= \Delta v_{DF} = \int_{T_D}^{T_F} a(t)\,dt\end{aligned} \tag{A.6}$$

where $T_{BC} = T_C - T_B$, $T_{BD} = T_D - T_B$, $T_{CD} = T_D - T_BC$, $T_{DE} = T_E - T_D$, $T_{DF} = T_F - T_D$ and $T_{EF} = T_F - T_E$. Acc_C and Acc_E are set as

$$Acc_C = \frac{2\int_{T_B}^{T_D} a(t)\,dt - Acc_B(T_C - T_B) - Acc_D(T_D - T_C)}{T_D - T_B} \tag{A.7}$$

$$Acc_E = \frac{2\int_{T_D}^{T_F} a(t)\,dt - Acc_D(T_E - T_D) - Acc_F(T_F - T_E)}{T_F - T_D} \tag{A.8}$$

A.3.2 Models for Various Speed

To show the variance of the proposed model, a series of crashes are simulated by the FE method. In these crashes, the 2010 Toyota Yaris is crashing to a rigid wall at the speed of 20km/h, 25km/h, 32km/h, 40km/h, 48km/h, 56km/h and 65km/h. The FE model of Yaris comes from the National Crash Analysis Center (NCAC) of George Washington University.

The parameters of the modelling results are shown in the table (See Table A.1).

Table A.1: Parameters of modelling results for crash simulations in various initial velocities

No.	Initial Velocity	At(s) A1(m/s^2)	Bt(s) B(m/s^2)	Ct(s) C(m/s^2)	Dt(s) D(m/s^2)	Et(s) E(m/s^2)	Ft(s) F(m/s^2)	Note
1	$20km/h$	0.0203 0	**0.0473** **-114.4992**	**0.1159** **-127.7229**	0.0736 -93.6547	0.1026 22.6533	0.1499 2.0482	Bad
2	$25km/h$	0.0172 0	0.0368 -125.1086	0.0569 -199.2543	0.0749 -87.6170	0.0985 20.3931	0.1499 -0.5908	Good
3	$32km/h$	0.0145 0	**0.0541** **-178.0036**	**0.1058** **35.2196**	0.0933 -3.2184	0.0989 -1.1863	0.1499 14.3759	Bad
4	$40km/h$	0.0125 0	0.0403 -187.4030	0.0516 -285.4251	0.0774 -84.9810	0.1030 37.3893	0.1499 -17.9486	Good
5	$48km/h$	0.0111 0	0.0337 -195.5635	0.0578 -379.2445	0.0745 -110.9681	0.0927 25.4419	0.1499 17.3587	Good
6	$56km/h$	0.0102 0	0.0330 -195.0890	0.0474 -484.4808	0.0873 40.1901	0.0963 40.0699	0.1499 -12.1832	Good
7	$65km/h$	0.0096 0	0.0278 -202.8010	0.0456 **-399.5320**	**0.1042** **44.3387**	0.1049 **21.1624**	0.1499 -22.8631	Bad
8	$20km/h$	0.0203 0	0.0323 -97.2563	0.0481 -172.514	0.0736 -93.6547	0.1026 22.6533	0.1499 2.0482	Good after adjustment
9	$32km/h$	0.0145 0	0.0362 -150.5192	0.0503 -229.4992	0.0933 -3.2184	0.0989 -1.1863	0.1499 14.3759	Good after adjustment
10	$65km/h$	0.0096 0	0.0278 -202.8010	0.0456 -500.0374	0.0905 38.564	0.1049 35.1197	0.1499 -22.8631	Good after adjustment

This table shows that:

1) Generally speaking, the model has good applicability for the crashes with the initial velocity from 25 56km/h.

2) For the No. 3, the model has a wrong identification of T_B and T_C and therefore fails to fit the crash response. By studying the crash responses of 32km/h crash (See Figure A.3(b)), it can be found that the engine acceleration at 0.0362s is the first local minimum value with the abrupt turn of trend. According to the physical meaning, this abrupt turn refers to the contact between the engine and firewall and T_B should be 0.0362s. Consequently, T_C is 0.0503s. After this adjustment (as No. 9), the model fits the crash response well. This is because of the less compression of the engine in the lower speed crashes. So for the crashes with initial speed lower than 32km/h, it is highly recommended to check the model again according to the physical meaning.

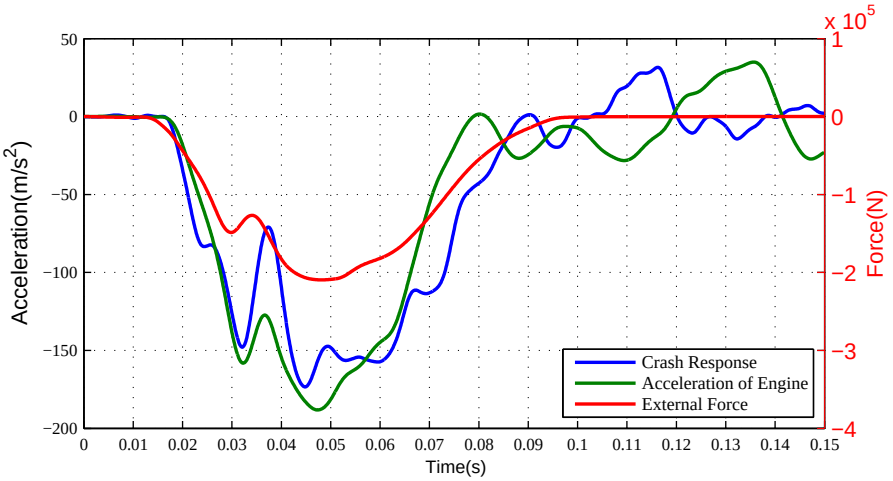

(a) Crash responses and references of No.1 simulation

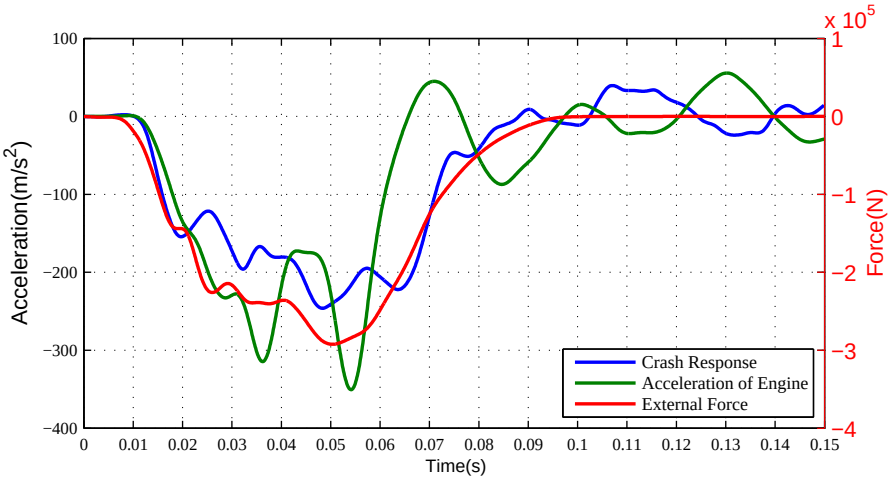

(b) Crash responses and references of No.3 simulation

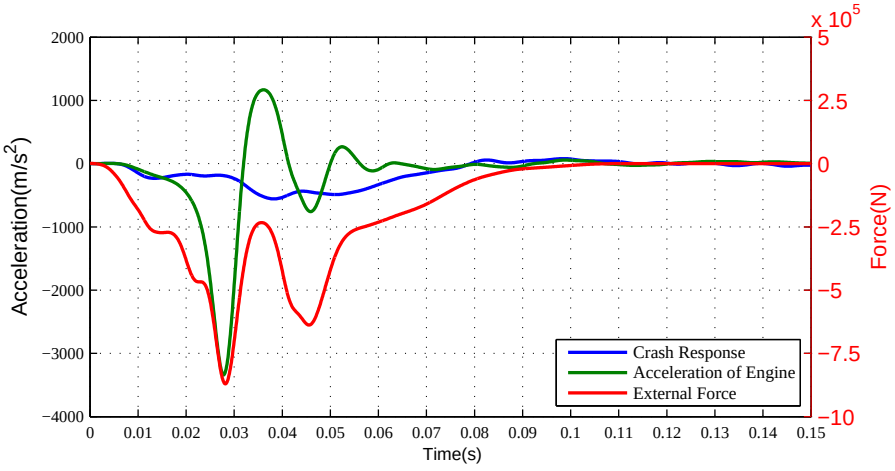

(c) Crash responses and references of No.7 simulation

Figure A.3: Crash responses and references (a. No.1; b. No.3; c. No.7)

3) No. 1 suffers similar problems with Test 3 and can be adjusted (as No. 8) to achieve good performance. However, the minimum value is not much lower than

other values in this crash response (See Figure A.3(a)). Specifically, the process B∼D (i.e. the engine influence) is not as significant as other crashes. This means the crash process, as well as model structure, is different from high speed crashes. For this reason, the proposed model may cannot represent the responses well for the crashes with initial velocity lower than 20km/h.

4) No. 7 is for the 65km/h crash and have a problem in the identification of T_D. In the crash responses (See Figure A.3(c)), there are oscillations with big amplitude in the process D∼E and lead the wrong identification. Obviously, in this crash, the vibration of the engine is much stronger than 56km/h crash. An adjustment can be made manually to improve the model (as No. 10). But it should be mentioned that for a higher speed crash, the model can hardly present the crash process very well.

A.3.3 Complex Condition

In this subsection, a full car crash test will be studied. In this crash, the Yaris is crashed by a moving deformable barrier (RMDB) with a target speed of 86.7km/h. The crash mode is 7°angle and 20.6% offset (See Figure A.4(a)). The test data come from NHTSA Test 7434.

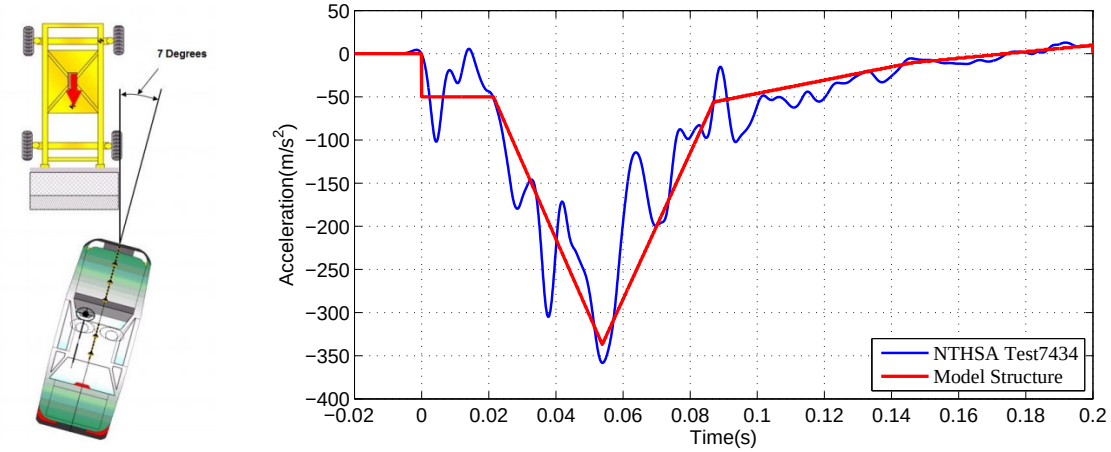

(a) Configuration of NHTSA Test 7434

(b) Crash responses and modelling of NHTSA Test 7434

Figure A.4: NHTSA crash Test 7434 (a. Crash configuration; b. Crash response)

From this response, we can find that:

1) Because of the deformable barrier, the maximum acceleration in this test is $358.3208 m/s^2$ in negative direction, which is near the value in 40km/h rigid wall crash. So it is possible to have an experience that the maximum acceleration of a deformable barrier crash can be estimated by the rigid wall crash with half speed. Of course, this is a rough estimation and the barrier should have similar mechanical characteristics as the vehicle body.

2) In 0∼0.02s, the bumper, crash box and longitudinal beam are deforming. But due to the offset, only left half part of the crush zone is crushed and therefor this crash response during this time is different from 100% overlap crash. The most important difference is the average value in this period is about $50m/s^2$, which is about only 1/4 of the Acc_B in No. 4 in Table A.1. In other words, the absorbed energy is much lower than the full overlap crash

3) There is also a process like B-D in the model, which indicates that the engine is also crushed into the firewall and compressed. This shows all the crashworthiness structures will work in the crashes with an offset.

In conclusion, this crash test can also be described roughly by the proposed model structure, shown as the red dash line in Figure A.4(b). However, some local performances are different, such as the mode of B-C stage. And consequently the related parameters should also be revalued.

A.4 Estimation of Vehicle Kinematics

The proposed model can be used for the estimation of vehicle kinematics. The NTHSA Test 6069 can be used as an example. The crash condition is: 39.6km/h full overlap crash to a rigid wall barrier. To make an estimation, the parameters of the proposed model can be set as the average value of No. 5 and No. 9 in Table A.1. That is $A_t = 0.0128$, $Acc_A = 0$, $B_t = 0.0350$, $Acc_B = -173.0414$, $C_t = 0.0541$, $Acc_C = -304.3719$, $D_t = 0.0825$, $Acc_D = -40.4034$, $E_t = 0.0958$, $Acc_E = 12.3273$, $F_t = 0.1499$ and $Acc_F = 15.8673$. Note: the T_D of No. 9 is obviously higher than other T_D. This may be because of the uncertainty of simulations. To get better estimation, the estimation of T_D and Acc_D should be adjusted as the average of No. 2∼6, as the 39.6km/h is the average of the corresponding velocities. The estimated model will be compared with the Test 6069 and simulation result (See Figure A.5).

A.5 Conclusion

Comparing to finite element models and multibody modes, the mathematical models have advantages on conciseness and usability. For this reason, the mathematical models can be used in the early design of vehicles, as well as accident reconstruction. This paper presents a novel modelling scheme of crashes, which is based on the acceleration signals and vehicle structure. The proposed model can reflect the crash process clearly and therefore describe the crash response exactly. In addition, this model suits for the crash in various conditions by adjusting the parameters. At the end of paper, an estimation of vehicle kinematics shows the good performance of the proposed model for a frontal crash at 40km/h.

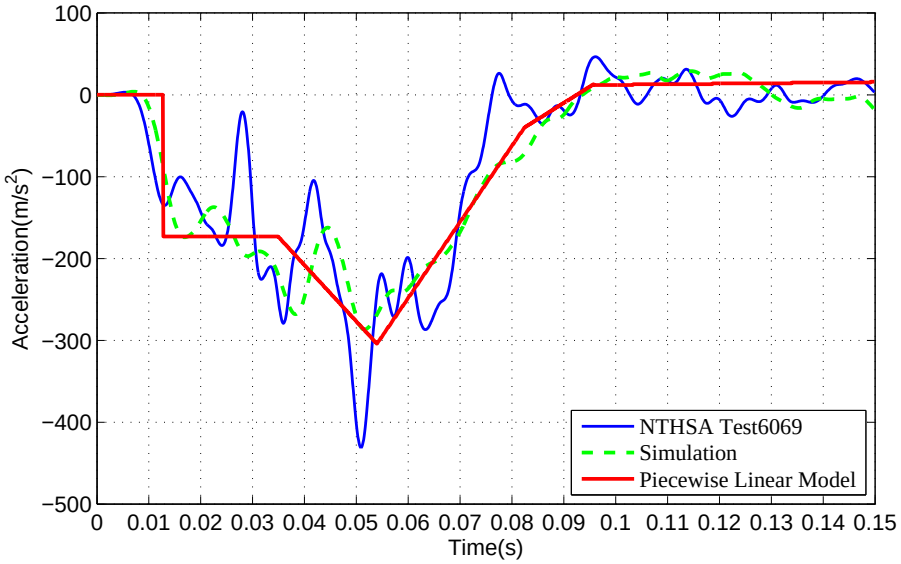

(a) Acceleration signals

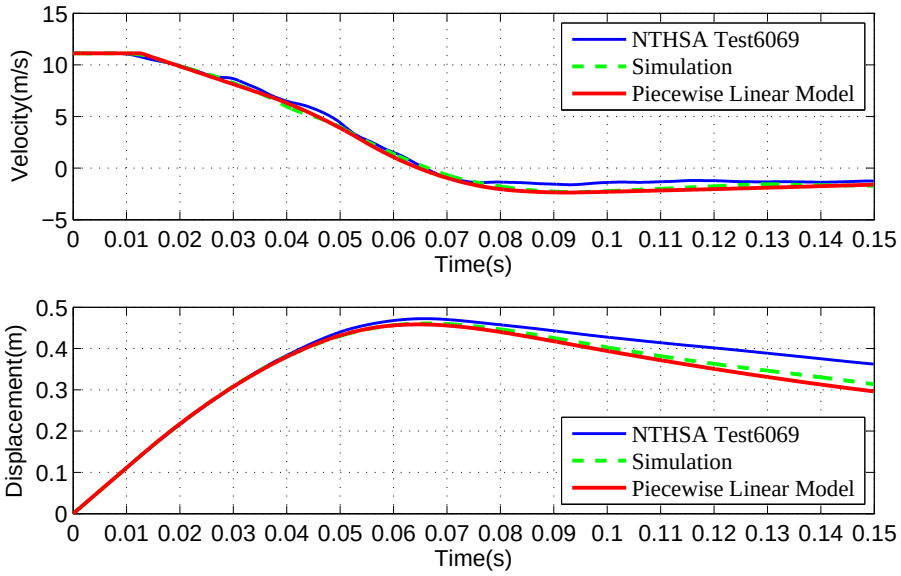

(b) Velocity and displacement signals

Figure A.5: Validation of the estimation (a. Acceleration; b. Velocity and displacement)

References

[1] W. Pawlus, H. R. Karimi, and K. G. Robbersmyr, "Investigation of vehicle crash modeling techniques: theory and application," *The International Journal of Advanced Manufacturing Technology*, vol. 70, no. 5-8, pp. 965–993, 2014.

[2] K. T. Hamza, *Design for vehicle structural crashworthiness via crash mode matching*. PhD thesis, University of Michigan, Ann Arbor, MI., 2008.

[3] M. Huang, *Vehicle crash mechanics*. Boca Raton, Florida: CRC press, 2002.

[4] M. M. Kamal, "Analysis and simulation of vehicle to barrier impact," *SAE Technical Paper 700414*, 1970.

[5] W. Pawlus, K. G. Robbersmyr, and H. R. Karimi, "Mathematical modeling and parameters estimation of a car crash using data-based regressive model approach," *Applied Mathematical Modelling*, vol. 35, no. 10, pp. 5091–5107, 2011.

[6] T. W. Simpson, A. J. Booker, D. Ghosh, A. A. Giunta, P. N. Koch, and R.-J. Yang, "Approximation methods in multidisciplinary analysis and optimization: a panel discussion," *Structural and multidisciplinary optimization*, vol. 27, no. 5, pp. 302–313, 2004.

[7] H. R. Karimi and K. G. Robbersmyr, "Signal analysis and performance evaluation of a vehicle crash test with a fixed safety barrier based on haar wavelets," *International Journal of Wavelets, Multiresolution and Information Processing*, vol. 9, no. 01, pp. 131–149, 2011.

[8] L. Zhao, W. Pawlus, H. R. Karimi, and K. G. Robbersmyr, "Data-based modeling of vehicle crash using adaptive neural-fuzzy inference system," *IEEE/ASME Transactions on mechatronics*, vol. 19, no. 2, pp. 684–696, 2014.

[9] M. Varat and S. E. Husher, "Crash pulse modeling for vehicle safety research," in *Proceedings of 18th International Technical Conference on the Enhanced Safety of Vehicles (ESV)*, no. 501, (Nagoya, Japan), National Highway Traffic Safety Administration, May 2003.

[10] C. C. Chou, J. Le, P. Chen, and D. Bauch, "Development of cae simulated crash pulses for airbag sensor algorithm/calibration in frontal impacts," in *Proceedings of 17th International Technical Conference on the Enhanced safety of Vehicles (ESV)*, (Amsterdam, Netherlands), National Highway Traffic Safety Administration, June 2001.

Paper B

EEMD Based Analysis of Vehicle Crash Responses

Zuolong Wei[1], Hamid R. Karimi[1], Kjell G. Robbersmyr[1]

1. Department of Engineering Sciences, University of Agder, PO Box 509, N-4898 Grimstad, Norway

The paper has been published as:

Z. Wei, H. R. Karimi, and K. G. Robbersmyr, "EEMD based analysis of vehicle crash responses," in *IECON 2015 - 41st Annual Conference of the IEEE Industrial Electronics Society*, pp. 005206–005210, 2015.

The layout has been revised.

Abstract

The vehicle crash is a complex process with nonlinear large deformation of structures. The analysis of the crash process is one of the challenges for all vehicle safety researchers. In this paper, the Ensemble Empirical Mode Decomposition (EEMD) method is applied in the analysis of crash responses in order to achieve some meaningful results. With the help of EEMD, the crash responses are decomposed into a trend signal and some high frequency fluctuations. By studying the load path of vehicle design, each component is corresponding to the structure of vehicle body. Consequently, some parameters of vehicle crash model can be identified. A frontal crash of Toyota Yaris is employed for demonstration.

B.1 Introduction

Vehicle Crash is the major casualties of road accidents. One of the most important aspects of vehicle safety is the crashworthiness of vehicles (a kind of passive safety), which refers to the ability of the vehicle structure to protect the occupants during crashes. For this reason, the study of vehicle crashworthiness is widely concerned by both vehicle manufacturers and research institutes.

The crash responses, i.e. the acceleration, velocity and displacement signals of the concerned parts of vehicles and occupants, are the base of vehicle safety studies. In most cases, they will be used for the analyses, calibration and evaluation of vehicle safety performance, and then help to provide the reference for vehicle safety improvements. They are also the basis of the vehicle safety evaluation.

However, the analysis of the crash responses is a great challenge for the vehicle designers and researchers. As the vehicle crash is a complex process with large deformation of vehicle structure, the crash responses are generally non-linear and non-stationary. In addition, the crash responses also suffer the noise and uncertainty in the measurement procedure. To the authors' knowledge, the development of special technologies for the vehicle crash analysis has not been completely investigated in literature. Therefore, this partly motives us for this study..

By studying the signal processing methods, the time-domain analysis can only get the rough estimation of crash features. Traditional frequency-domain analysis, i.e. the Fourier Transform (FT), can hardly reflect the relationship between the frequency information and the crash process. The time-frequency analysis is a potential method as an efficient tool for the crash response research. The wavelet Transform (WT) has already been applied in the model validation [1] and vehicle crash studies [2]. However, the selection of mother wavelet is arbitrary. In this paper, the Ensemble Empirical Mode Decomposition (EEMD), a self-adaptive time-frequency analysis method, is used for the analysis of vehicle crash responses. Comparing to other time-frequency analysis method, the EEMD supposes no based signal for decomposition and only based on the properties of original signal. It can be shown that the EEMD has excellent performance in the analysis of crash signals.

The rest of this paper is organized as follows. Section II introduces the physical

model of crashes and related features. In Section III, the theory and properties of EEMD method is reviewed firstly. And then, the crash responses are decomposed by EEMD. The analysis of the crash signals will also be presented in this section. The conclusions are presented in the last section.

B.2 Features of vehicle crash responses

Vehicle crash responses reflect the performance of crashworthiness structures. For the frontal crash, the input impulses work on the head of vehicles and transfer through the whole structure. In this section, some features of vehicle crash responses will be illustrated.

B.2.1 Transfer Features Through Kelvin Structures

Typically, the vehicle structure have two basic characteristics when undergoing deformation: elastic and viscous characteristic. There are different mechanisms which can describe the crash process [3] and Kelvin element is a common one, shown in Fig.B.1. Kelvin element contains a spring and a parallel damper. Although the spring stiffness k and damping coefficient c are not always linear with time when a stress is applied, they can be treated as equivalent parameters k_e and c_e in research. In the crash, the input signal works on the front of Kelvin structure and is transported to end.

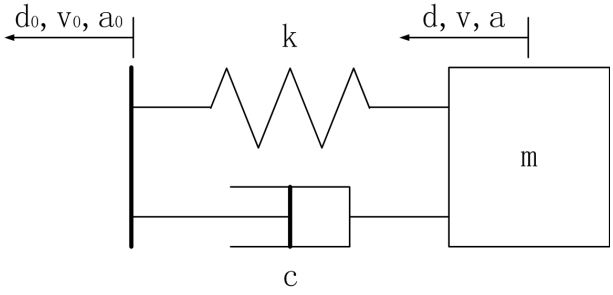

Figure B.1: Kelvin element

Kelvin element contains a spring and a parallel damper. Although the spring stiffness k and damping coefficient c are not always linear with time when a stress is applied, they can be treated as equivalent parameters k_e and c_e in research.

For the system shown in Fig.B.1, the relationship between a_0 and a are studied. For simplicity, the initial status are $v_0(0) = v(0) = 0$, $d_0(0) = d(0) = 0$. The Equation of motion (EOM) are

$$\ddot{d}_2 = F/m_2 = \frac{1}{m_2}\left[k_e\left(d_0 - d\right) + c_e\left(\dot{d}_0 - \dot{d}\right)\right] \tag{B.1}$$

Its characteristic equation looks like

$$s^2 + 2\zeta\omega_e s + \omega_e^2 = 0 \tag{B.2}$$

where $\zeta = \frac{c_e}{2m_2\omega_e}$ and $\omega_e = \sqrt{\frac{k_e}{m_2}}$. The general solution is

$$d = e^{\alpha t}\left[\beta_1 \sin(\omega t) + \beta_2 \cos(\omega t)\right] d_0 \tag{B.3}$$

in which $\alpha = -\zeta\omega_e$, $\omega = \omega_e\sqrt{1-\zeta^2}$. β_1 and β_2 are the constants based on the system conditions. Therefore the transfer function from a_0 to a can be formulated as

$$a = \left[A \sin(\omega t) + B \cos(\omega t)\right] a_0 + C \tag{B.4}$$

where A, B and C are the calculated component which will decay along the time.

For the input $a_0 = p_0 \sin(w_0 t)$, where $\omega \ll w_0$ in real crashes, the response of a manifests the following expression:

$$\begin{aligned} a &= \left[A \sin(\omega t) + B \cos(\omega t)\right](p_0 \sin\omega_0 t) + C \\ &= \frac{1}{2} A p_0 \left[\cos\left((\omega_o + \omega)\, t\right) - \cos\left((\omega_o - \omega)\, t\right)\right] \\ &+ \frac{1}{2} B p_0 \left[\sin\left((\omega_o + \omega)\, t\right) + \sin\left((\omega_o - \omega)\, t\right)\right] + C \\ &\approx P_0 \sin(\omega_0 t) + D \end{aligned} \tag{B.5}$$

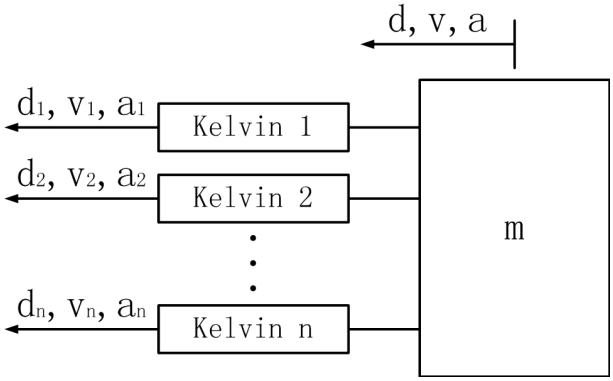

Figure B.2: Parallel system

This means the acceleration of m_2 may keep the frequency feature of input. In a complex system as Fig.B.2, in which Kelvin elements are parallel connected, acceleration of the mass will be the linear combination of input signals.

$$a = \sum_{i=1}^{n} p_i \sin(\omega_i t + \varphi_i) \tag{B.6}$$

The phases φ_i are caused by the start time, initial phase and non-linearity of each inputs.

Fig.B.3 shows the response of a 3-input system, in which $a_1 = -50\sin(10t + \pi/12)$, $a_2 = 10\sin(40\pi t + \pi/3)$ and $a_3 = 10\sin(100\pi t)$ in $t = 0.02 \sim 0.03s$. The corresponding component of each input can be seen clearly in the graph.

For this reason, the time-frequency decomposition is a potential tool for the crash analysis.

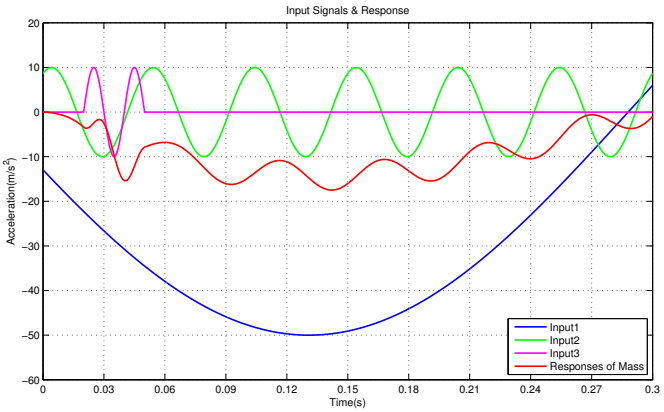

Figure B.3: Demo of a 3-input system

B.2.2 Vehicle Crashes Responses

In most crashes, the body of vehicle experience a large deformation to absorb the energy. Generally, the crash responses can also be split into a "base pulse" and several "shocks" [4]. The base pulse reflects the trend of structure response and is regards as an estimation of crash process in some modelling work, such as [5]. The shocks are high frequency oscillations around zero. They are caused by the deformation or impact of some parts in the vehicle. For example, the collapse of longitudinal beam may generate a periodic vibration. These shocks are sensitive with the uncertainties of start time, frequency and crash condition. The combination of shocks may mask the base pulse and lead unstable of crash features. Fig.B.4 shows the two signals, which are combined by three shocks.

$$\begin{aligned} s_0 &= 200\sin(20\pi t) + 80\sin\left(120\pi t + \frac{\pi}{4}\right) \\ s_1 &= s_0 + 40\sin\left(200\pi t + \frac{\pi}{3}\right) \\ s_2 &= s_0 + 40\sin(180\pi t) \end{aligned} \tag{B.7}$$

There are only small errors on the frequency and phase in the third components of two signals. However, the time of peak points of two signals various from 0.204s to 0.357s.

In addition, the characteristics still various in some content, although the structure of vehicle structure is designed to collapse steadily. For such a non-linear and time-varying system, the crash responses are even more complex An effective scheme is in need to acquire useful information from the crash responses.

B.3 Analysis of Vehicle Crash Responses

B.3.1 Ensemble Empirical Mode Decomposition (EEMD)

Empirical Mode Decomposition (EMD) is proposed by Huang in [6] to analysis the non-linear, non-stationary signals. In EMD, original signals are decomposed into a

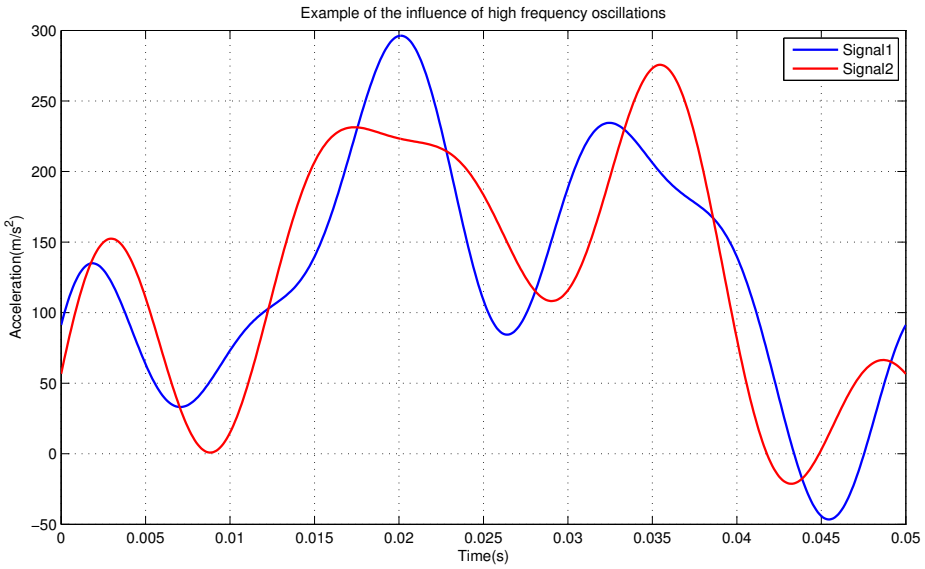

Figure B.4: Example of combined shocks

set of Intrinsic Mode Functions (IMFs), which represent the natural oscillatory mode embedded in the signal. That is

$$x(t) = \sum_{i=1}^{m} s_i(t) \tag{B.8}$$

where each IMF is an amplitude modulated-frequency modulated (AM-FM) signal

$$s_i(t) = A_i(t) \sin(\phi_i(t)) \tag{B.9}$$

Typically, $A_i(t)$ and $\phi_i'(t)$ various slowly and therefore $s_i(t)$ can be regarded as a harmonic signal locally.

Comparing with other time-frequency analysis methods, such as Short-Time Fourier Transform (STFT) and Wavelet Transform (WT), the EMD suppose no template, i.e. the base function, for decomposition. EMD extract the IMFs from original signal $x(t)$ by the shifting process, shown as Algorithm B.1.

Each IMF from EEMD may fall into a specific frequency interval. Without the base function, the EMD avoids the distortion caused by the inconsistence on the templates and original signals. In vehicle crashes, the parameters of structure are non-linear and time-varying, which means the frequency of each component are not constant. For this reason, the advantage of EMD is of great meaning for crash responses analysis.

The Esemble EMD (EEMD) is an improvement of EMD to overcome the mode mixing problem caused by intermittence and noise [7]. In the EEMD method, some trial decompositions of the noised signals are conducted. The noises here is white noise with finite amplitude. The true IMF component is defined as the mean of an ensemble of trials and the added noise will be filtered by EMD process. With this improvement, the EEMD can perform a stable decomposition of original signal.

Algorithm B.1 Shifting Process of EMD

Step1: Set $p = 1$, $h_p(t) = x(t)$; $q = 0$, $r_q(t) = h_p(t)$.
Step2: Extract the local maxima and minima of signal $r_q(t)$ and construct the upper and lower envelops of $r_q(t)$ by interpolation method (generally the cubic spline function).
Step3: Calculate the mean of the upper and lower envelops, recorded as $m_q(t)$. Set $r_{q+1}(t) = r_q(t) - m_q(t)$.
Step4: Calculate the standard division between $r_q(t)$ and $r_{q+1}(t)$: $SD = \sum [r_q(t) - r_{q+1}(t)]^2 \Big/ \sum r_q^2(t)$.
Step5: If $SD \leq threhold$, then stop the shifting process; or else repeat Step 2∼4 until $SD \leq threhold$. After the shifting process, the residual signal $r_i(t)$ is the IMF_p.
Step6: Repeat the shifting process (Step 1∼5) for signal $h_{p+1}(t) = h_p(t) - IMF_p$ to get other IMFs until the IMF_p has only one or no extrema.

B.3.2 Decomposition of Crash Responses

The essential idea of EEMD is to identify the natural oscillation modes according to the scales of fluctuations in the signals and then and decompose the original signals into a series of IMFs. Each signal can be decomposed into $\log_2 N - 1$ IMFs at the most. In most cases, especially for vehicle crash responses, the IMFs are excessively extracted. For this reason, only the high frequency IMFs should be kept and the else are summed to satisfy the definition of a trend. The criterion for IMFs is

$$\int s_i(t)dt \approx 0 \tag{B.10}$$

So the EEMD result of signal $x(t)$ is

$$x(t) = \sum_{i=1}^{n} s_i(t) + T \tag{B.11}$$

where $s_i(t)$ are the IMFs, which is corresponding to the shocks of vehicle crash. And T is the base pulse, i.e. the trend component of crash response.

To illustrate the EEMD performance, a finite element (FE) simulation of Toyota Yaris is employed. In this simulation, Yaris crashed to the rigid wall frontally with the initial velocity of 56km/h. The crash responses of gravity center and engine and their EEMD decompositions are shown in Fig.B.5 and Fig.B.6. These two responses are two typical types of crash signals.

It can be seen in the two figures, the trend signals can roughly present the original responses while the IMFs fluctuate around zero. However, the difference between them is the trend components. The trend of gravity center response is low frequency and exist in the whole crash process, while the trend of engine is a strong pulse in a specified period. Generally, the responses from passenger cabin are similar to the gravity center. In fact, the parts of passenger cabin can be supposed to connected to gravity center rigidly. The shape of engine response is common for the components in the front crumple zone of vehicles.

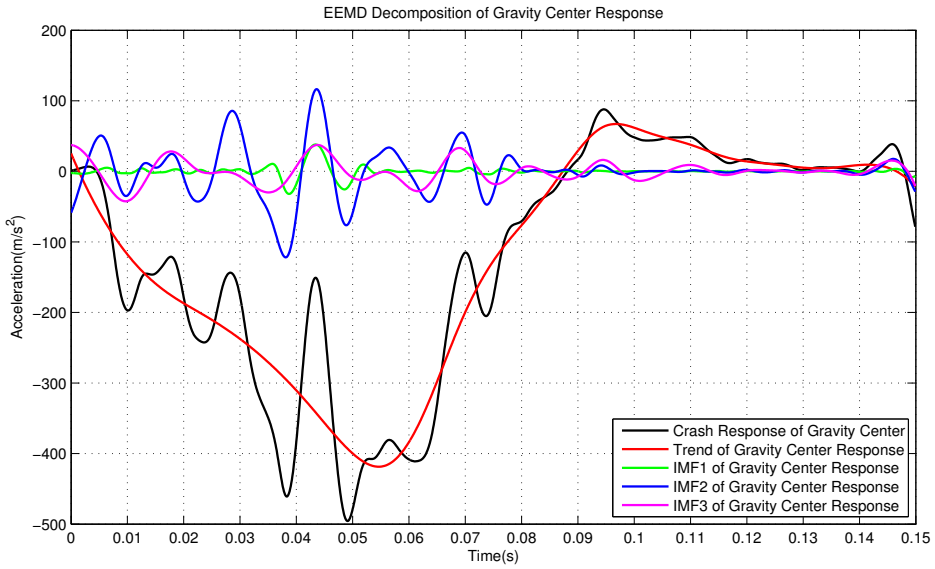

Figure B.5: EEMD result of gravity center response in the 56km/h frontal crash of Toyota Yaris

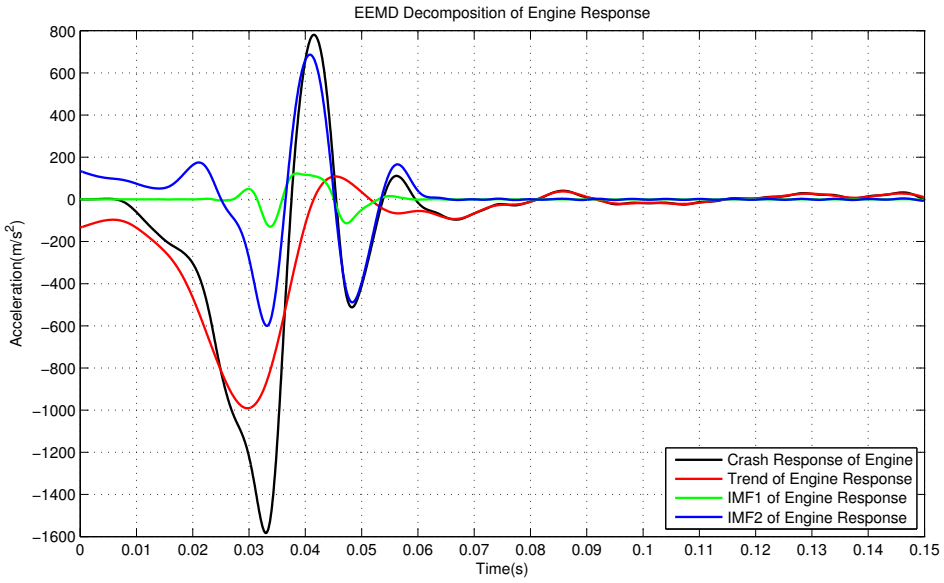

Figure B.6: EEMD result of engine response in the 56km/h frontal crash of Toyota Yaris

B.3.3 Analysis of Trend Components

The trend components are generally used for the identification of global features. Some concerned parameters which characterize car's behavior during a crash are:

1) maximum deceleration a_m and its time t_{am}

2) crash period (from t_{start} to t_{end})

3) maximum dynamic crush d_m and its time t_{dm}

4) equivalent spring stiffness k_e and damping coefficient c_e

By removing the high frequency oscillations form the original signal, the trend can improve the stability of identification of time. Specifically, the time of maximum deceleration can to be identified from the trend T directly as

$$T\left(t_{am}\right) = \min T\left(t\right) \tag{B.12}$$

and the maximum dynamic crush time t_{dm} as

$$d\left(t_{dm}\right) = \max \iint x\left(t\right) \tag{B.13}$$

The crash process can be regarded as the period from t_{start} to t_{end}, which

$$\int_0^{t_{start}} T\left(t\right) dt = \gamma \int_0^{+\infty} T\left(t\right) dt \tag{B.14}$$

$$\int_{t_{end}}^{+\infty} T\left(t\right) dt = \gamma \int_0^{+\infty} T\left(t\right) dt \tag{B.15}$$

Here,the parameter γ is a pre-set threshold and 0.05 is recommended for most cases.

Considering that the magnitude of trend suffers attenuation of original signal in some extent, the identification of amplitude related parameters should be use the original signal. So the maximum deceleration a_m and maximum dynamic crush d_m are calculated as follow.

$$a_m = \min x\left(t\right) \tag{B.16}$$

and

$$d_m = \max d\left(t\right) = \max \iint x\left(t\right) \tag{B.17}$$

There exist some different methods for the identification of the equivalent spring stiffness k_e and damping coefficient c_e. For example, W. Pawlus gives an estimation scheme based on the Kelvin model in [8]. Known the mass of vehicle $m = 1100kg$ and initial velocity $v = 56km/h$, k_e and c_e can be calculated based on previous parameters.

Table B.1 list the identified parameters of gravity center responses.

Table B.1: Parameters of center gravity response in 56km/h frontal crash

No.	Parameters	Identified Value
1	maximum deceleration a_m	$0.0547s$
2	time of maximum deceleration t_{am}	$-495.66m/s^2$
3	start time of crash period t_{start}	$0.0116s$
4	end time of crash period t_{end}	$0.1022s$
5	maximum dynamic crush d_m	$0.62m$
6	time of maximum dynamic crush t_{dm}	$0.0623s$
7	equivalent spring stiffness k_e	$591877N/m$
8	equivalent damping coefficient c_e	$6379Nm/s$

B.3.4 Analysis of High Frequency Components

The high frequency components are mostly generated by the vehicle components in energy absorbing zone and are transferred to the center of gravity through the load path. Similar to the trend component, the IMFs have two style as well: long term oscillations and strong pulses. Generally, the oscillations cannot influence the global trends significantly as they exist the same period with trends. This is especially true when considering the amplitude of them are always much smaller than trend signals. For this reason, only pulse style IMFs are studied in this paper.

The most important pulse is caused by the impact of engine to the firewall before the passenger cabin and then transferred to the center of gravity.

As discussed previously, the frequency feature of engine response will be inherited and the amplitude will be reduced. According to this, the IMFs of two responses are to compared. The instantaneous frequency of $s\,(i)$ can be calculated by Hilbert Transform:

$$f\,(i) = H\,(s)\,(i) \tag{B.18}$$

The average frequency of each IMF are shown in Table B.2.

Table B.2: Comparison of average frequency of IMFs

IMFs.	Average Frequency
IMF1 of Gravity Center Response	134.3Hz
IMF2 of Gravity Center Response	66.3Hz
IMF3 of Gravity Center Response	47.8Hz
IMF1 of Engine Response	120.7Hz
IMF2 of Engine Response	57.1Hz

It shows that the two pulse component of gravity center response have similar frequency with IMFs of engine response. The comparison of two pairs of IMFs are shown in Fig.B.7. The attenuation ration of amplitude are defined as the ratio between the maximum amplitude of two IMFs, i.e.

$$\rho = \frac{\|\sum s_i\|_\infty}{\|\sum s'_i\|_\infty} \tag{B.19}$$

In this example, $\rho = 0.1926$. The small time errors between two pairs of IMFs are small and can be ignored.

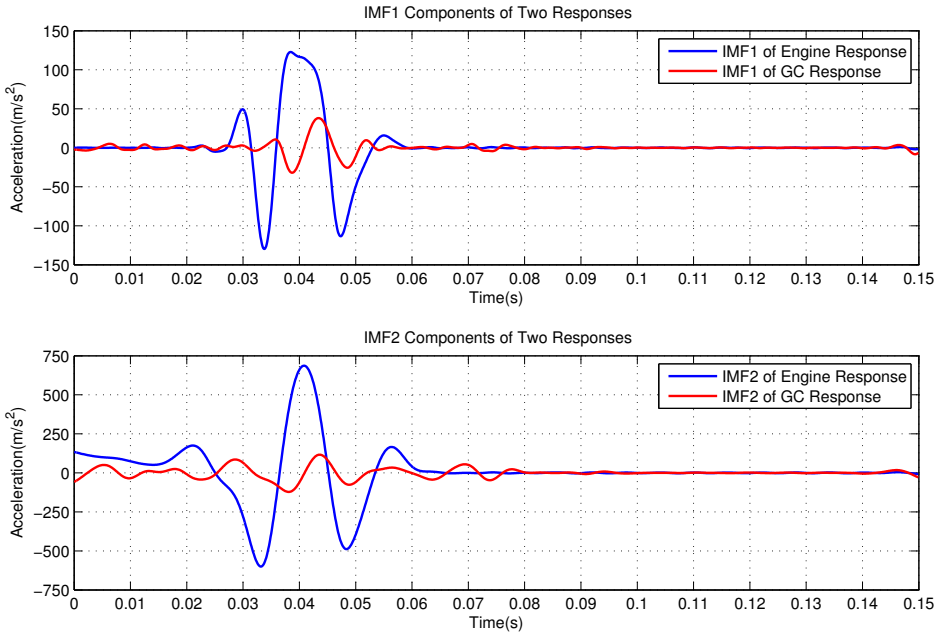

Figure B.7: Comparison of IMFs

In conclusion, the pulse components of engine response are transferred to the center of gravity with an attenuation rate of 0.1926 and no significant delay exists.

B.3.5 Application based on the analysis

The presented analysis can be used in many aspects of vehicle safety research. One of them is the estimation of crashes responses in different. In this subsection, the 40km/h frontal crash of Yaris is employed for illustration.

The estimation of trend component is based on the trend component of 56km/h. The meanifest function is

$$\tilde{T} = \left(\frac{\tilde{v}}{v}\right)^2 T \tag{B.20}$$

And the pulse component from engine is

$$\tilde{s}_{GC}(t) = \rho \tilde{s}_{EC}(t) = \frac{\rho \tilde{v}}{v} s_{EC}(t - t_{delay}) \tag{B.21}$$

where the $t_{delay} = \frac{1}{2}\left(\frac{v}{\tilde{v}} - 1\right)(t_{start} + t_{end})$.

Fig.B.8 shows the estimation of the center gravity response in 40km/h frontal crash. It can be seen that the estimation result can represent the main features of the simulation result.

This example shows that the proposed analysis scheme is effective. The estimation can be therefore used for the design process. More clearly, the designer can adjust the crash response by move the pulse of engine quantify. And modify the base trends of

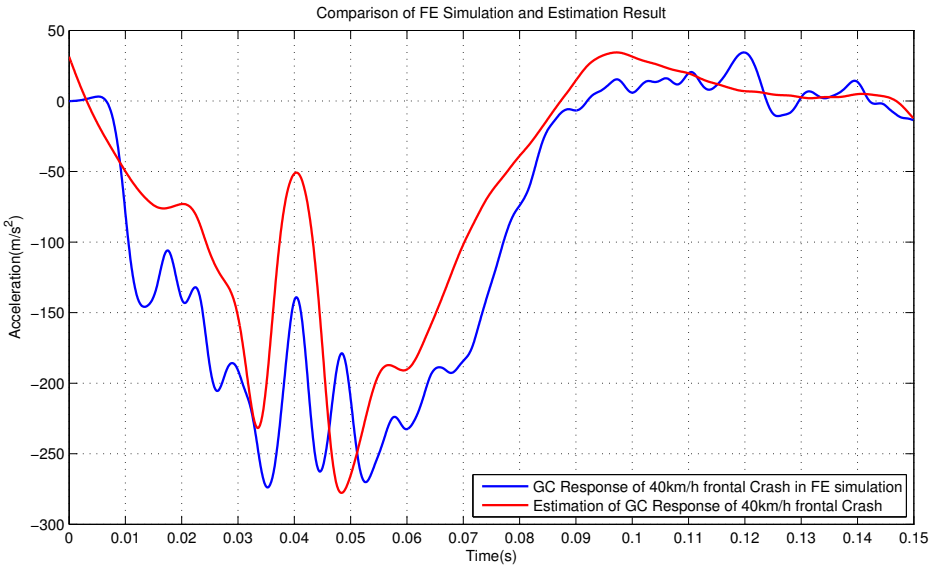

Figure B.8: Comparison of FE simulation and estimation result

crash response of cabin by change the equivalent spring stiffness and damping coefficient.

B.4 Conclusion

This paper proposed an analysis scheme for vehicle crash responses. With the help of EEMD decomposition, the crash responses are split into the trend and IMF signals, which can be analysed separately. The trend component removes the uncertainty and presents the global variation of the crash response. The high frequency oscillations are contained in the IMFs. Especially, the IMFs of crashworthiness structures are transported to the passenger cabin and keep their frequency features. Based on this feature, the crash responses of gravity center contains the component which is decided by the engine crash pulse. The example and estimation demonstrates that the proposed method is an useful tool for vehicle safety researchers.

References

[1] J. R. McCusker, K. Danai, and D. O. Kazmer, "Validation of dynamic models in the time-scale domain," *Journal of Dynamic Systems, Measurement, and Control*, vol. 132, no. 6, pp. 061402:1–9, 2010.

[2] H. R. Karimi and K. G. Robbersmyr, "Signal analysis and performance evaluation of a vehicle crash test with a fixed safety barrier based on haar wavelets," *International Journal of Wavelets, Multiresolution and Information Processing*, vol. 9, no. 01, pp. 131–149, 2011.

[3] W. Pawlus, H. Reza, and K. G. Robbersmyr, "Application of viscoelastic hybrid models to vehicle crash simulation," *International Journal of Crashworthiness*, vol. 16, no. 2, pp. 195–205, 2011.

[4] C. C. Chou, J. Le, P. Chen, and D. Bauch, "Development of CAE simulated crash pulses for airbag sensor algorithm/calibration in frontal impacts," in *Proceedings of 17th International Technical Conference on the Enhanced safety of Vehicles (ESV)*, (Amsterdam, Netherlands), National Highway Traffic Safety Administration, June 2001.

[5] M. Varat and S. E. Husher, "Crash pulse modeling for vehicle safety research," in *Proceedings of 18th International Technical Conference on the Enhanced Safety of Vehicles (ESV)*, no. 501, (Nagoya, Japan), National Highway Traffic Safety Administration, May 2003.

[6] N. E. Huang and Z. Wu, "A review on Hilbert-Huang transform: Method and its applications to geophysical studies," *Reviews of Geophysics*, vol. 46, no. 2, 2008.

[7] Z. Wu and N. E. Huang, "Ensemble empirical mode decomposition: a noise-assisted data analysis method," *Advances in Adaptive Data Analysis*, vol. 1, no. 01, pp. 1–41, 2009.

[8] W. Pawlus, J. E. Nielsen, H. R. Karimi, and K. G. Robbersmyr, "Mathematical modeling and analysis of a vehicle crash," in *Proceedings of The 4th European Computing Conference*, (Bucharest, Romania), April 2010.

Paper C

Analysis of the Relationship between Energy Absorbing Components and Vehicle Crash Response

Zuolong Wei[1], Hamid R. Karimi[1], Kjell G. Robbersmyr[1]

1. Department of Engineering Sciences, University of Agder, PO Box 509, N-4898 Grimstad, Norway

The paper has been published as:

Z. Wei, H. R. Karimi, and K. G. Robbersmyr, "Analysis of the relationship between energy absorbing components and vehicle crash response", *SAE Technical Paper*, Paper No. 2016-01-1541, 2016.

The layout has been revised.

Abstract

The analysis of the vehicle crash performance is of great meaning in the vehicle design process. Due to the complexity of vehicle structures and uncertainty of crashes, the analysis of vehicle crashworthiness is generally depending on the researchers' experiences. In this paper, different deformation modes of energy absorption components are studied. More specifically, the bumper, crash box, the front longitudinal beam and the engine/firewall have different frequency characteristics in the deformation process. According to these characteristics, it is possible to identify the performance of each component in the crash process of assembled structures. To achieve this goal, the crash response of the passenger cabin is decomposed by the time-frequency transformation. Different frequency components exist mainly in a specified period of the crash process. By comparing the features of each period and structural components, the relationship between the components and the crash responses of vehicle is identified. As an example, a frontal crash of Toyota Yaris at 56km/h is introduced for demonstration. The identified performance of each component is consistent with the real crash test and Finite Element simulation, which shows the effectiveness of the proposed method. Another two cases are also given for further discussion. The main advantage of the proposed scheme is that only the passenger cabin deceleration signal is used and the crash performance of a complex structure can be identified accurately. This is helpful in the vehicle design, crash tests as well as accident analysis.

C.1 Introduction

Vehicle crashes cause great number of casualties all over the world. To protect the occupants during crash accidents, crashworthiness is one of the most important abilities of vehicles and widely concerned by the vehicle designer and consumer.

In the design and development process, the crashworthiness of vehicles is always investigated by crash tests. These tests may be conducted either by experiments of prototype or by using computer simulations (e.g. LS-DYNA, RADIOSS). The crash responses, i.e. the accelerations, of different positions in the vehicle structure are recorded. Due to the large deformation of the complex structure and various materials used, these responses are normally nonlinear and non-stationary [1]. In addition, the recorded signals may also suffer the noise and uncertainty in the tests. For this reason, the analysis of these crash responses is a challenging work, which requires experience of engineers. Some work has been published about the analysis of crash responses, such as [2–4]. But most of these work focused on the modeling of responses. To the best of the authors' knowledge, there is no result in open literature about the relationship between crash responses and vehicle structure up to now, which motives us for this study.

This paper proposes a time-frequency analysis scheme, which can extract meaningful information from the crash responses. Comparing with traditional analysis in the frequency domain, the time-frequency transformation can reflect the frequency variations along the time. This enables the time-frequency analysis to investigate the

relationship between the frequency information and the crash process. There are several time-frequency methodologies, such as Short-time Fourier Transform (STFT), Wavelet Transform (WT) and Wigner Distribution Function (WDF). The wavelet transform is a typical one and has already been used in model validation [5] and vehicle crash studies [6, 7]. However, most of these time-frequency techniques are based on the "template" selection. In other words, the original signal is decomposed into the specified base signal and its scaled group signals. For the vehicle crash responses, it is difficult to find a proper base signal and the decomposition is arbitrary. For this reason, the Ensemble Empirical Mode Decomposition (EEMD) is employed in the proposed scheme. The advantage of EEMD is that it is intuitive and adaptive and requires no base signals. With the help of EEMD, the deformation mode of energy absorbing components can be extracted from the crash responses of vehicle gravity center. The proposed scheme offers a normative and quantificational analysis tool for vehicle engineers.

The rest of this paper is organized as follows. First, preliminary knowledge of EEMD is introduced. Second, the deformation process of the vehicle structure in crash is studied. Next Section presents a comprehensive analysis scheme of vehicle crash response in detail. After that, another two cases are studied to validate the effectiveness of the proposed scheme. The conclusions are presented in the last section.

C.2 Ensemble Empirical Mode Decomposition (EEMD)

The crash response of vehicle crash is a typical time histories signal. Although the time domain analysis is of great meaning, the features on frequency domain can provide even more information. Time-frequency decomposition is a powerful tool to investigate the structure of a complex signal. This is especially useful for the signal consisting of several components, such as vehicle crash response.

Ensemble Empirical Mode Decomposition (EEMD) is an adaptive time-frequency analysis algorithm. The Empirical Mode Decomposition (EMD) is the main core of this methodology.

C.2.1 Empirical Mode Decomposition (EMD)

In [8, 9], Huang proposed the Empirical Mode Decomposition (EMD) to analyze the non-linear, non-stationary signals. In EMD, original signals are decomposed into a set of Intrinsic Mode Functions (IMFs), which are amplitude modulated-frequency modulated (AM-FM) signals and oscillate around zero. That is

$$x(t) = \sum_{i=1}^{k} s_i(t) = \sum_{i=1}^{k} A_i(t) \cos(\phi_i(t)) \tag{C.1}$$

with $A_i(t) > 0, \phi_i'(t) > 0$ where $x(t)$ is the original signal, $s_i(t)$ is the i-th Intrinsic Mode Function (IMF), $A_i(t)$ is the amplitude modulated function of the i-th IMF, $\phi_i(t)$ is the frequency modulated function of the i-th IMF.

Typically, $A_i(t)$ and $\phi_i'(t)$ vary much slower than $\phi_i(t)$ itself. So $s_i(t)$ can be locally regarded as a harmonic signal with amplitude $A_i(t)$ and frequency $\phi_i'(t)$. In this condition, the IMFs are "physically meaningful" and can represent the natural oscillatory modes embedded in the original signal.

Although the decomposition in Eq. C.1 is not unique, the EMD is typically applied to decompose a signal into fewer components with mild variations in frequency and amplitude [10]. To achieve this goal, the shifting process is used to construct the decomposition, which is shown in the following:

1) Step 1: Extract the local maxima and minima of signal $x_{i,j}(t)$. Set initial $i = 1$, $j = 1$ and $x_{1,1}(t) = x(t)$.

2) Step 2: Based on the local maxima and minima, construct the upper and lower envelops by an interpolation method (generally the cubic spline function), i.e. $u_j(t)$ and $l_j(t)$.

3) Step 3: Calculate the mean of the upper and lower envelops, that is $m(t) = \frac{u_j(t)+l_j(t)}{2}$. And define $h_j(t) = x_{i,j}(t) - m(t)$.

4) Step 4: Repeat Steps 1$\sim$3 for signal $x_{i,j+1}(t) = h_j(t)$, until $h_j(t)$ fulfills the definition of IMF. The i-th IMF is recorded as $s_i(t) = h_j(t)$.

5) Step 5: Define the residual signal $r_i(t) = x_{i,1}(t) - s_i(t)$. If $r_i(t)$ has only one or no extremum, $r_i(t)$ is the trend component, then stop the shifting process. Otherwise, repeat Steps 1$\sim$4 for signal $r_i(t)$ to get other IMFs. .

The shifting process will remove the low frequency carrier and extract the high frequency IMF at first. As no base function is used for the shifting process, the EMD is more adaptive and suitable for non-stationary signals.

C.2.2 Noise-Assisted Empirical Mode Decomposition

In the EMD process, there exists mode mixing problem, i.e. an IMF includes disparate scales oscillations or a similar scale component exists in different IMFs. The main cause of this problem is the intermittence of signals. Wu and Huang have proposed the Ensemble Empirical Mode Decomposition (EEMD) as a noise-assisted method to solve this problem in [11].

According to the EEMD method, the white noise is added to the original signal and makes the EMD decomposition for the noisy signal. By repeating this process many times, a number sets of IMFs are acquired. The true IMFs are the average of these sets of IMFs. This method is based on the observation that the white noise background will be cancelled out in the time-frequency ensemble mean and only the original signal remains in the final result. The detailed algorithm of the EEMD is:

1) Step 1: Set initial $j = 1$. Create white noise $n_j(t)$ with the given amplitude and add it to the original signals, i.e. $x_j(t) = x(t) + n_j(t)$.

2) Step 2: Decompose the noisy signal $x_j(t)$ by EMD method and get $x_j(t) = \sum_{i=1}^{k} s_{i,j}(t)$. $s_{i,j}(t)$ is the j-th trial of the i-th IMF.

3) Step 3: Repeat Step1$\sim$2 for N times with $j = j + 1$.

4) Step 4: Compute the ensemble mean of the N trials for each IMF as the final result, i.e. $s_i(t) = \frac{1}{N} \sum_{j=1}^{N} s_{i,j}(t)$. .

The amplitude of white noise is suggested as 0.2 of the standard deviation of $x(t)$ [11]. In conclusion, the EEMD can perform a stable decomposition of the original signal with each IMF falls into a specific frequency interval.

C.3 Structural Deformation of Vehicle Crash

In vehicles, the structures are always meticulously designed to achieve the high standard of safety, economy and aesthetics. As an important aspect of passive safety, the crashworthiness should meet strict criteria. Generally speaking, frontal crashes have higher impact velocity than other kinds of accidents. For this reason, the frontal structure of vehicles has comprehensive schemes for energy absorption. In this work, only the crashworthiness of frontal structure is considered. The 2010 Toyota Yaris passenger sedan is used for illustration and its main frontal structure is shown in Figure C.1.

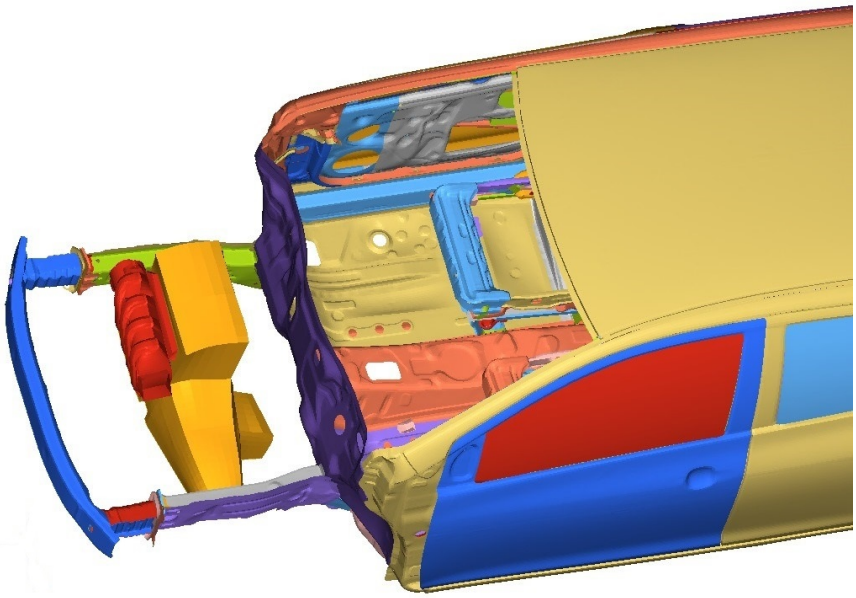

Figure C.1: Main crashworthiness structure of 2010 Toyota Yaris passenger sedan

C.3.1 Energy Absorbing Components

During the crash, the impact load is transmitted from the impact point to the passenger cabin in specified path along the specified load-carrying paths. The energy absorbing

components are arranged as the crumple zone, which will deform and absorb energy to ensure the low deceleration of the passenger cabin. Three typical energy absorbing components are bumper, crash box and frontal longitudinal beam, as shown in Figure C.1.

1) Bumper: it is a reinforcement bar made of metal, composite material or plastic and mainly used for low speed crashes. The bumpers of recent cars are also considered to protect the pedestrian.

2) Crash box: crash box is a thin-walled structure equipped between the bumper and longitudinal beam. In crashes, it is expected to be collapsed prior to the other component. To achieve this goal, some crumple points, such as ditches and crash beads, are set on the crash box. The purpose of the crash box is to absorb energy as well as reduce repair costs.

3) Frontal longitudinal beam: most longitudinal beams are also thin-walled structure with a specified cross-section shape. However, it is generally longer and stronger than crash boxes. Different from the stable collapse mode of crash boxes, the longitudinal beam may bend and not fully compressed.

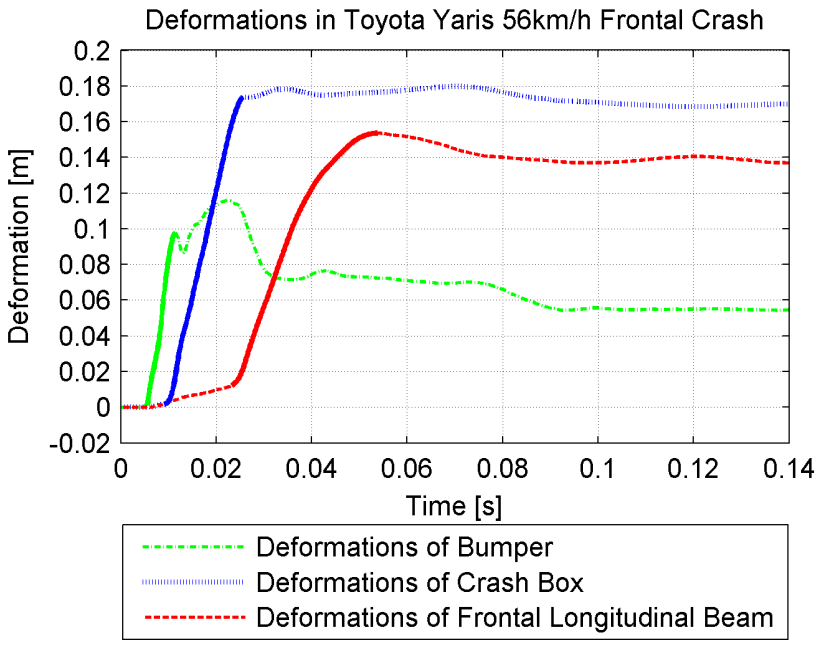

Figure C.2: Deformations in Toyota Yaris 56km/h frontal crash

In most cases, the deformations of these components are not occurred at the same time, but in the order from front to rear. For example, a Toyota Yaris crashed into a rigid wall in 56 km/h in a finite element simulation. The compression of each component is shown in Figure C.2.

It can be seen that the bumper compression mainly happened in 0.006 0.011s and the deformation of crash boxes followed immediately in 0.01∼0.024s. While in this period, the frontal longitudinal beams were only slightly crushed. The deforming process of

longitudinal beams was 0.024∼0.054s. The deformation period of each component is marked by bold in Figure C.2.

In addition, the release process can also be seen in Figure 2. After fully crushed (the largest deformation) at 0.054s, the longitudinal beams released immediately until 0.074s. The release length was about 0.013m. However, the crash boxes had very small release length in 0.074∼0.09s. At the same time, the bumper started releasing.

C.3.2 Engine and Firewall

Although not energy absorbing component, the engine and firewall of a vehicle play important roles in the crash process. The firewall is a separator between the engine compartment and the passenger cabin. It is also a strong component to minimize the intrusion of the passenger cabin.

There are many components located in the vehicle front space and the engine is one of them. Influenced by other components (not shown in Figure C.1), the movement of the engine is complex in the crash. Especially, the engine will pitch a lot during the crash. In other words, the movements of engine top and bottom are not the same.

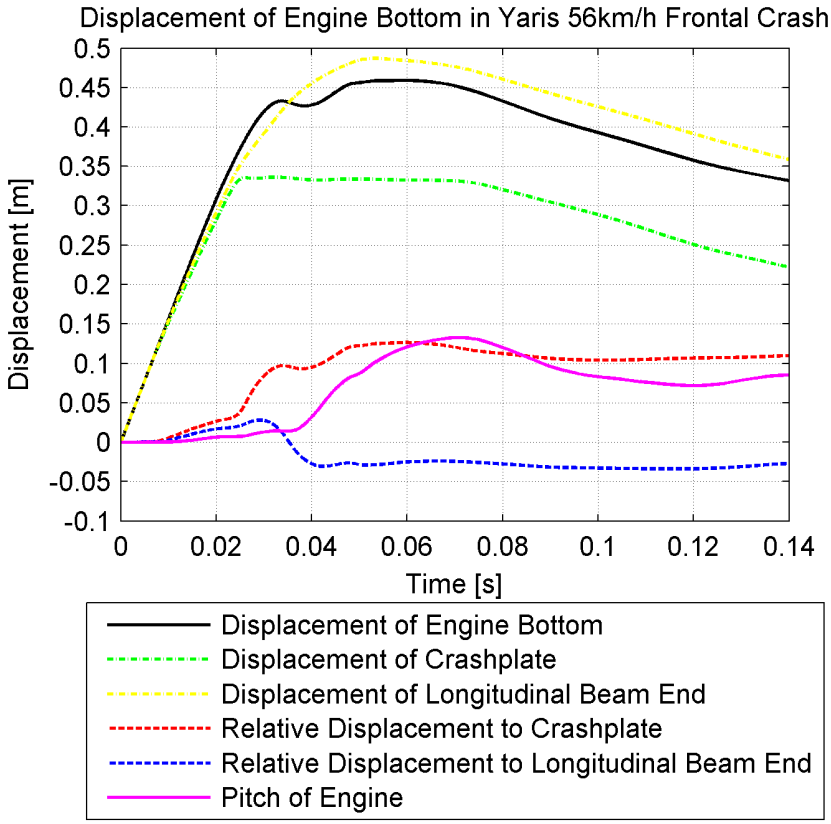

Figure C.3: Displacement of engine bottom in Toyota Yaris 56km/h frontal crash.

Figure C.3 shows displacement of engine bottom in the crash. The crash plate refers to the connection between the crash box and longitudinal beam. The pitch of the engine is defined by the longitude distance between the top and bottom of the engine.

As shown in Figure C.3, the significant pitch of engine started at about 0.037s and reached the biggest value at about 0.07s. The relative displacement of engine bottom to the crash plate (the red dash line) shows that the engine continued moving ahead during 0.024∼0.034s, after the crash boxes were fully compressed.

During 0.034∼0.038s, the engine bottom moved in reverse slightly. At about 0.035s, the difference in displacement between the engine bottom and the end of longitudinal beam was zero. Then the gap between engine bottom and firewall started to be compressed. This indicates that the reaction force between engine and firewall occurred and may lead the deceleration of vehicle cabin to increase suddenly.

After 0.038s, engine bottom kept going ahead until 0.06s, as shown by the black line in Figure C.3. This indicates the space between the engine and bumper was compressed. For this reason, the reaction force between the engine and firewall reached the biggest around 0.038s and consequently the cabin experienced a peak of deceleration.

In conclusion, the deceleration of the passenger cabin was decided by the bumper, crash box, frontal longitudinal beam and engine together. The first three components may work in order and combine the whole crash period, while the engine may only have significant influence in about 0.034∼0.06s period.

C.4 EEMD Aided Analysis of Crash Responses

Although the simulation technology is widely used in vehicle crash studies, the crashworthiness analysis is still mainly based on the full car crash tests [12]. Different with the simulation, there are generally not so many signals can be recorded in crash tests. So it is important for engineers to mine useful information from limited signals. As discussed previously, the crash response of passenger cabin is tightly associated with the structural performance. Therefore, this section proposes a novel scheme to acquire meaningful information by analysis the cabin response. In most crashes, the response of the passenger cabin is recorded by a high frequency accelerometer located at the vehicle mass center, the bottom of B pillar or the cross-member of rear seat. For illustration, the response of vehicle mass center in the previous simulation is used.

C.4.1 EEMD of Cabin Response

According to the algorithm of EEMD, the stop criterion is that the residual has only one or no extremum. However, the original signal is always over decomposed in vehicle crash analysis. To make a proper decomposition, the trend is defined as the sum of some low frequency IMFs, i.e.

$$T(t) = \sum_{i=m+1}^{k} s_i(t) \tag{C.2}$$

where $T(t)$ is trend of original signal and m is number of high frequency IMFs. The criterion of $T(t)$ and m is that for $1 \leqslant i \leqslant m$.

$$\int s_i(t)\,dt \leqslant thr * \int x(t)\,dt \tag{C.3}$$

where thr is the threshold and a recommended value is 5%.

So the original signal can be rewritten as

$$x(t) = \sum_{i=1}^{m} s_i(t) + T(t) \tag{C.4}$$

The EEMD result of cabin response in previous simulation is shown in Figure C.4.

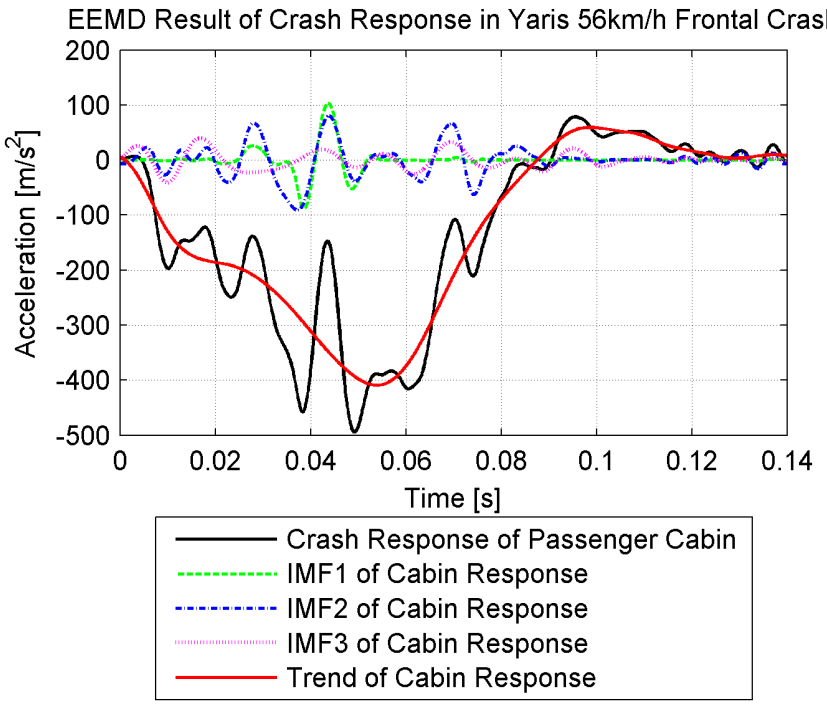

Figure C.4: EEMD result of passenger cabin response in Toyota Yaris 56km/h frontal crash

By checking the original response, some points can be noted as follows:

1) In $0.005sim0.01$s, the response fell rapidly and had no oscillations. This is consistent with the discussion in previous as only the bumper is compressed in this period. As no other structure was crushed, the deceleration increased steadily and suffered no disturbance.

2) After 0.01s, the high frequency oscillations occurred. Although the trend of deceleration can be roughly seen, it is difficult to identify the important time points (i.e. the time when deformations start or stop).

3) A peak of deceleration existed at about 0.038s. The previous analysis is validated. However, the working period of the engine is still not clearly shown.

With the help of EEMD, the trend of original response is extracted. As shown in Figure C.4, the trend signal can represent the variance of the original response well. High frequency oscillations are removed and presented as IMFs. To make an effective analysis, the trend signal and IMFs will be studied respectively in the following part.

C.4.2 Analysis of Trend Component

The trend is the low frequency component of the original response. It can be clearly divided into 4 stages: first increase period, steady period, second increase period and decline period. Obviously, the first three stages are corresponding to the deformation process of bumper, crash box and longitudinal beam respectively. And the last stage is the release process. The time points of each stage can be identified by the second derivative of the trend signal (i.e. $ddT(t)$), as shown in Figure C.5. For clearance, the differential and double differential signals are linear scaled on value.

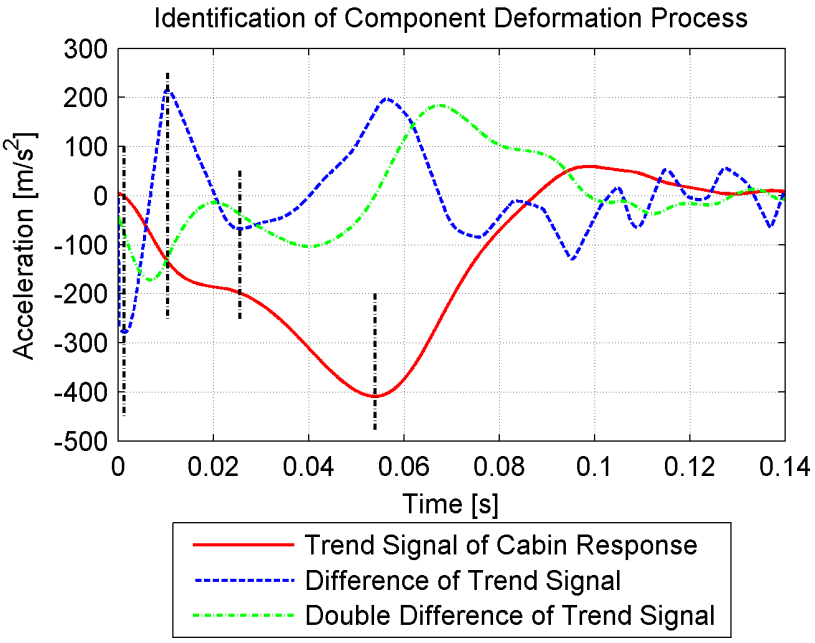

Figure C.5: Identification of component deformation process in Toyota Yaris 56km/h frontal crash.

The identified results are listed in Table C.1. Comparing with the analysis in Section C.3, there is only small error on the start time of bumper crush.

Table C.1: Identified period of component deformation in Toyota Yaris 56km/h frontal crash

Component	Deformation Period
Bumper	0.0013 0.0104s
Crash Box	0.0104 0.0256s
Frontal Longitudinal Beam	0.0256 0.0539s

C.4.3 Analysis of IMF Components

Different with the energy absorbing components, some inner structures, such as the engine, is not designed to control the deceleration of vehicle. So the influence of it cannot be reflected in the trend of crash response. On the other hand, however, the

performance of the engine may lead an extra pulse of crash response, which should be considered in the design procedure. To solve this problem, the features of each component deformation in frequency domain are studied in this section.

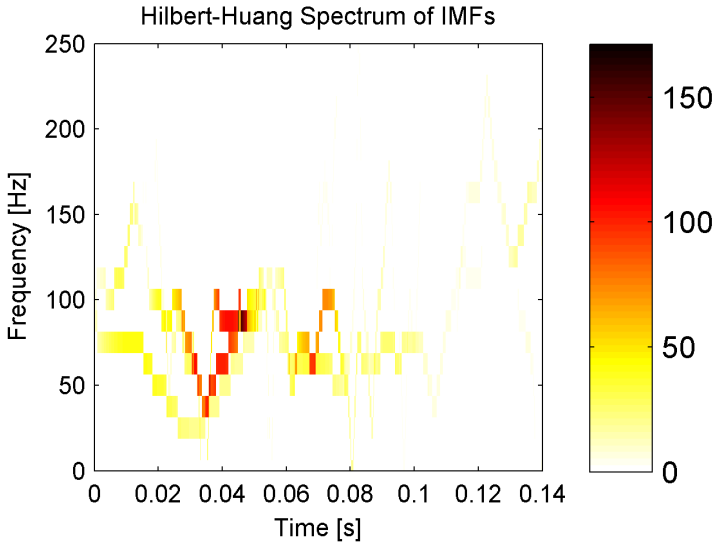

Figure C.6: Time-frequency representation of IMFs

Figure C.6 is the Hilbert-Huang representation of the high frequency oscillations. The color indicates the amplitude of signals, as well as the energy that can be seen mainly between 20∼160Hz. The whole crash process last between 0∼0.1s, when the energy of oscillations is significantly high. The highest energy occurs at 0.465s, same with the peak point of cabin deceleration. To investigate the features of each component, the Hilbert-Huang spectrum of every IMF is studied. Figures C.7∼C.9 are corresponding to IMF1∼IMF3 respectively.

By comparing with result of trend analysis, some conclusions can be drawn as follows:

1) The energy of IMF1 focused in about 0.024∼0.055s and nearly zero in the other time. This indicates that IMF1 is corresponding to the engine, which moved significantly in a short period.

2) The energy of IMF2 existed in the whole crash period. In addition, in the period of 0.023∼0.051s, the amplitude was higher than any other time. This matches the deformation period of frontal longitudinal beam well.

3) Similar with the IMF2, the amplitude of IMF3 was significant all the time. However, the highest amplitude occurred from 0.003s to 0.025s, just before the IMF2. So IMF3 reflects the oscillations caused by crash boxes.

4) No IMF is corresponding to the bumper due to no significant oscillations caused by the bumper. This is consistent with the observation of original crash response.

5) In Figure C.7, 0.033∼0.0353s is a singular period. Generally, this indicates that an "interruption" occurred. The "interruption" is mainly caused by the sudden structure changes, such as impact between components, failure of welding spots

and active structure changes. In this case, it can be regarded as the instruction (deformation) of the firewall caused by the engine. Together with previous conclusion (item 1)), the duration of engine and firewall connection was about 0.034 0.055, close to the finite element result (0.038∼0.06s).

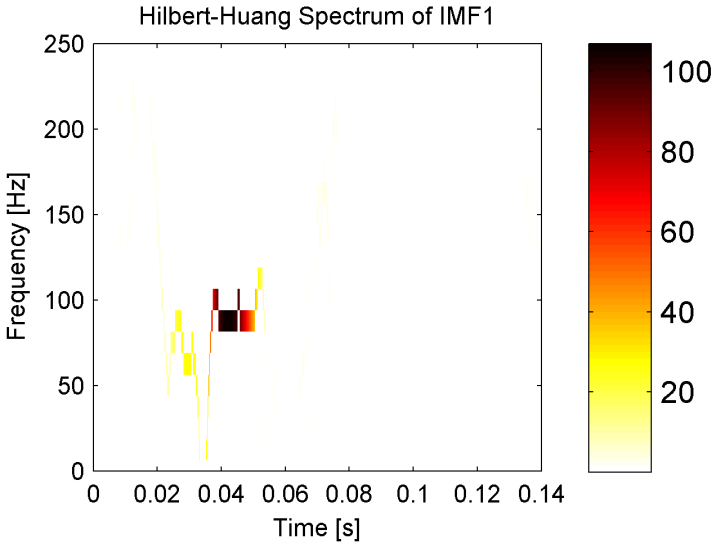

Figure C.7: Time-frequency representation of IMF1, which is corresponding to the engine

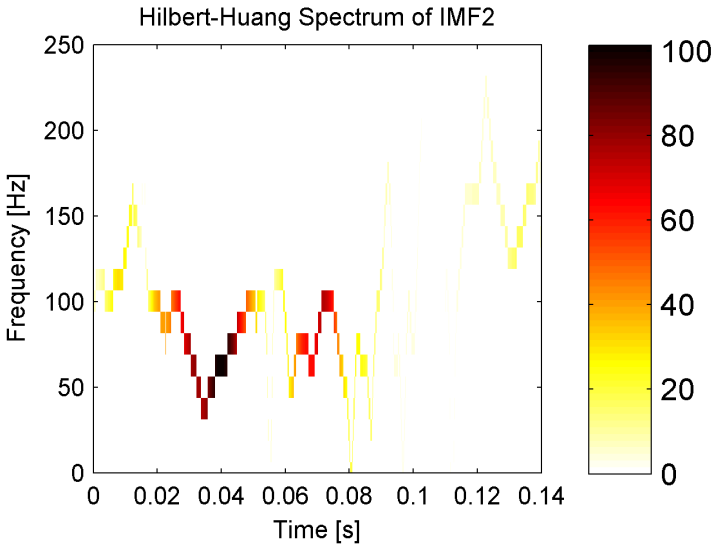

Figure C.8: Time-frequency representation of IMF2, which is corresponding to frontal longitudinal beams

These analyses show that the component deformation and the oscillations caused by them are recorded by IMFs. The deformation process can therefore be identified by the frequency information of IMFs. The results from IMFs and trend are consistent with each other. Especially, the performance of the engine can also be investigated by IMFs.

The features of the components are summarized here. First, the frequency of the engine IMF is higher than the crash box and longitudinal beam. Second, the amplitude of engine IMF may only exist in a short period, as the engine may not contact with

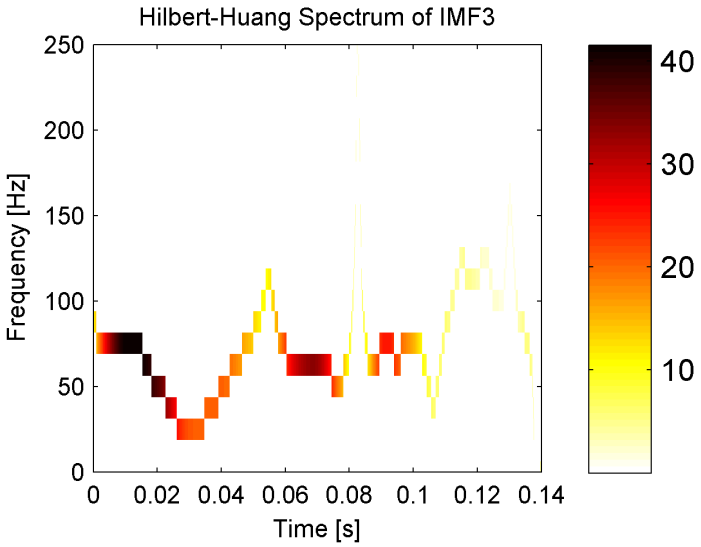

Figure C.9: Time-frequency representation of IMF3, which is corresponding to crash boxes

the cabin/firewall all the time. In addition, the amplitude of the IMF related to the longitudinal beam is much higher than the IMF of crash box. Finally, the high amplitude period of longitudinal beam may be just after the crash box. The further analysis should mainly base on these features.

C.5 Case Studies

Vehicle crashes are complex and various. A good analysis tool is required to keep effective for most cases. To check the performance of the proposed scheme, another two crashes are studied in this section and further discussion will also be given. For each case, the finite element model of Toyota Yaris will be used for the simulations, where the cabin responses come from. The analysis process are only based on the features concluded previously. The analysis result will be checked by the simulations.

C.5.1 Case1: Low Speed Crash

In this case, Yaris crashed to the rigid wall at 32km/h. By checking the simulation, some key points about the crash can be found.

1) The bumper deformed in 0.098∼0.0194s and finally reached the biggest deformation. At about 0.07s, the bumper started to release.

2) The crash boxes were crumpled since 0.0186s. The deformation of crash boxes stop at 0.05s. The kinetic energy of vehicle is absorbed completely and the crash boxes were not fully compressed.

3) There was no big deformation of the longitudinal beam and the space around engine was not compressed. For this reason, the influence of cabin response from the engine was not significant.

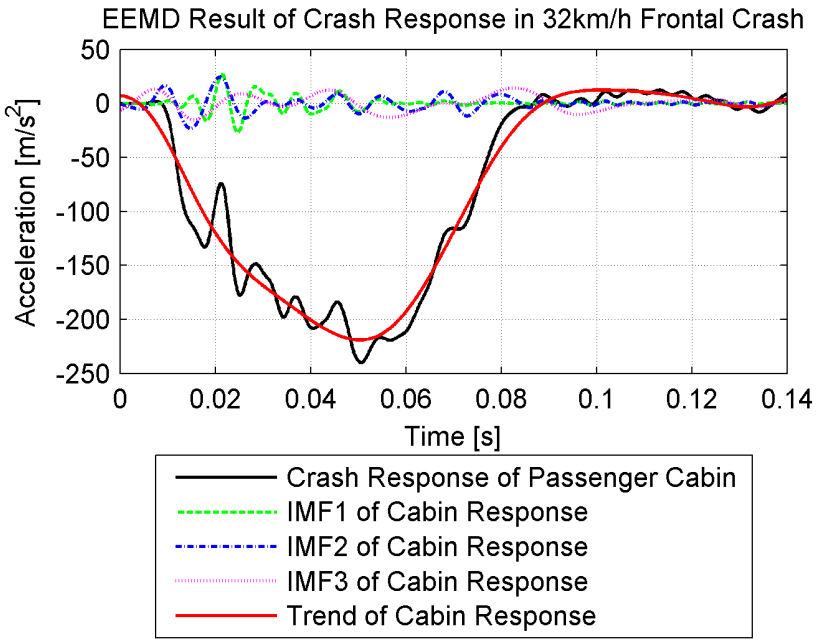

Figure C.10: EEMD result of passenger cabin response in Toyota Yaris 32km/h frontal crash

Figure C.10 is the EEMD result of the cabin response. The trend signal has only two turns before the peak time. This refers to only two components, i.e. bumper and crash boxes are compressed in this crash. The deforming periods are 0.0052∼0.0203s and 0.0203∼0.0504s respectively. The Hilbert-Huang Spectrum of three IMFs are shown in Figure C.11.

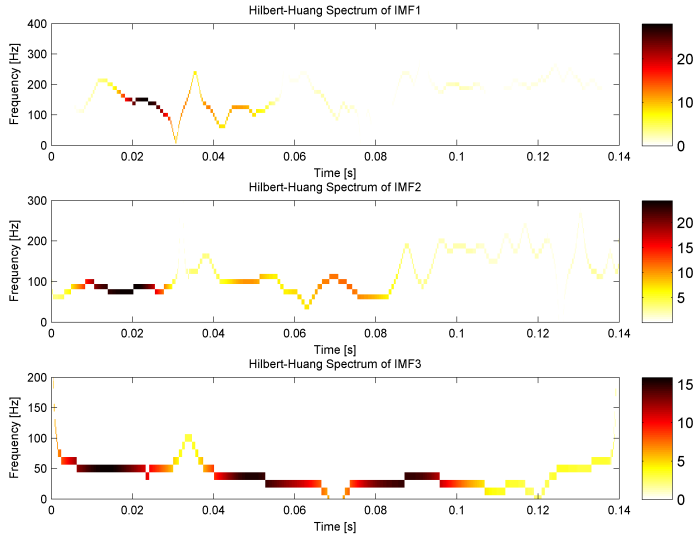

Figure C.11: Time-frequency representation of IMFs in Toyota Yaris 32km/h frontal crash

Different with the previous example, the crash in this case is low speed and the oscillations are therefore small. This makes some small amplitude "noise", which is caused by other part of vehicle, are extracted as IMF signal. The main feature of these "noise"

is that the amplitude of it keep steady in the whole crash, as the IMF3 in this case. The energy of IMF1 and IMF2 are focused on 0.0183∼0.0482s and 0.0075∼0.0284s respectively. The identified results from Hilbert-Spectrum are acceptable but not as good as those from trend signal.

C.5.2 Case2: Oblique Crash

To show the effectiveness of the proposed scheme in complex crash condition, an oblique crash case will be studied in this section. The configuration of the crash is shown in Figure C.12. The initial velocity of Yaris is 56km/h and the oblique angle is 10 degrees.

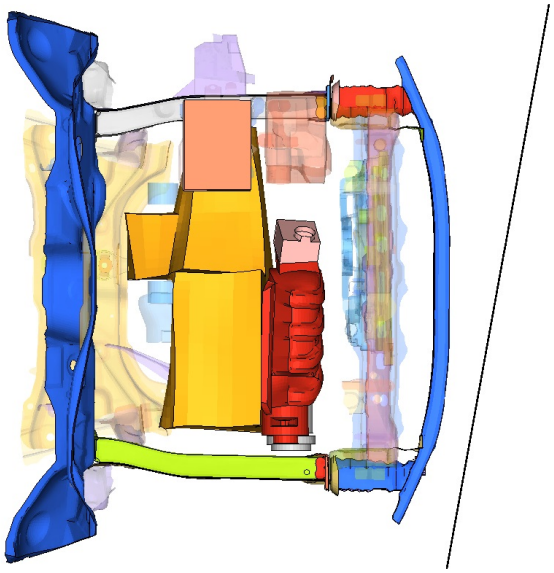

Figure C.12: Crash configuration of oblique crash case

Because the oblique barrier, the deformation periods of the components in both sides are different. Some components may fail to be fully compressed. By check the simulation result, the whole crash process are list in Table C.2.

Table C.2: Deformation process of each component in Case2.

Component	Deformation Period
Right Crash Box	0.006 0.0298s
Right Longitudinal Beam	0.0204 0.0478s
Left Bumper	0.0056 0.021s
Left Crash Box	0.016 0.0337s
Left Longitudinal Beam	0.0313 0.0590s
Engine	0.033 0.0455s

Figure C.13 is the crash response of passenger cabin and its EEMD result. Obviously, due to the complexity of this case, more IMFs are extracted and consequently there is

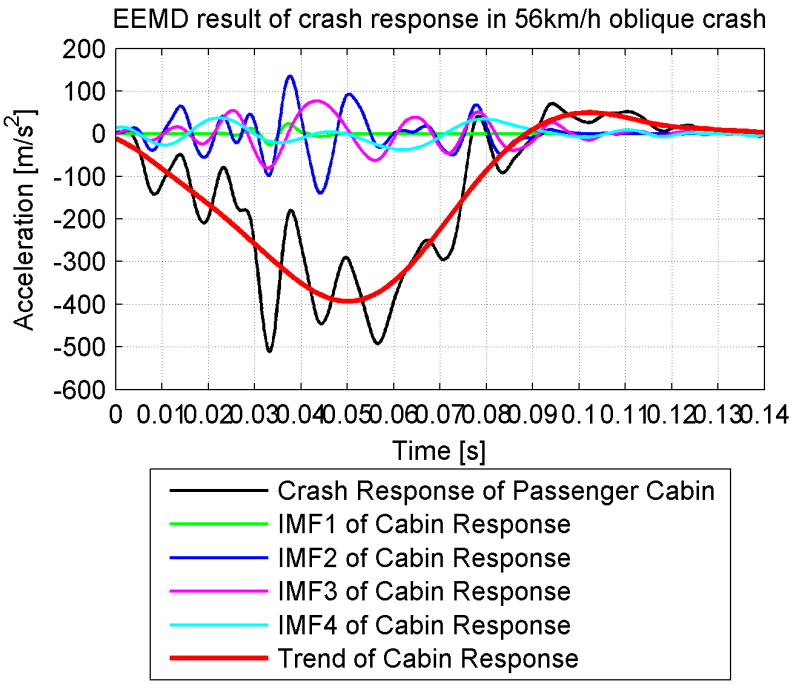

Figure C.13: EEMD result of passenger cabin response in Toyota Yaris 56km/h oblique crash

no useful information in the trend signal. It is impossible to identify the crash details only by the trend signal in this case.

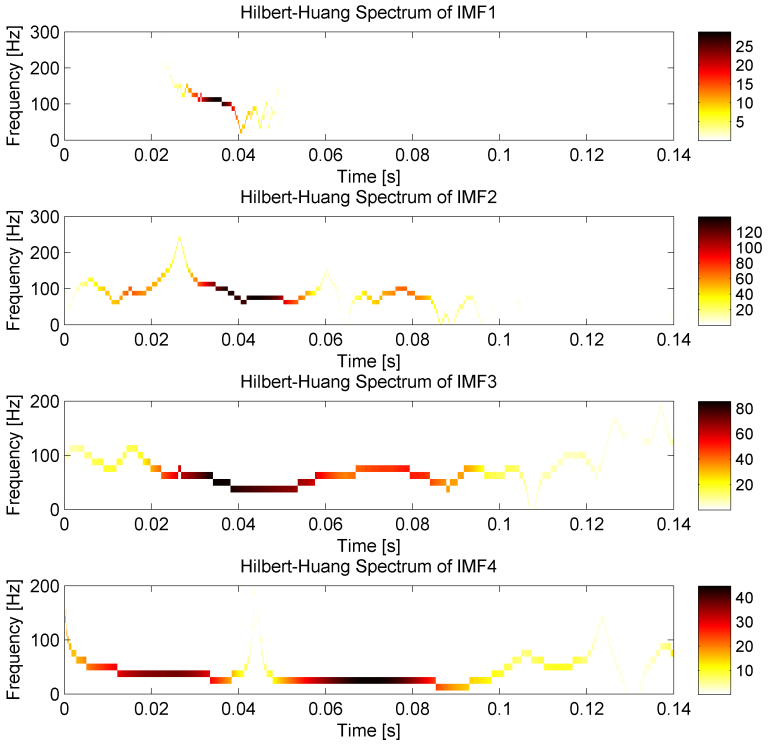

Figure C.14: Time-frequency representation of IMFs in Toyota Yaris 56km/h oblique crash

Figure C.14 shows the Time-frequency representation of the four IMFs. IMF only exist in the period of 0.0292∼0.0434s. This refers that the IMF1 is corresponding to the engine. IMF2 and IMF3 have high amplitude and lower frequency (than engine). So they are corresponding to the longitude beams. Especially, the high amplitude period of IMF2 is 0.0304∼0.0564s, which is late than IMF3. IMF2 is therefore corresponding to the left longitudinal beam and IMF3 to the right one. IMF3 is mainly started at 0.0216s and ended at 0.061s. The first part of IMF4 is 0.0045∼0.0364s, which is just before the period of longitudinal beams. So the first part of IMF4 is related to the both crash boxes. The second part of IMF4 is very low frequency and low amplitude. It may refer to the release process of the whole structure.

Comparing with Table C.2, there is only an error, which is about the end time of IMF3 (right longitude beam). The rest analyses are accurate and meaningful. The error of IMF3 may be caused by the mode mixing problem. A good decomposition is of great importance in the analysis.

C.6 Conclusion

This work presented a novel scheme for analysis of vehicle crash responses. The basic idea is that the deceleration signal of passenger cabin is decided by the deformable structure of the vehicle. Each component in the structure has unique deformation mode and happens at a specified period. When these deformations start or end, the crash response is consequently influenced. The time-frequency transform can scan the changes and locate the time. EEMD is a time-frequency analysis algorithm suitable for the crash responses, which are nonlinear and non-stationary. It can decompose the responses effectively into the low frequency trend and some high frequency oscillations. Both of them can be used for the crash process identification. Especially, the IMFs based scheme is more effective in complex condition than the trend based scheme. The proposed scheme enables engineers to make an objective and quantitative analysis of crashes effectively. This is helpful for the designer to make a target-oriented improvement of crashworthiness design.

References

[1] A. Ferrer and E. Infantes, "Load cell wall analysis in oblique tests," *SAE Technical Paper 2015-01-1479*, 2015.

[2] J. Kral, "Yet another look at crash pulse analysis," *SAE Technical Paper 2006-01-0958*, 2006.

[3] Z. Wei, H. R. Karimi, and K. G. Robbersmyr, "A model of vehicle-fixed barrier frontal crash and its application in the estimation of crash kinematics," in *24th International Technical Conference on the Enhanced Safety of Vehicles (ESV)*, no. 15-0161, 2015.

[4] W. Pawlus, H. R. Karimi, and K. G. Robbersmyr, "Investigation of vehicle crash modeling techniques: theory and application," *The International Journal of Advanced Manufacturing Technology*, vol. 70, no. 5-8, pp. 965–993, 2014.

[5] J. R. McCusker, K. Danai, and D. O. Kazmer, "Validation of dynamic models in the time-scale domain," *Journal of Dynamic Systems, Measurement, and Control*, vol. 132, no. 6, p. 061402, 2010.

[6] H. R. Karimi and K. G. Robbersmyr, "Signal analysis and performance evaluation of a vehicle crash test with a fixed safety barrier based on haar wavelets," *International Journal of Wavelets, Multiresolution and Information Processing*, vol. 9, no. 01, pp. 131–149, 2011.

[7] D. M. ONCHIŞ and E. M. SUArez SANchez, "The flexible gabor-wavelet transform for car crash signal analysis," *International Journal of Wavelets, Multiresolution and Information Processing*, vol. 7, no. 04, pp. 481–490, 2009.

[8] N. E. Huang, Z. Shen, S. R. Long, M. C. Wu, H. H. Shih, Q. Zheng, N.-C. Yen, C. C. Tung, and H. H. Liu, "The empirical mode decomposition and the Hilbert spectrum for nonlinear and non-stationary time series analysis," *Proceedings of the Royal Society of London A: Mathematical, Physical and Engineering Sciences*, vol. 454, no. 1971, pp. 903–995, 1998.

[9] N. E. Huang and Z. Wu, "A review on hilbert-huang transform: Method and its applications to geophysical studies," *Reviews of Geophysics*, vol. 46, no. 2, 2008.

[10] I. Daubechies, J. Lu, and H.-T. Wu, "Synchrosqueezed wavelet transforms: an empirical mode decomposition-like tool," *Applied and computational harmonic analysis*, vol. 30, no. 2, pp. 243–261, 2011.

[11] Z. Wu and N. E. Huang, "Ensemble empirical mode decomposition: a noise-assisted data analysis method," *Advances in adaptive data analysis*, vol. 1, no. 01, pp. 1–41, 2009.

[12] S. R. Wu and N. Saha, "Some challenges to crashworthiness analysis," *SAE Technical Paper 2006-01-0669*, 2006.

Paper D

Data-based Modeling and Estimation of Vehicle Crash Processes in Frontal Fixed-barrier Crashes

Zuolong Wei[1], Kjell G. Robbersmyr[1], Hamid R. Karimi[2]

1. Department of Engineering Sciences, University of Agder, PO Box 509, N-4898 Grimstad, Norway
2. Department of Mechanical Engineering, Politecnico di Milano, 20156 Milan, Italy

The paper has been submitted as:

Z. Wei, K. G. Robbersmyr, and H. R. Karimi, "Data-based modeling and estimation of vehicle crash processes in frontal fixed-barrier crashes", *Journal of the Franklin Institute*, 2016.

The layout has been revised.

Abstract

As a complex process, vehicle crash is challenging to be described and estimated mathematically. Although different mathematical models are developed, it is still difficult to balance the complexity of models and the performance of estimation. The aim of this work is to propose a novel scheme to model and estimate the processes of vehicle-barrier frontal crashes. In this work, a piecewise model structure is predefined to represent the accelerations of vehicle in frontal crashes. Each segment in the model is corresponding to the energy absorbing component in the crashworthiness structure. With the help of Ensemble Empirical Mode Decomposition (EEMD), a robust scheme is proposed for parameter identification. By adjusting the model structure and parameters according to the initial velocity, crash processes in different conditions are estimated effectively. The estimation results exhibit good agreement with finite element (FE) simulations in three different cases. It is shown that, the proposed model keeps low complexity. Furthermore, the structure information of vehicle is involved in improving the accuracy and ability of crash estimation.

Keywords: *vehicle crash, crashworthiness structure, piecewise model, crash process estimation, Ensemble Empirical Mode Decomposition(EEMD)*

D.1 Introduction

Vehicle crashes are the main traffic accidents and cause great casualties all over the world. Although some manufacturers put forward the scope of no accident, the passive safety, especially the crashworthiness design, is still serving as the base of vehicle safety and therefore widely concerned by vehicle engineers and researchers.

In this area, modeling of vehicle crash remains a topic of interest in both academia and industry. Up to now, many kinds of models are developed to describe or estimate the crash process. These models fall into two categories. The first category includes the lumped parameter models [1, 2], hybrid models [3], multi-body models [4] and finite element (FE) models [5], which can be used to represent the vehicle body for the simulations of vehicle crashes. The essential difference of these models are the details involved in the vehicle model. The lumped parameter models use mass, spring and damper to describe the structure only, while the finite element models contains the geometry, material and connection of every component in the vehicle. Although the accuracy are improved with more information involved in the models, the computation load will increase significantly accordingly. This is especially true for the detailed finite element models.

The second category of models will focus on the crash acceleration signals and describe the vehicle movement directly, such as the crash pulse model proposed in [6, 7]. With simple mathematical functions, these models can only offer rough representations of crashes process. Especially, these models ignore the relationship between the vehicle structure and crash responses [8]. Consequently, it is difficult to give an reasonable estimation of parameter variance in different crash scenarios. To solve this problem, the scope of this work is to build a surrogate model of crash process based on the crash

test data, which is corresponding to vehicle structure.

In the design of crashworthiness structure, different components (e.g. bumper, crash boxes and frontal longitudinal beams)are integrated to absorb the energy during crashes. Inspired by [9], each component has a specified crash mode, which can be observed using the crash signals. As illustrated in [10], the crash process can be investigated by time-frequency analysis. The relationship between crashworthiness components and crash signals are consequently identified. Based on relationship, a structure related piecewise model of vehicle crash signal was proposed in this work. This model represents the acceleration signal of the vehicle gravity center and each segment in the model is corresponding to the deformation process of an energy absorbing component. The parameters of model are identified from the measured data of 56km/h frontal crash test. In addition, the frontal crashes in different velocities are also studied in this work. An integrated scheme is proposed to estimate the variance of model structure and parameters. The main contributions of this work are threefold: 1) The piecewise model structure combines the knowledge of vehicle structure and crash signals properly. 2) An EEMD aided scheme is proposed for the identification of model parameters, which is based on the crash test data only. 3) The crashes are classified into three catalogues and the crash processes of them are estimated separately.

The rest of this paper is organized as follows. Section D.2 investigates the crashworthiness structure and proposes a piecewise model to describe the vehicle crash. In Section D.3, the identification scheme of the piecewise model is given in detail. The frontal crashes with different velocities are studied and estimated in the next section. To demonstrate the effectiveness of the proposed scheme, three cases are also employed. The conclusions are presented in the last section.

D.2 Model Structure of Vehicle Crash Response

Currently, the most used models in vehicle safety area based on the numerical technology, which obtains the models behavior through time-stepping procedure and generally has large computation load. Although model reduction is highly considered in engineering [11] and some work have been done for vehicle crash, such as [12, 13], it is difficult to reducing the model complexity significantly. For this reason, some researchers attempted to use mathematics formulations, such as sine and wavelet signals, to describe the crash acceleration. However, they are not accurate enough and lack of physical interpretation. To overcome these problems, a piecewise model for vehicle crashes is proposed in this section.

D.2.1 Crashworthiness Components of Vehicle

In modern vehicles, the crashworthiness structure is meticulously designed to improve the passive safety. The impact load is transmitted through the specified load-carrying paths. In most passenger vehicles, the bumper, crash boxes and front longitudinal beams are the main energy absorbing components, which afford more than half of the total energy in crashes.

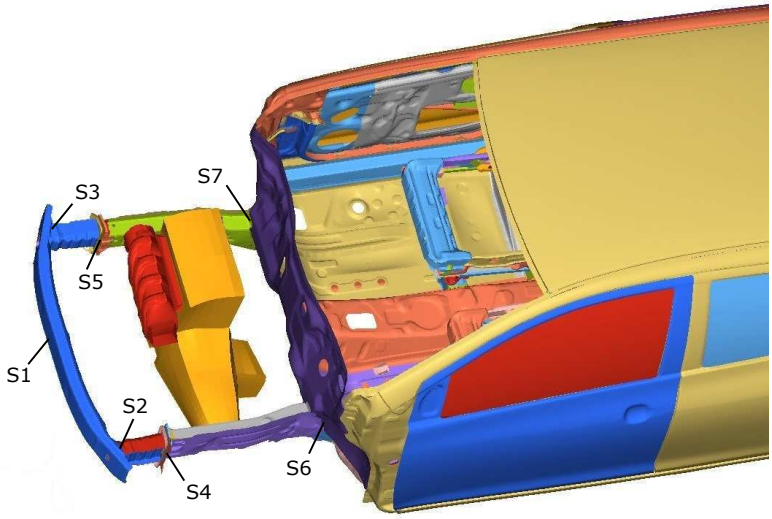

Figure D.1: Energy absorbing components of Toyota Yaris in detailed Finite Element model

To analysis the performance of energy absorbing components in the crash process, a finite element simulation of the 2010 Toyota Yaris passenger sedan is employed. The detailed FE model, which contains 1,514,068 elements, is developed by the National Crash Analysis Center (NCAC). More information about the FE model can be found in [14].

As shown in Figure D.1, these components combine an important load-carrying path of vehicle. Except the gravity center of vehicle, extra accelerometers were located on the energy absorbing components to measure their deformation, as listed in Table D.1.

Table D.1: Locations of accelerometers

No.	Symbol	Description
1	S1	Center of Bumper Front Surface
2	S2	Connection of Bumper and Left Crash box
3	S3	Connection of Bumper and Right Crash box
4	S4	Connection of Left Crash box and Left Beam
5	S5	Connection of Right Crash box and Right Beam
6	S6	End Point of Left Beam
7	S7	End Point of Right Beam

The vehicle was crashed into the rigid wall with an initial velocity of 56km/h. The accelerations were double integrated to calculate the displacements. Deformations of each component is defined as relative displacement of relative sensors, i.e.

$$Def_{Bumper} = Dis_{S1} - (Dis_{S2} + Dis_{S3})/2 \tag{D.1}$$

$$Def_{Crashbox} = (Dis_{S2} + Dis_{S3} - Dis_{S4} - Dis_{S5})/2 \tag{D.2}$$

$$Def_{Beam} = (Dis_{S4} + Dis_{S5} - Dis_{S6} - Dis_{S7})/2 \tag{D.3}$$

Figure D.2 shows the deformation process of main crashworthiness components. It can be seen that the crushes of different components occur within a specified time. As shown by bold line, the bumper, crash boxes and longitudinal beams (including firewall) are crushed in 0.005s∼0.011s, 0.011s∼0.0255s and 0.0255s∼0.1s respectively. This indicates that the energy absorbing components deformed in order without coincidence on time.

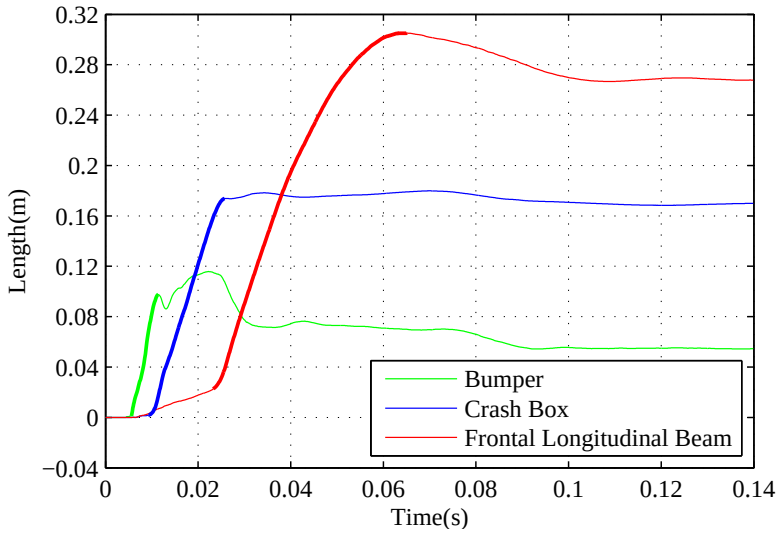

Figure D.2: Structure deformations of Toyota Yaris in 56km/h frontal barrier crash

D.2.2 Piecewise Model Structure

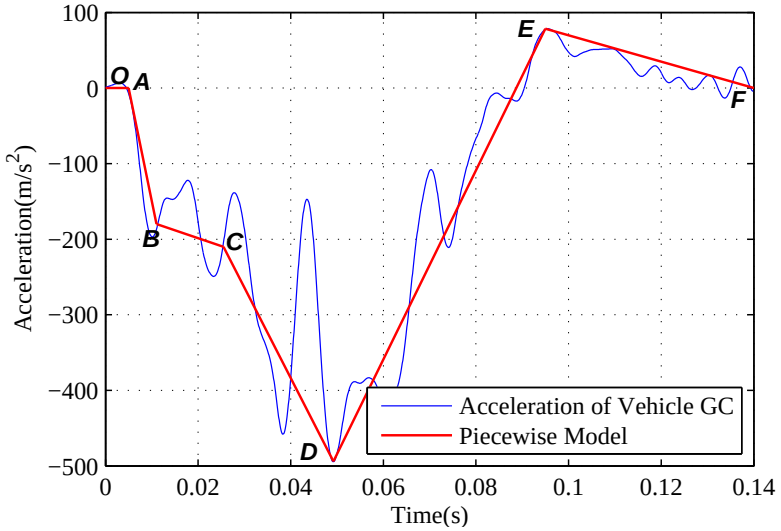

Figure D.3: Structure of piecewise model for vehicle frontal crashes

Figure D.3 shows the crash response (acceleration of Gravity Centre of vehicle) in the simulations. It can be seen that the crash response experienced some stages. In each stage, the trends of the acceleration signal are significantly different, as shown

by the red line in the figure. Comparing against the previous analysis, a corresponding relation can be stated as follows:

1) O-A: This duration is very short and there is no significant deceleration. In fact, only cover and accessories (designed for pedestrian protection) are crushed in this stage.

2) A-B: This stage is related to the bumper deformation. As the bumper has limited ability for the energy absorbing, the deceleration increases significantly during this period.

3) B-C: The crash boxes are working in this period. In this stage, the acceleration varies around a fixed level or increases slightly.

4) C-D-E: This is a long period, which is corresponding to the deformations of longitudinal beams and firewall. In this process, the deceleration changes a lot and experiences a peak. At time E, the crash process is almost finished and the vehicle is separated from the barrier.

5) E-F: Post crash process. There is no significant external force and consequently the deceleration turns to 0.

Based on this analysis, a piecewise model with 6 segments can be used to represent the crash processes of vehicles, if they have similar frontal crashworthiness structures. It should be noted that the 6-segment structure is suitable for the 56km/h crashes, which is tested in New Car Assessment Programme (NCAP). As all types of vehicle should pass the NCAP tests, the proposed model can be applied for different cars. The crashes in other velocities will be discussed in Section D.4.

D.3 Identification of Model Parameters in NCAP Crash Tests

Due to the difficulty of physical modeling for complicated processes, the data-based techniques are widely used in various industrial applications [15]. In the vehicle safety area, Pawlus reproduce crash kinematics if vehicle by nonlinear autoregressive (NAR) model of measured data [16]. In this section, a parameter identification scheme, which is based on the NCAP tests data, will be proposed for previous model structure.

In NCAP tests, the crash responses are recorded by the accelerometers, which are normally located on the engine, brake calipers and rear seats. In this paper, the data of rear seat is investigated, as it refers to the acceleration of passenger cabin and can reflect the performance of whole crashworthiness structure: energy absorbing components, engine and other parts (fan, battery etc.).

D.3.1 Ensemble Empirical Mode Decomposition (EEMD)

The complex structure of vehicle leads the responses of vehicle frontal crashes to become nonlinear, non-stationary and uncertain. Especially, the local oscillations may

mask the main variance of accelerations during crashes. For the analysis of crash responses, the time-frequency analysis methods, such as Short-Time Fourier Transform (STFT) and Wavelet Transform (WT), are used for decomposition in the literature [17–19]. However, it is difficult to give a reasonable selection of the base signal for decomposition.

In this work, EEMD is employed to filter the original crash responses and consequenctly extract the trend signals. EEMD is a advanced data analysis method proposed by Huang etc. [20, 21] and especially suitable for nonlinear and non-stationary process, such as [22]. In EEMD, the shifting process, as shown in Algorithm D.1, decomposes the original signal into a series of Intrinsic Mode Functions (IMFs) without the base signal.

Algorithm D.1 Shifting Process of EMD

Step 1: Set initial $i = 1$, $j = 1$ and $x_{1,1}(t) = x(t)$.
Step 2: Extract the local maxima and minima of signal $x_{i,j}(t)$ and construct the upper and lower envelops of $x_{i,j}(t)$ by interpolation of the maxima and minima, i.e. $u_{i,j}(t)$ and $l_{i,j}(t)$.
Step 3: Calculate the mean of the upper and lower envelops, recorded as $m_{i,j}(t) = \frac{1}{2}(u_{i,j}(t) + l_{i,j}(t))$. Define $h_{i,j}(t) = x_{i,j}(t) - m_{i,j}(t)$.
Step 4: Repeat Steps 2 and 3 for signal $x_{i,j+1}(t) = h_{i,j}(t)$, until $h_{i,j}(t)$ fulfills the definition of IMF. The i-th IMF is recorded as $s_i(t) = h_{i,j}(t)$.
Step 5: Calculate residual $x_{i+1,1}(t) = x_{i,1}(t) - s_i(t)$. Stop the shifting process until $x_{i+1,1}(t)$ has only one or no extremum. Otherwise, repeat Steps 2 to 4 for signal $x_{i+1,1}(t)$ to get other IMFs.

In addition, a noise aided method is also employed to achieve a stable decomposition [23] for intermittent signals. For this reason, EEMD is suitable for the analysis of crash responses. The integrated scheme of EEMD is shown in Algorithm D.2.

Algorithm D.2 Ensemble Empirical Mode Decomposition

Step 1: Set initial $j = 1$. Create white noise $n_j(t)$ with the given amplitude and add it to the original signals, i.e. $x_j(t) = x(t) + n_j(t)$.
Step 2: Decompose the noisy signal $x_j(t)$ by the EMD method and get $x_j(t) = \sum_{i=1}^{n} s_{i,j}(t)$. $s_{i,j}(t)$ is the j-th trial of the i-th IMF.
Step 3: Repeat Step 1 and Step 2 for N times with $j = j + 1$.
Step 4: Compute the ensemble mean of the N trials for each IMF as the final result, i.e. $s_i(t) = \frac{1}{N}\sum_{j=1}^{N} s_{i,j}(t)$.

The IMF is a function oscillating around 0, albeit not necessarily with constant frequency. Especially, some low frequency IMFs are summed as the trend component, i.e.

$$x(t) = \sum_{i=1}^{k} s_i(t) + T(t) \tag{D.4}$$

where $x(t)$ is the original crash response of vehicle, $s_i(t)$ are the high frequency IMFs of $x(t)$ with the average amplitude 0. $T(t)$ is the trend component of $x(t)$. In Figure D.4, the trend signal $T(t)$ is shown by red dash line. It can be seen that the trend signal has removed high frequency oscillations but kept the features of each crash stage. For this reason, the trend signal can be used for model identification.

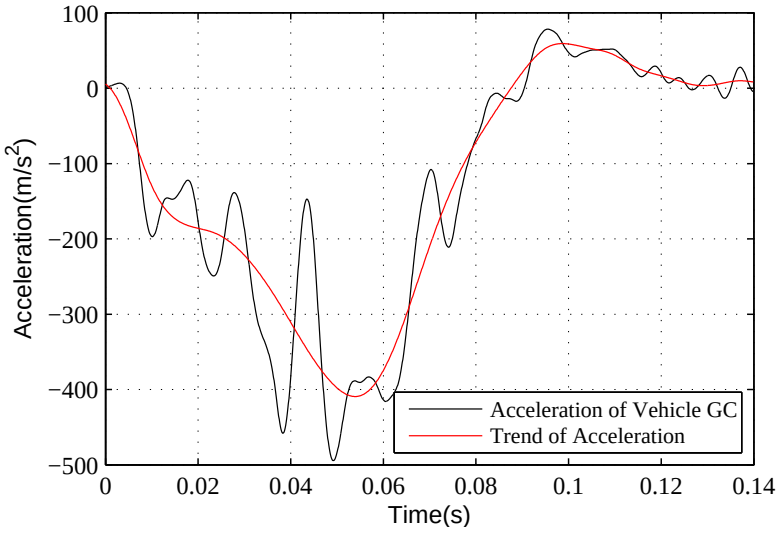

Figure D.4: The trend of original crash acceleration

D.3.2 Parameters Identification

In the previous model structure, some parameters can be pre-defined. Point F is the end of model and therefore the time and value of F are set as the end time of the trend signal, i.e. $t_F = t_{end}$ and $acc_F = T(t_{end})$. In addition, the acceleration of A is zero, i.e. $acc_A = 0$.

The time points are identified by the trend signal according to the analysis in pre-subsection. The crush of crashworthiness components mainly happens since A to E. In other time, i.e. the period O-A and E-F, there is no significant external force between vehicle and barrier. For this reason, the time of points A and E satisfy

$$Force(t) \leqslant \theta_1 \times Force_{max}, 0 \leqslant t \leqslant t_A \tag{D.5}$$

$$Force(t) \leqslant \theta_2 \times Force_{max}, t_E \leqslant t \leqslant t_F \tag{D.6}$$

where $Force$ is the external force from rigid wall, $Force_{max}$ is the maximal value of $Force$, θ_1 and θ_2 are the thresholds.

Point D is the peak of the deceleration, i.e.

$$T(t_D) = \min T(t) \tag{D.7}$$

The time of points B and C are corresponding to the sharp turns between A and D. They can be identified by the following equations

$$T''(t_B) = \max T''(t), t_A \leqslant t \leqslant t_D \tag{D.8}$$

$$T''(t_C) = \min T''(t), t_B \leqslant t \leqslant t_D \tag{D.9}$$

Although the acceleration of every point in the model can be roughly estimated by the trend signal, the error between the model and original signal should be limited. Specifically, the model has same velocity with the original crash response at time C, i.e.

$$\int_{t_O}^{t_C} acc(t)\,dt = \frac{1}{2}acc_B(t_B - t_A) + \frac{1}{2}(acc_B + acc_C)(t_C - t_B) = \Delta v_{OC} = \int_{t_O}^{t_C} x(t)\,dt \tag{D.10}$$

where the acceleration of C can be directly set as $acc_C = Trend(t_C)$. So acc_B is calculated as

$$acc_B = \left(2\int_0^{t_C} x(t)\,dt - acc_C(t_C - t_B)\right) \Big/ (t_C - t_A) \tag{D.11}$$

As to the value of points D and E, they should follow these two conditions:

1) ensuring the model has the same velocity change with original crash response in the duration C to F.

2) minimizing the error of displacement between the model and original signals.

That is

$$\begin{aligned} \min \quad & Err_{Dis} = \left\| \iint_0^{t_F} [acc(t) - x(t)]\,dtdt \right\| \\ \text{s.t.} \quad & \int_{t_C}^{t_F} acc(t)\,dt = \Delta v_{CF} = \int_{t_C}^{t_F} x(t)\,dt \end{aligned} \tag{D.12}$$

where

$$\int_{t_C}^{t_F} acc(t)\,dt = \int_{t_C}^{t_D} acc(t)\,dt + \int_{t_D}^{t_E} acc(t)\,dt + \int_{t_E}^{t_F} acc(t)\,dt$$

$$= \frac{1}{2}\left[(acc_C + acc_D)(t_D - t_C) + (acc_D + acc_E)(t_E - t_D) + (acc_E + acc_F)(t_F - t_E)\right] \tag{D.13}$$

then, Eq.D.12 can be simplified as

$$\begin{aligned} \min \quad & Err_{Dis} = \left\| \iint_0^{t_F} [acc(t) - x(t)]\,dtdt \right\| \\ \text{s.t.} \quad & acc_D(t_E - t_C) + acc_E(t_F - t_D) \\ & = 2\int_{t_C}^{t_F} x(t)\,dt - acc_C(t_D - t_C) - acc_F(t_F - t_E) \end{aligned} \tag{D.14}$$

Previous simulation of Yaris 56km/h crash is also used as an example. Table D.2 lists the identified parameters and the piecewise model is shown in Figure D.5 by the blue line. Compared with the analyses in subsection D.2.1, the piecewise model represent the crash durations of bumper, crashboxes and frontal beams exactly. In addition,

Table D.2: Identified model parameters of Yaris frontal crash simulation

	A	B	C	D	E	F
Time (s)	0.0041	0.0107	0.0259	0.0540	0.0942	0.1400
Acceleration (m/s^2)	0	-167.72	-199.41	-392.48	52.22	8.34

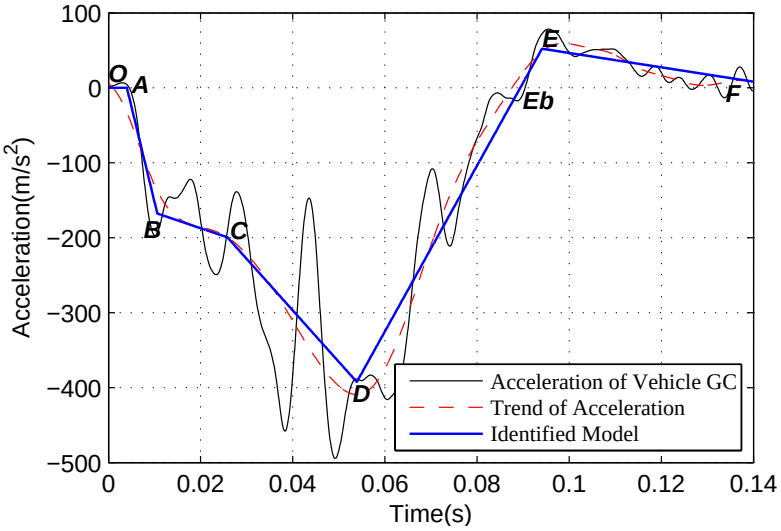

Figure D.5: Identified model of Yaris 56km/h frontal crash

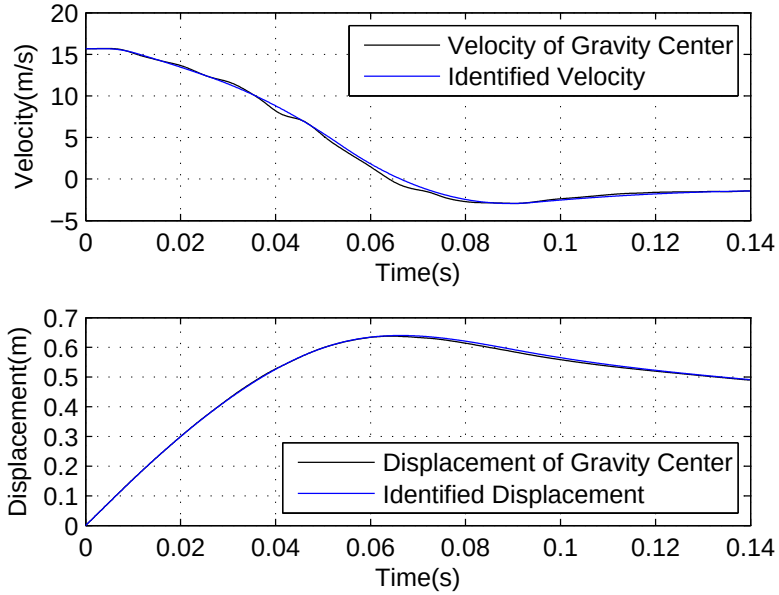

Figure D.6: Identified model and its comparison with original signal

Figure D.6 shows the comparison of velocity and displacement between the identified model and original simulation.

It can be seen that, the proposed model fits the trend signal very well and consequently reflect the global variance of original acceleration. The main discrepancy comes from the local oscillations. The Sprague & Geers (S&G) metric and ANOVA metric

are employed for quantitative comparison, as recommended by [24]. The S&G metric treats the magnitude error and phase error separately using two different metrics and combine them into a comprehensive metric [25]. The ANOVA, which contains average residual and standard deviation (SD) of Residuals, is a standard statistical assessment of whether the variance between two curves can be attributed to random error [26]. The criteria and comparison results are list in Table D.3.

Table D.3: Validation of identified model

Metrics	Items	Criteria, %	Error, %	Conclusion
S&G	Magnitude Error	<40.0	-9.0	Pass
	Phase Error	<40.0	8.2	Pass
	Comprehensive Error	-	12.2	Pass
ANOVA	Average Residual Error	<5.0	0.9	Pass
	SD of Residuals	<35.0	11.0	Pass

D.4 Estimation of Various Velocity Crashes

Although the model variance of different crashes are discussed in [6], there is still no quantitative estimation of model parameters.

In the 56km/h frontal crashes, every crashworthiness components work only within a specified stage, which is shown by the corresponding segment in the identified model. To estimate the process of different speed crashes, the feature of crashworthiness components should be investigated firstly.

According to the identified model and vehicle mass, the energy absorbed by each component, i.e. ΔJ_{AB} and ΔJ_{BC} can be roughly calculated as the kinetic energy change in the corresponding duration.

In different crashes, if the initial kinetic energy of vehicle is less than ΔJ_{AB}, i.e. the initial velocity is lower than $v_1 = \sqrt{2\Delta J_{AB}/m}$, only the bumper will be crushed and other components will not deform. In the case that the initial kinetic energy is less than $\Delta J_{AB} + \Delta J_{BC}$, the bumper and crash boxes will deform and the longitudinal beams will remain the same. The corresponding velocity is $v_2 = \sqrt{2\left(\Delta J_{AB} + \Delta J_{BC}\right)/m}$. For this reason, the frontal crashes can be classified into three types according to the initial velocity: 1) light crashes with initial velocity v_{Ol} lower than v_1, 2) moderate crashes with initial velocity v_{Om} between v_1 and v_2 and severe crashes with initial velocity v_{Os} higher than v_2. Due to the different deformed components, the model structures of each case are shown in Figure D.7.

In these model structures, the initial and end points can be pre-defined as zero, i.e. $t_{Ol} = t_{Om} = t_{Os} = 0$, $acc_{Ol} = acc_{Om} = acc_{Os} = 0$, $t_{Fl} = t_{Fm} = t_{Fs} = t_F = 0.14s$ and $acc_{Fl} = acc_{Fm} = acc_{Fs} = 0$. For each case, the stage O-A is corresponding to the accessories crush and therefore $acc_{Al} = acc_{Am} = acc_{As} = 0$.

For a specified car, the length of crash duration remains the same in different velocity crashes. However, in previous identified model, Eb is the point whose acceleration is

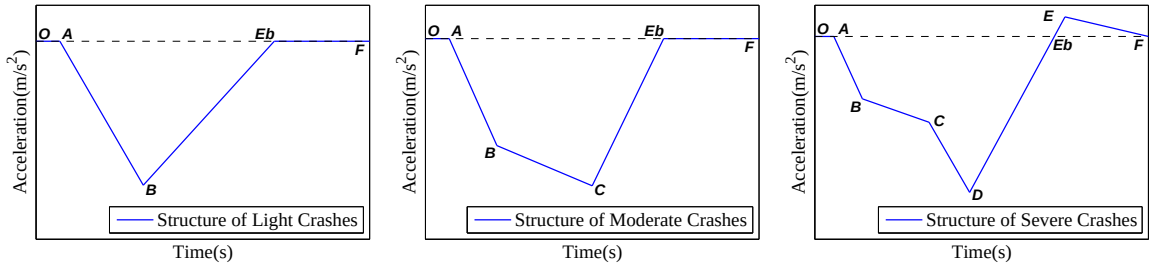

(a) Light crashes (b) Moderate crashes (c) Severe crashes

Figure D.7: Model structure to estimate the process of different crashes

zero. Eb-E is the overshoot of the restitution process and only exists in the sever crashes. In other words, the crash process will end at Eb in light and moderate crashes. So for light and moderate crashes, the length of crash duration is fixed as $T_{AEb} = t_{Eb} - t_A$ and accelerations are zero. The estimation of E (and Eb) in severe crashes will be discussed in Subsection D.4.5.

D.4.1 Estimation of post-crash velocity

The post-crash velocity is of importance in the crash estimation and may be decided by many factors [27]. In the crashes, the main deformation pattern of crash boxes and longitudinal beams are fold deformation and only a small amount of energy can be released in the restitution process. To make a rough estimation of the post-crash velocity, the following assumptions are made:

1) All the kinetic energy after crash is transformed from the restitution of bumper.
2) The released energy of bumper is proportional to the maximum deformation of bumper.

For all moderate and severe crashes, the post-crash velocities are same as the 56km/h case, i.e. $v_{Fm} \approx v_{Fs} \approx v_F$. For light crashes, $v_{Fl} \approx v_F \times v_{Ol}/v_1$.

D.4.2 Estimation of slopes of AB and BC

According to the identified model, the force-displacement graph is shown in Figure D.8. The external force is in direct proportion to the displacement during A-C, i.e. $F \approx k_{df} Dis$ [28]. k_{df} refers to the force-deformation ratio, which keeps stable in different crashes. Considering $F = ma$,

$$\frac{da}{dt} \approx \frac{d\left[\frac{k_{df}}{m} Dis\right]}{dt} = \frac{k_{df}}{m}\frac{dDis}{dt} = \frac{k_{df}}{m} v \tag{D.15}$$

This means the change ratio of deceleration will vary according to the velocity. For a piecewise model, it can be simplified as $\frac{da}{dt} = k_p \bar{v}$, where $\bar{v}$ is the average velocity of the corresponding period. In addition, the slopes in the Yaris 56km/h crash are defined as the average slops of trend signal T in the corresponding duration.

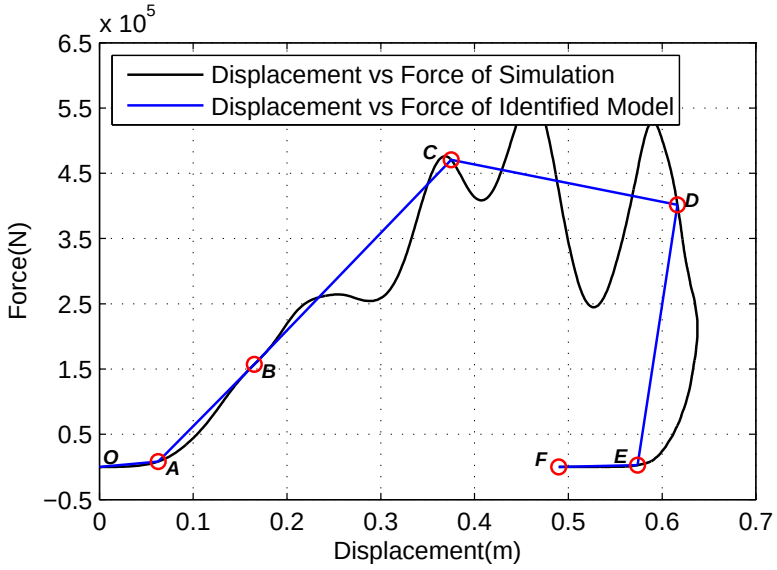

Figure D.8: Force vs. displacement of the crashes in Yaris

D.4.3 Light Crashes Estimation

In these cases, the deformation of bumper starts at $t_{Al} = \frac{v_{Ol}}{v_0} t_A$, where v_{Ol} is the initial velocity and $v_0 = 56km/h$. The restitution starts at $t_{Ebl} = t_{Al} + T_{AEb}$. The velocity change in light crashes are

$$\Delta v_l = v_{Fl} - v_{Ol} = \frac{1}{2} acc_{Bl} \left(t_{Ebl} - t_{Al}\right) \tag{D.16}$$

So the peek deceleration can be calculated as

$$acc_{Bl} = \frac{2\left(v_{Fl} - v_{Ol}\right)}{t_{Ebl} - t_{Al}} \tag{D.17}$$

The time of B, i.e. t_{Bl}, is solved by

$$\begin{cases} v_{Bl} = v_{Al} - \frac{1}{2} acc_{Bl} \left(t_{Bl} - t_{Al}\right) \\ t_{Bl} = t_{Al} + \frac{acc_{Bl}}{k_{ABl}} = t_{Al} + \frac{acc_{Bl}}{k_{AB} \cdot \frac{v_{Al} + v_{Bl}}{v_A + v_B}} \end{cases} \tag{D.18}$$

D.4.4 Moderate Crashes Estimation

In the moderate crashes with the initial velocity between v_1 and v_2, both the bumper and crash boxes will be crushed.

Same as the low speed crashes, we have $t_{Am} = \frac{v_{Om}}{v_0} t_A$ and $t_{Ebm} = t_{Am} + T_{AEb}$.

For point B, the velocity is $v_{Bm} = \sqrt{{v_{Om}}^2 - \frac{2\Delta J_{AB}}{m}}$. In this condition, the slopes of AB is

$$k_{ABm} = \frac{v_{Am} + v_{Bm}}{v_A + v_B} k_{AB} = \frac{v_{Om} + v_{Bm}}{v_A + v_B} k_{AB} \tag{D.19}$$

Considering $\Delta v_{ABm} = v_{Bm} - v_{Am} = v_{Bm} - v_{Om} = \frac{1}{2}\frac{acc_{Bm}^2}{k_{ABm}}$, the acceleration and time of B are

$$acc_{Bm} = -\sqrt{2\left(v_{Bm} - v_{Om}\right)k_{ABm}} = -\sqrt{\frac{2\left(v_{Bm}^2 - v_{Om}^2\right)k_{AB}}{v_A + v_B}} = -\sqrt{\frac{-4\Delta J_{AB}k_{AB}}{m\left(v_A + v_B\right)}} \tag{D.20}$$

$$t_{Bm} = t_{Am} + \frac{acc_{mB}}{k_{ABm}} \tag{D.21}$$

Note that acc_{Bm} is independent of the initial velocity of the crash and only decided by the features of bumper. To decide point C, t_{Cm} and acc_{Cm} can be solved by the following equations.

$$\begin{cases} acc_{Cm} = acc_{Bm} + k_{BCm}\left(t_{Cm} - t_{Bm}\right) \\ k_{BCm} = \dfrac{v_{Bm} + v_{Cm}}{v_B + v_C}k_{BC} \\ \Delta v_{BEm} = \dfrac{1}{2}\left[acc_{Bm}\left(t_{Cm} - t_{Bm}\right) + acc_{Cm}\left(t_{Ebm} - t_{Bm}\right)\right] \end{cases} \tag{D.22}$$

where $\Delta v_{BEm} = v_{Ebm} - v_{Bm} = v_{Fm} - v_{Bm} = v_F - v_{Bm}$.

D.4.5 Severe Crashes Estimation

For high speed cases, all crashworthiness components will be deformed and therefore the vehicle will experience the full process of the model. Different than the previous cases, the crash has a significant release process and therefore the overshoot will occur.

For simplification, the time of D and E are set as $t_{Ds} = t_{As} + T_{AD}$ and $t_{Ebs} = t_{As} + T_{AEb}$, where $t_{As} = \frac{v_{Os}}{v_0}t_A$ and $T_{AD} = T_D - T_A$. In addition, the acceleration of E can be estimated as $acc_{Es} = acc_E \cdot (v_{Os} - v_2)/(v_0 - v_2)$.

The velocity at time points B and C are

$$v_{Bs} = \sqrt{v_{Os}^2 - \frac{2\Delta J_{AB}}{m}} \tag{D.23}$$

and

$$v_{Cs} = \sqrt{v_{Os}^2 - \frac{2\left(\Delta J_{AB} + \Delta J_{BC}\right)}{m}} \tag{D.24}$$

respectively. Similar with the middle speed case, the parameters related to points B and C are decided as follows:

$$acc_{Bs} = -\sqrt{\frac{2\left(v_{Bs}^2 - v_{Os}^2\right)k_{AB}}{v_A + v_B}} = -\sqrt{\frac{-4\Delta J_{AB}k_{AB}}{m\left(v_A + v_B\right)}} \tag{D.25}$$

$$t_{Bs} = t_{As} + \frac{acc_{Bh}}{k_{ABs}} = t_{As} + \sqrt{\frac{2\left(v_{Bs} - v_{Os}\right)\left(v_A + v_B\right)}{\left(v_{Bs} + v_{Os}\right)k_{AB}}} \tag{D.26}$$

and

$$acc_{Cs} = -\sqrt{acc_{Bs}^2 + \frac{2\left(v_{Cs}^2 - v_{Bs}^2\right)k_{BC}}{v_B + v_C}} = -\sqrt{\frac{-4\Delta J_{AB}k_{AB}}{m\left(v_A + v_B\right)} + \frac{-4\Delta J_{BC}k_{BC}}{m\left(v_B + v_C\right)}} \quad \text{(D.27)}$$

$$t_{Cs} = t_{Bs} + \frac{acc_{Cs} - acc_{Bs}}{k_{BCs}} = t_{Bs} + \frac{\left(acc_{Cs} - acc_{Bs}\right)\left(v_B + v_C\right)}{\left(v_{Bs} + v_{Cs}\right)k_{BC}} \quad \text{(D.28)}$$

The initial velocity has no influence on acc_{Bs} and acc_{Cs}. The acceleration of D, i.e. acc_{Ds}, should ensure the velocity change of duration C-F is $\Delta v_{CFs} = v_{Fs} - v_{Cs} = v_F - v_{Cs}$.

$$\frac{1}{2}acc_{Cs}\left(t_{Ds} - t_{Cs}\right) + \frac{1}{2}acc_{Ds}\left(t_{Ebs} - t_{Cs}\right) + \frac{1}{2}acc_{Es}\left(t_{Fs} - t_{Ebs}\right) = v_F - v_{Cs} \quad \text{(D.29)}$$

That is

$$acc_{Ds} = \frac{1}{t_{Ebs} - t_{Cs}}\left[2\left(v_F - v_{Cs}\right) - acc_{Cs}\left(t_{Ds} - t_{Cs}\right) - acc_{Es}\left(t_{Fs} - t_{Ebs}\right)\right] \quad \text{(D.30)}$$

Consequently,

$$t_{Es} = t_{Ebs} + \frac{acc_{Es}\left(t_{Ds} - t_{Ebs}\right)}{acc_{Ds}} \quad \text{(D.31)}$$

D.4.6 Case Study

In this subsection, three crash cases of Yaris will be estimated by the proposed scheme. Table D.4 lists the velocity and displacement at each time point of piecewise model.

Table D.4: Velocity and displacement at each time point

	A	B	C	D	E	F
Velocity (m/s)	15.698	15.035	12.336	3.646	-2.779	-1.451
Displacement (m)	0.0627	0.1651	0.3751	0.6163	0.5737	0.4897

The mass of Yaris in the finite element model is 1100kg. According to the identified model in Section D.3, the bumper absorbed energy is $\Delta J_{AB} = 8.766kJ$ and $\Delta J_{BC} = 40.62kJ$ for crash boxes. Consequently, $v_1 = 14.37km/h$ and $v_2 = 34.11km/h$. So the crash velocities are setted as 12km/h, 25km/h and 48km/h, which are corresponding to the light, moderate and severe conditions respectively. In the model of 56km/h, the end velocity is $v_F = -5.22km/h$. The slopes of AB and BC are $-17118m/s^3$ and $-1956.4m/s^3$ respectively. According to the previous scheme, the estimations of three crashes are listed in Table D.5.

The estimation results are compared with the corresponding finite element simulations. Table D.6 lists the quantitative comparison results, which indicate that the proposed scheme make effective estimations for three crashes. Figures D.9∼D.11 show the comparison of accelerations and velocities. It can be seen that the error of the

Table D.5: Estimation of three crash cases

	$12km/h$ Crash	$25km/h$ Crash	$48km/h$ Crash
$t_A\ (s)$	0.0191	0.0096	0.0041
$t_B\ (s)$	0.0427	0.0294	0.0139
$acc_B\ (m/s^2)$	-104.30	-133.56	-133.56
$t_C\ (s)$	-	0.0589	0.0361
$acc_C\ (m/s^2)$	-	-146.49	-168.51
$t_D\ (s)$	-	-	0.0547
$acc_D\ (m/s^2)$	-	-	-367.34
$t_{Eb}\ (s)$	0.1045	0.0949	0.0902
$t_E\ (s)$	-	-	0.0934
$acc_E\ (m/s^2)$	-	-	33.13

start time t_A is magnified in the estimation of low speed crashes. This is the main cause of phase error, especially in light crash cases. Furthermore, the main error of moderate and severe crashes exist in duration BC. In moderate and severe crashes, the estimation of BC slopes is simplified as linear correlation with the k_{BC} in 56km/h crash and consequently result in the inherent error.

Table D.6: Comparison metrics of estimations and simulations

Metrics	Items	$12km/h$ Crash	$25km/h$ crash	$48km/h$ crash
S&G	Magnitude Error	-7.4%, Pass	-11.7, Pass	-5.8, Pass
	Phase Error	9.8%, Pass	7.7, Pass	7.3, Pass
	Comprehensive Error	12.3%, Pass	14, Pass	9.4, Pass
ANOVA	Average Residual Error	0.9%, Pass	0.9%, Pass	1.2%, Pass
	SD of Residuals	13.5%, Pass	10.8%, Pass	11.3%, Pass

D.5 Conclusion

This work is essentially based on the inherent relationship between the crashworthiness structure and acceleration of vehicle. The piecewise model of frontal crashes is proposed to represent the acceleration of passenger cabin in the whole crash duration. Especially, the deformation processes of bumper, crash boxes and frontal beams are clearly corresponded to the segments in the model. Compared with previous crash models, the proposed model describes the kinetic signal of model directly and involves the deformation features of vehicle structure. Consequently, the piecewise model can balance the model accuracy and complexity properly.

The 56km/h frontal crash test is recommended for the parameter identification of model, as it is NCAP standard test and available for most vehicles. The features

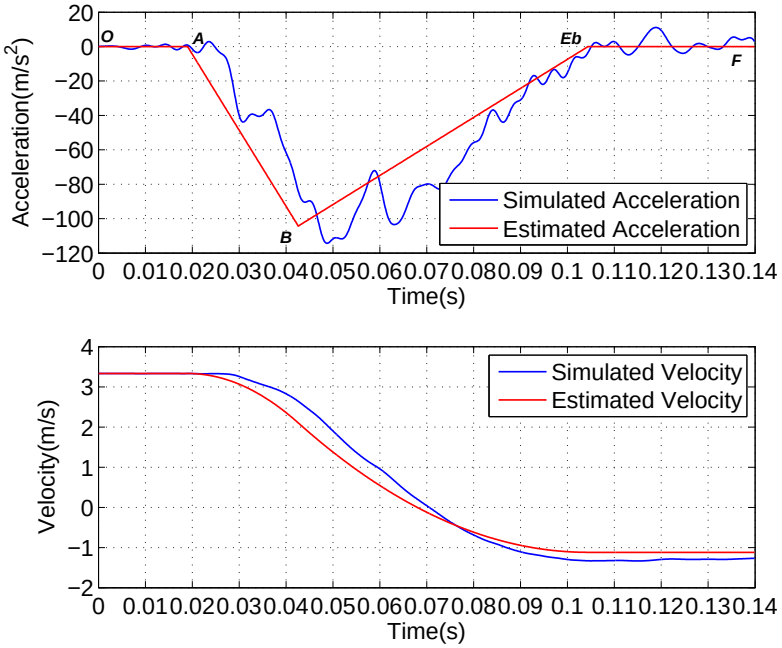

Figure D.9: Estimation of 12km/h frontal crash of Toyota Yaris

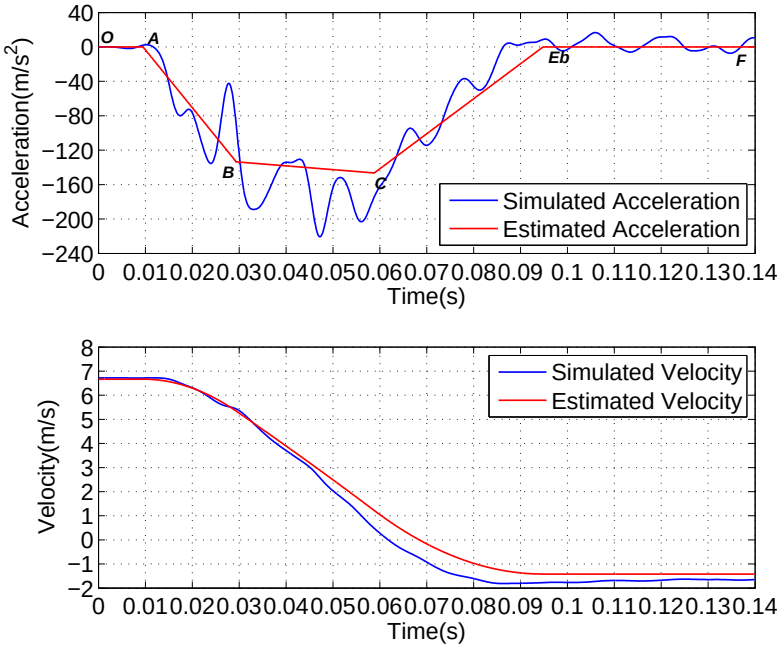

Figure D.10: Estimation of 25km/h frontal crash of Toyota Yaris

of crahworthiness components, including energy absorbing abilities and acceleration change rates, can be calculated from the model. Based on these, the frontal crashes are classified as light, moderate and severe crashes according to the initial crash velocities. The structure deformation may vary in different types of crashes. An integrated crash estimation scheme is also proposed in this work. The case studies give examples for the proposed scheme and demonstrate the effectiveness.

Comparing with other existing models in engineering and literature, the proposed model has two significant advantages. Firstly, the proposed model can achieve better

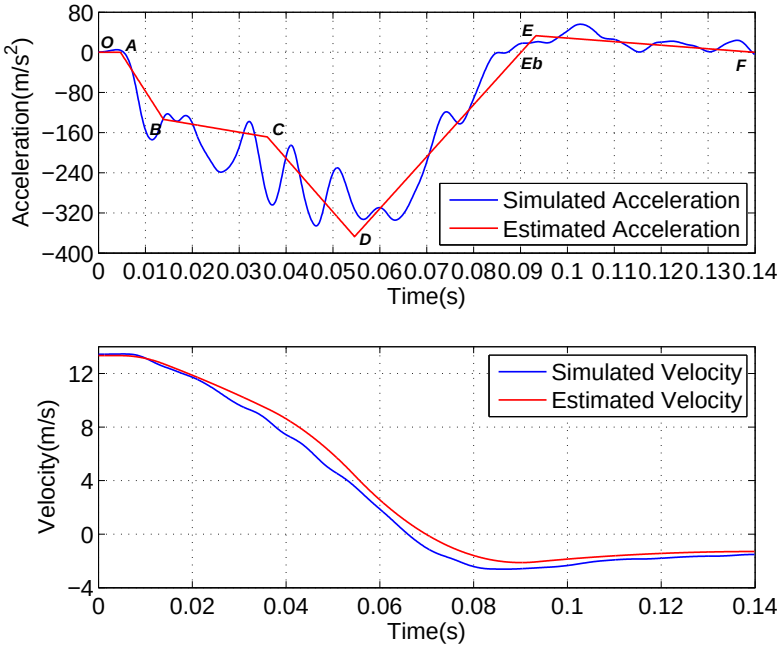

Figure D.11: Estimation of 48km/h frontal crash of Toyota Yaris

estimation performance with extremely low complexity. Secondly, without the requirements of detailed information of vehicle, the modeling process is based on the crash test data only. The model is easy to be established with low cost on time, as well as economic. This work is potential to benefit the design of other safety functions. The crashes in more complex conditions, such as oblique and offset cases, should be studied in the future.

References

[1] P. Jonsén, E. Isaksson, K. Sundin, and M. Oldenburg, "Identification of lumped parameter automotive crash models for bumper system development," *International Journal of Crashworthiness*, vol. 14, no. 6, pp. 533–541, 2009.

[2] M. Pahlavani and J. Marzbanrad, "Crashworthiness study of a full vehicle-lumped model using parameters optimisation," *International Journal of Crashworthiness*, vol. 20, no. 6, pp. 573–591, 2015.

[3] W. Pawlus, H. R. Karimi, and K. G. Robbersmyr, "Application of viscoelastic hybrid models to vehicle crash simulation," *International Journal of Crashworthiness*, vol. 16, no. 2, pp. 195–205, 2011.

[4] M. El Kady, A. Elmarakbi, J. MacIntyre, and M. Alhariri, "Multi-body integrated vehicle-occupant models for collision mitigation and vehicle safety using dynamics control systems," *International Journal of System Dynamics Applications (IJSDA)*, vol. 5, no. 2, pp. 80–122, 2016.

[5] A. R. Yildiz and K. N. Solanki, "Multi-objective optimization of vehicle crashworthiness using a new particle swarm based approach," *International Journal of Advanced Manufacturing Technology*, vol. 59, no. 1-4, pp. 367–376, 2012.

[6] M. Varat and S. E. Husher, "Crash pulse modeling for vehicle safety research," in *Proceedings of 18th International Technical Conference on the Enhanced Safety of Vehicles (ESV)*, no. 501, (Nagoya, Japan), National Highway Traffic Safety Administration, May 2003.

[7] J. Iraeus and M. Lindquist, "Pulse shape analysis and data reduction of real-life frontal crashes with modern passenger cars," *International Journal of Crashworthiness*, vol. 20, no. 6, pp. 535–546, 2015.

[8] Z. Wei, H. R. Karimi, and K. G. Robbersmyr, "A model of vehicle-fixed barrier frontal crash and its application in the estimation of crash kinematics," in *24th International Technical Conference on the Enhanced Safety of Vehicles (ESV)*, no. 15-0161, National Highway Traffic Safety Administration, 2015.

[9] K. T. Hamza, *Design for vehicle structural crashworthiness via crash mode matching*. PhD thesis, University of Michigan, Ann Arbor, MI., 2008.

[10] Z. Wei, H. R. Karimi, and K. G. Robbersmyr, "Analysis of the relationship between energy absorbing components and vehicle crash response," *SAE Technical Paper 2016-01-1541*, 2016.

[11] H. Li, S. Yin, Y. Pan, and H.-K. Lam, "Model reduction for interval type-2 Takagi–Sugeno fuzzy systems," *Automatica*, vol. 61, pp. 308–314, 2015.

[12] J. Fehr, "Non-modal based model reduction for explicit crash codes," *IFAC-PapersOnLine*, vol. 48, no. 1, pp. 176–177, 2015.

[13] S. Mukherjee, R. Mittal, *et al.*, "Model order reduction using response-matching technique," *Journal of The Franklin Institute*, vol. 342, no. 5, pp. 503–519, 2005.

[14] D. Marzougui, R. R. Samaha, C. Cui, C. Kan, and K. S. Opiela, "Extended validation of the finite element model for the 2010 toyota yaris passenger sedan," Working Paper NCAC 2012-W-005, The National Crash Analysis Center (NCAC), July 2012.

[15] S. Yin, X. Li, H. Gao, and O. Kaynak, "Data-based techniques focused on modern industry: an overview," *IEEE Transactions on Industrial Electronics*, vol. 62, no. 1, pp. 657–667, 2015.

[16] W. Pawlus, H. R. Karimi, and K. G. Robbersmyr, "Data-based modeling of vehicle collisions by nonlinear autoregressive model and feedforward neural network," *Information Sciences*, vol. 235, pp. 65–79, 2013.

[17] D. M. Onchiș and E. M. Súarez Sánchez, "The flexible Gabor-wavelet transform for car crash signal analysis," *International Journal of Wavelets, Multiresolution and Information Processing*, vol. 7, no. 04, pp. 481–490, 2009.

[18] H. R. Karimi and K. G. Robbersmyr, "Signal analysis and performance evaluation of a vehicle crash test with a fixed safety barrier based on haar wavelets," *International Journal of Wavelets, Multiresolution and Information Processing*, vol. 9, no. 01, pp. 131–149, 2011.

[19] H. R. Karimi, W. Pawlus, and K. G. Robbersmyr, "Signal reconstruction, modeling and simulation of a vehicle full-scale crash test based on morlet wavelets," *Neurocomputing*, vol. 93, pp. 88–99, 2012.

[20] N. E. Huang, Z. Shen, S. R. Long, M. C. Wu, H. H. Shih, Q. Zheng, N.-C. Yen, C. C. Tung, and H. H. Liu, "The empirical mode decomposition and the Hilbert spectrum for nonlinear and non-stationary time series analysis," *Proceedings of the Royal Society of London A: Mathematical, Physical and Engineering Sciences*, vol. 454, no. 1971, pp. 903–995, 1998.

[21] N. E. Huang and Z. Wu, "A review on Hilbert-Huang transform: Method and its applications to geophysical studies," *Reviews of Geophysics*, vol. 46, no. 2, 2008.

[22] Y. Yang, H. Chen, and T. Jiang, "Nonlinear response prediction of cracked rotor based on EMD," *Journal of The Franklin Institute.*, vol. 352, no. 8, pp. 3378–3393, 2015.

[23] Z. Wu and N. E. Huang, "Ensemble empirical mode decomposition: a noise-assisted data analysis method," *Advances in Adaptive Data Analysis*, vol. 1, no. 01, pp. 1–41, 2009.

[24] M. H. Ray, M. Mongiardini, and C. Plaxico, "Quantitative methods for assessing similarity between computational results and full-scale crash tests," in *91th Annual Meeting of the Transportation Research Board*, (Washington, DC), Citeseer, January 2012.

[25] M. A. Sprague and T. L. Geers, "Spectral elements and field separation for an acoustic fluid subject to cavitation," *Journal of Computational Physics*, vol. 184, no. 1, pp. 149–162, 2003.

[26] M. Ray, "Repeatability of full-scale crash tests and criteria for validating simulation results," *Transportation Research Record: Journal of the Transportation Research Board*, no. 1528, pp. 155–160, 1996.

[27] P. Niehoff and H. C. Gabler, "The accuracy of winsmash delta-V estimates: the influence of vehicle type, stiffness, and impact mode," in *Annual Proceedings / Association for the Advancement of Automotive Medicine*, vol. 50, pp. 73–89, 2006.

[28] M. Huang, *Vehicle crash mechanics*. Boca Raton, Florida: CRC press, 2002.

Paper E

An EEMD Aided Comparison of Time Histories and Its Application in Vehicle Safety

Zuolong Wei[1], Kjell G. Robbersmyr[1], Hamid R. Karimi[2]

1. Department of Engineering Sciences, University of Agder, PO Box 509, N-4898 Grimstad, Norway
2. Department of Mechanical Engineering, Politecnico di Milano, 20156 Milan, Italy

The paper has been published as:

Z. Wei, K. G. Robbersmyr, and H. R. Karimi, "An EEMD aided comparison of time histories and its application in vehicle safety", *IEEE Access, Special Section: Recent Advances on Modelling, Optimization and Signal Processing Methods in Vehicle Dynamics and Crash-worthiness*, 2016.

The layout has been revised.

Abstract

In the context of signal processing, the comparison of time histories is required for different purposes, especially for the model validation of vehicle safety. Most of the existing metrics focus on the mathematical value only. Therefore, they suffer the measuring errors, disturbance and uncertainties and can hardly achieve a stable result with a clear physical interpretation. This paper proposes a novel scheme of time histories comparison to be used in vehicle safety analysis. More specifically, each signal for comparison is decomposed into a trend signal and several intrinsic mode functions (IMFs) by Ensemble Empirical Mode Decomposition. The trend signals reflect the general variation and are free from the influence of high frequency disturbances. With the help of dynamic time warping, the errors of time and magnitude between trends are calculated. The IMFs, which contain high frequency information, are compared on frequency, magnitude and local features. To illustrate the full scope and effectiveness of the proposed scheme, this paper provides three vehicle crash cases.

Keywords: *Time-history, Model Validation, EEMD, DTW, Vehicle Crash.*

E.1 Introduction

histories can present the variation of signals over time and are often used to record the detailed processes of events. In some areas, such as pattern recognition, fault diagnosis, data mining and numerical simulations, an objective, proper and accurate comparison is in great request [1]. An integrated scheme of comparison contains the pre-process, discrepancy calculation and optional post-process (e.g. the evaluation of discrepancies). Typically, the fundamental problem is to define a proper comparison metric, which refers to mathematical measures that quantify the level of agreement between different signals, for the discrepancy calculation [2]. According to the features of signals and the purposes of comparison, the metrics should be diverse in different applications.

One of the purposes of time histories comparison is to validate computational models, a critical topic of numerical simulation, which is particularly rigorous in the field of vehicle safety. More specifically, the validation process is to assess to which degree that the simulation can replicate the corresponding physical event [3]. In the context of vehicle safety, the crashes are usually recorded by electronic and photographic instruments [4, 5]. And model validation is normally conducted by quantitative comparisons of response signals, i.e. the accelerations during crashes and simulations, which are measured by accelerometers. Therefore, both engineering and academic researchers developed many comparison metrics to achieve an accurate and reliable validation for simulations of vehicle safety. However, as far as the authors' knowledge, these developed metrics focus on the mathematical value only and ignore the physical meaning of the comparative signals.

In this paper, the existing metrics are presented firstly with respect to their advantages and disadvantages. Then a signal processing methodology is proposed to be involved in the comparison process. More specifically, the signals are decomposed

by the Ensemble Empirical Mode Decomposition (EEMD) algorithm in different frequency domains. This makes it possible to introduce more features into the detailed comparison, which will consequently improve the performance of comparisons. Although emphasizes on the application in vehicle safety, the proposed metric is universal and can be introduced into related fields.

The remainder of this paper is organized as follows. Section E.2 reviews and analyses the existing metrics. A discussion about the comparison metrics is also given in this section. In Section E.3, the proposed comparison scheme and related technologies are presented in detail. The next section shows some case studies of the vehicle crashes to show the performance of the proposed scheme. The conclusions are presented in the last section.

E.2 A Review of The Existing Comparison Schemes

Up to now, various comparison schemes have been proposed and employed by researchers to validate the vehicle safety simulations. In these methods, the stochastic metrics focus on the distribution of the residuals between the signals from test and simulation, see for instance [6–8] and the references therein. Although they consider the uncertainties of parameters, the features of original signals are lost. For this reason, only the deterministic metrics will be introduced and discussed in this section.

E.2.1 Basic Metrics

The basic metrics refer to those metrics which involve only one error measure. Compare to the composite metrics, the basic metrics can only reflect the difference on one particular aspects of time histories.

L_1 and L_2 norms of residual signals are the most popular metrics. Generally, they are used to measure the magnitude errors. As a common mathematical tool, the norm can also be used to measure the errors on other aspects, such as time error and frequency error. The shortage of using norms can be listed in twofold: 1) the norms are not normalized and 2) the norms are highly depended on the number of time points. To overcome this shortage, many uniformed metrics are proposed. Some typical ones are listed in Tab. E.1. (Note: r_i means the reference signal, t_i stands for the test and n is the number of sample points.)

Different from the norm methods considering the errors, the coefficient of correlation

$$\rho = \frac{n\sum_{i=1}^{n} t_i r_i - \sum_{i=1}^{n} t_i \sum_{i=1}^{n} r_i}{\sqrt{n\sum_{i=1}^{n} t_i^2 - \left(\sum_{i=1}^{n} t_i\right)^2}\sqrt{n\sum_{i=1}^{n} r_i^2 - \left(\sum_{i=1}^{n} r_i\right)^2}} \tag{E.1}$$

reflects on how much degrees a signal can be determined by the other one. However, this method is too sensitive to the time error. So the cross-correlation coefficient (also called sliding dot product) is modified from the coefficient of correlation, shown in

Table E.1: Norm-Based Metrics

Name of Metric	Equations
Weighted Integrate Factor	$\sqrt{\frac{\sum \max\left(r_n^2, t_n^2\right)\left(1-\frac{\max(0, r_n, t_n)}{\max\left(r_n^2, t_n^2\right)}\right)^2}{\sum \max\left(r_n^2, t_n^2\right)}}$
Zilliacus error	$\frac{\sum \lvert t_n - r_n \rvert}{\sum \lvert r_n \rvert}$
RMS error	$\frac{\sqrt{\sum (t_n - r_n)^2}}{\sqrt{\sum t_n^2}}$
Theil's inequality	$\frac{\sqrt{\sum (t_n - r_n)^2}}{\sqrt{\sum t_n^2} + \sqrt{\sum r_n^2}}$
Whang's inequality	$\frac{\sum \lvert t_n - r_n \rvert}{\sum \lvert t_n \rvert + \sum \lvert r_n \rvert}$
Regression efficient	$\sqrt{1 - \frac{(n-1)\sum (t_n - r_n)^2}{n \sum (r_n - \bar{r})^2}}$

Eqn. (E.2). It is a good measure of time delay (i.e. phase errors) [9, 10] and used in some composite metrics.

Each of these basic metrics can hardly describe the difference effectively, but they provide some tools to develop composite metrics. To achieve better performance, a composite metric may consider the discrepancy on various aspects, including the magnitude, phase or time-of-arrival (TOA), frequency or slope, shape, etc. Different measures will be designed specifically for each kind of features and combined into a comprehensive assessment. According to different features involved, composite metrics can be divided into several groups.

E.2.2 Magnitude-Phase-Composite (MPC) Metrics

MPC metrics measure the discrepancies on two axes, i.e. the amplitude axis and time axis. Four typical MPC metrics are listed in Tab. E.2, where $\alpha = sign\left(\sum t_n r_n\right)$ and $m = \frac{\sum t_n^2 - \sum r_n^2}{\sqrt{\sum t_n^2 \sum r_n^2}}$.

For the magnitude discrepancy, the first three metrics from Geer share the same measure, while the Russell's measure modifies it to be symmetric. The symmetry keeps the same measure no matter to select which signal as the reference. But this advantage

$$\rho(n_0) = \frac{(n-n_0)\sum_{i=1}^{n-n_0} t_i r_{i+n_0} - \sum_{i=1}^{n-n_0} t_i \sum_{i=1}^{n-n_0} r_{i+n_0}}{\sqrt{(n-n_0)\sum_{i=1}^{n-n_0} t_i^2 - \left(\sum_{i=1}^{n-n_0} t_i\right)^2}\sqrt{(n-n_0)\sum_{i=1}^{n-n_0} r_{i+n_0}^2 - \left(\sum_{i=1}^{n-n_0} r_{i+n_0}\right)^2}} \quad \text{(E.2)}$$

Table E.2: Typical MPC metrics

	Magnitude	Phase	Comprehensive
Geers	$M_G = \sqrt{\frac{\sum t_n^2}{\sum r_n^2}} - 1$	$P_G = 1 - \frac{\sum t_n r_n}{\sqrt{\sum t_n^2 \sum r_n^2}}$	$\sqrt{M_G^2 + P_G^2}$
Geers CSA	$M_{GC} = \sqrt{\frac{\sum t_n^2}{\sum r_n^2}} - 1$	$P_{GC} = 1 - \frac{\lvert\sum t_n r_n\rvert}{\sqrt{\sum t_n^2 \sum r_n^2}}$	$\alpha\sqrt{M_{GC}^2 + P_{GC}^2}$
Sprague & Geers	$M_{SG} = \sqrt{\frac{\sum t_n^2}{\sum r_n^2}} - 1$	$P_{SG} = \frac{1}{\pi}\cos^{-1}\frac{\sum t_n r_n}{\sqrt{\sum t_n^2 \sum r_n^2}}$	$\sqrt{M_{SG}^2 + P_{SG}^2}$
Russell	$M_R = sign(m)\log_{10}(1 + \lvert m\rvert)$	$P_R = \frac{1}{\pi}\cos^{-1}\frac{\sum t_n r_n}{\sqrt{\sum t_n^2 \sum r_n^2}}$	$\sqrt{\frac{\pi}{4}(M_R^2 + P_R^2)}$

is not significant in model validation as the signal of the real test is commonly chosen as a reference. The measure of phase discrepancy in S&G and Russell is an improvement of that in Geer with a more clear meaning. All of these MPC metrics use the root-sum square of magnitude and phase as the composite result.

Reference [2] compared these metrics mentioned above (except the cross correlation coefficient) with a case study and analyzed the results. As a conclusion, the S&G metric is recommended for the use in roadside safety simulations, such as [11, 12]. Referencing this suggestion, a computer program for the verification and validation of numerical simulations in roadside safety is developed as RSVVP [13].

E.2.3 Normalized Integral Square Error (NISE)

NISE is proposed by Donnelly et al. in [14] to quantify the difference between repeated tests. NISE takes the phase, magnitude and shape discrepancies into account with corresponding formulations as follows:

$$M_{NISE} = \rho(n_*) - \frac{2\psi_{rt}(n_*)}{\psi_{rr} + \psi_{tt}} \tag{E.3}$$

$$P_{NISE} = \frac{2\psi_{rt}(n_*) - 2\psi_{rt}}{\psi_{rr} + \psi_{tt}} \tag{E.4}$$

$$S_{NISE} = 1 - \rho(n_*) \tag{E.5}$$

where $\psi_{rr} = \sum r_n^2/N$, $\psi_{tt} = \sum t_n^2/N$, $\psi_{rt} = \sum r_n t_n/N$, n_* is the "steps" to compensate for the error in phase and $\rho(n_*)$ is the cross-correlation in Eqn. (E.2).

The composite metric can be expresses as:

$$C_{NISE} = M_{NISE} + P_{NISE} + S_{NISE} = 1 - \frac{2\psi_{rt}}{\psi_{rr} + \psi_{tt}} \tag{E.6}$$

Obviously, the measure of shape is cancelled out in C_{NISE}. In addition, the magnitude measure is possible to be negative and then decrease the comprehensive metric.

E.2.4 Enhanced Error Assessment of Response Time Histories (EEARTH)

EEARTH is a comprehensive scheme to evaluate the difference of time histories. The core idea is the EARTH, presented in [1] and [15]. The EARTH metric is the composition of the measures of magnitude, phase and slope. Comparing to other metrics, the EARTH involves the slope as a description of the feature of frequency and therefore improves the assessment significantly. Another valuable idea of EARTH is that to keep the independence of each measure, which means to avoid the influence from other two factors when calculating each measure. Especially, the dynamic time warping (DTW) is employed in the magnitude measure to remove the influence of local time error.

Based on EARTH, the EEARTH scheme proposed by [16] makes the following improvements: 1) translate the original measures into intuitive scores between 0 and 100% and 2) involve an integrated calibration process which incorporates physical-based thresholds and knowledge of subject matter experts (SMEs) . The EEARTH is selected into ISO standard ISO/TR16250 and used in many cases, such as [17].

E.2.5 Summary and Discussion

Besides the metrics presented previously, some other metrics, such as Correlation and Analysis (CORA) [18], are also proposed in existing literatures. By studying these metrics, a short summary will be given in this subsection.

1) In general, to make an object and accurate comparison, various features are considered by different metrics. In these features, the magnitude and phase errors are most concerned by researchers. The magnitude error has clear physical meaning and should be measured undoubtedly. However, for vibration signals, the magnitude error will be influenced significantly by the time lag. For this reason, the magnitude measure used in EEARTH has superiority.

2) The measures for phase error are based on the cross-correlation coefficient in most related metrics. Unfortunately, the concept of phase error comes from periodic signals. For non-periodic signals, the cross-correlation coefficient based measures may only qualify the global phase error. That means the local time error is lost in the comparison.

3) Some metrics also try to define the difference of shape. But both the NISE and CORA suffer critical problems. In fact, the shape error can be divided into the errors on magnitude and time axes. In other words, shape error is superfluous if the magnitude and time errors are measured properly.

4) Only EEARTH try to compare the frequency of signals and employ the slope as a substitute. Although not given directly, the frequency, i.e. the oscillation rate of signals is an intuitional information in the comparison.

5) According to the experience of SMEs, some local features are of great value in comparisons, such as the peak values and times [19]. However, they are not included in the existing metrics.

E.3 An EEMD Aided Comparison of Time Histories

In this section, a novel scheme of time histories comparison is presented in this section. Vehicle crash is a complex process and therefore crash signals contain high frequency oscillations and uncertainties. According to [20], a crash impulse can be splitted into a "base" and several "shocks", which represent the low and high frequency components respectively. Generally, the "base" reflects the global trend of crash signal and can be decomposed as time and magnitude orthogonally. And the "shocks" may contain the frequency and local features of original signal, which should be analysed and checked to achieve a comprehensive result. In fact, the "shocks" of crash signals have two different catalogues. The first catalogue "shocks" occur in a specified period and keep zero in other time, which can be called as "pulse". While the others are sustained oscillations existing in the whole duration. The basic idea of the proposed scheme is to compare the "base" and "shocks" separately and get more meaningful comparison.

To illustrate the proposed scheme, a pair of signals are used as an example. Each signal consists three components:

$$X = S + P + O \tag{E.7}$$

where, S, P and O refer to the "base", "pulse" and "oscillation", respectively. In this example, the base pulses are shown as Fig. E.1, whose peak points are $M_1 = (0.40s, 1000)$ and $M_2 = (0.64s, 900)$. As shown, the test signal are later and smaller than the reference.

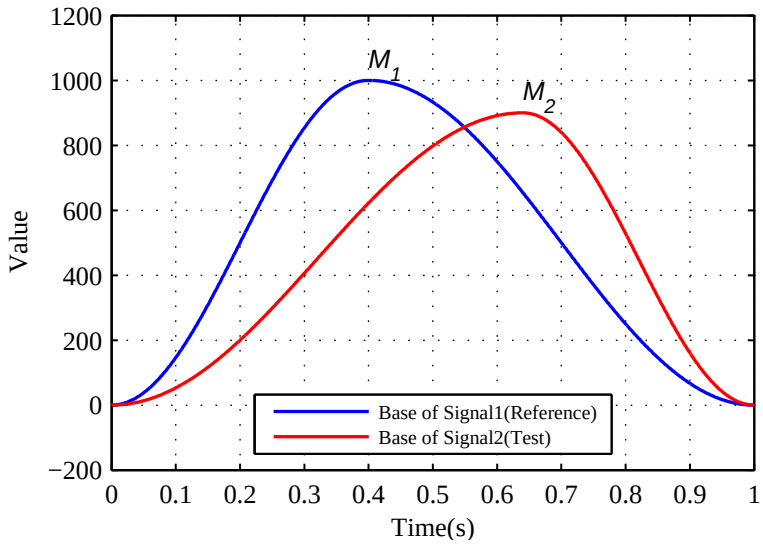

Figure E.1: Base signals in the example

The P and O are given as follows:

$$\begin{cases} P_c = A_1(t) * \sin(40\pi t + \pi) & 0.367 \le t \le 0.467 \\ P_m = A_2(t) * \sin(50\pi t) & 0.400 \le t \le 0.480 \end{cases} \tag{E.8}$$

and

$$\begin{cases} O_c = A_3(t) * \sin(30\pi t - \pi) \\ O_m = A_4(t) * \sin(25\pi t - \pi) \end{cases} \tag{E.9}$$

where $A_1(t) = 180\sin^2(10\pi(t-0.367))$, $A_2(t) = 200\sin^2(12.5\pi(t-0.367))$, and $A_3(t) = 60+12\sin(5\pi t)$ and $A_4(t) = 80+10\sin(4\pi t)$. The subscript c refers to the reference signal and m refers to the test signal. The signals for comparison are shown in Fig. E.2. Comparing with the reference signal, the test signal has a phase error of 14.54% and a magnitude error of -9.78%, which are calculated by S&G metric.

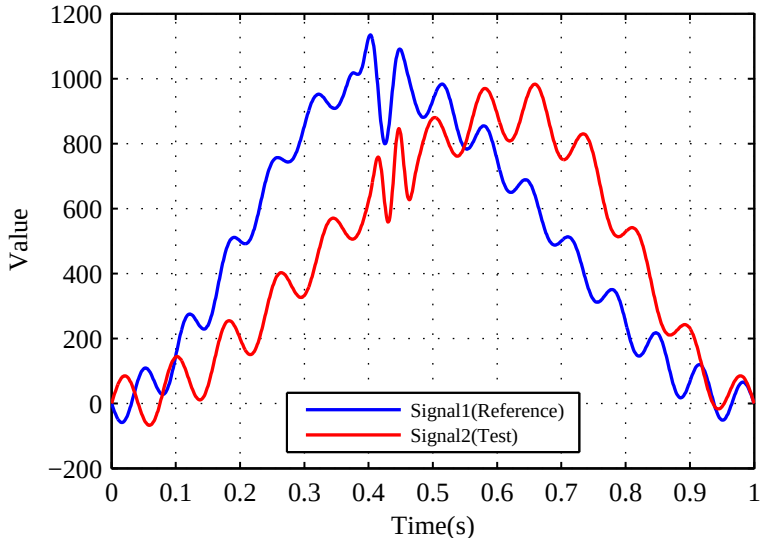

Figure E.2: Example signals for comparison

E.3.1 Pre-processing of Signals

As many other schemes, the pre-processing of signals is required before comparisons. For a pair of time histories, one of them (generally the signal measured from full car test) is selected as reference signal, and the other one is test signal. Typically, the pre-processing includes:

- Filtering: the influence of noise from measurements should be removed by the filtering of raw data. The digital filters can be designed for different purposes in vehicle safety according to the standard SAE J211.
- Re-sampling: two signals should share the same sampling interval.
- Synchronizing: ensure two crash signals start at the same stage. This step is always operated manually.
- Trimming: For the convenience and accuracy of comparison, the trimming process cuts off the unconcerned period and ensure two signals have the same length.

The Matlab based interactive interface RSVVP provides a friendly tool for pre-processing. More information can reference to [13] and will not be discussed in this paper.

E.3.2 Ensemble Empirical Mode Decomposition (EEMD)

To extract the trends of crash responses, original signals should be decomposed according to the frequency. The wavelet transformation (WT) has been applied in the model validation [21] and vehicle crash studies [22]. However, the crash responses are nonlinear and non-stationary signals in most cases and the selection of mother wavelet for crash signals is difficult. For this reason, Ensemble Empirical Mode Decomposition (EEMD) is employed in the proposed scheme.

According to Huang [23], a signal can be decomposed into a set of Intrinsic Mode Functions (IMFs), which represent the natural oscillatory modes embedded in the signal. The instantaneous frequency and amplitude of each time point on IMFs is of physics meaning. The goal of Empirical Mode Decomposition (EMD) is to acquire the IMFs of signal. Different from Fourier Transform and Wavelet Transform, EMD does not suppose any base function and conducts the decomposition according to the local time scale character of signals. EMD is a self-adaptive time-frequency analysis method for nonlinear and non-stationary signals and therefore suitable for the analysis of crash signals. Given a signal $x(t)$, the procedure of extracting IMFs is called shifting process, shown as Algorithm E.1.

Algorithm E.1 Shifting Process of EMD

Step1: Set $p = 1$, $h_p(t) = x(t)$; $q = 0$, $r_q(t) = h_p(t)$.
Step2: Extract the local maxima and minima of signal $r_q(t)$ and construct the upper and lower envelops of $r_q(t)$ by interpolation method (generally the cubic spline function).
Step3: Calculate the mean of the upper and lower envelops, recorded as $m_q(t)$. Set $r_{q+1}(t) = r_q(t) - m_q(t)$.
Step4: Calculate the standard division between $r_q(t)$ and $r_{q+1}(t)$: $SD = \sum [r_q(t) - r_{q+1}(t)]^2 \Big/ \sum r_q^2(t)$.
Step5: If $SD \leq threhold$, then stop the shifting process; or else repeat Steps 2$\sim$4 until $SD \leq threhold$. After the shifting process, the residual signal $r_i(t)$ is the IMF_p.
Step6: Repeat the shifting process (Steps 1$\sim$5) for signal $h_{p+1}(t) = h_p(t) - IMF_p$ to get other IMFs until the IMF_p has only one or no extrema.

EEMD is an improvement of EMD to overcome the mode mixing problem caused by intermittence [24]. In EEMD method, some trial decompositions of noised signals are conducted. The noise here is white noise with finite amplitude. The true IMF component is defined as the mean of an ensemble of trials. Because the noise in each trial is different, the added noise will be filtered by EMD process. With this improvement, EEMD can perform a stable decomposition of original signal. Each IMF from EEMD may fall into a specific frequency interval.

For model validation purposes, only first k IMFs should be treated as “oscillations" and the rest IMFs and residual are summated as “trend". Then the original signal is written as $X = \sum_{i=1}^{k} IMF_i + T$, where T is the trend signal. k is decided by the criterion that the integration of $IMF_1 \sim IMF_k$ are nearly zero.

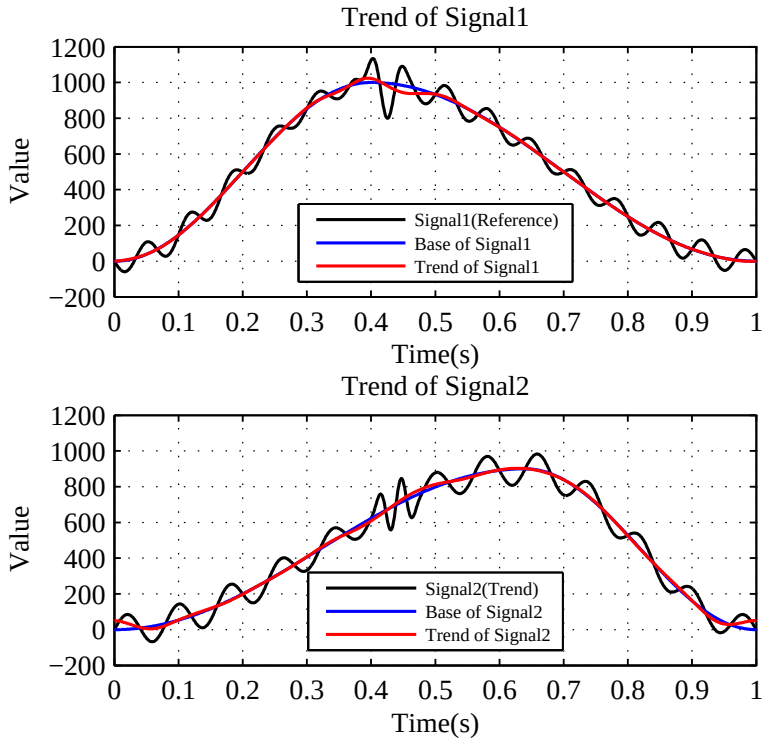

Figure E.3: Trends of original signals

In this example, the signals are decomposed into a trend and two IMFs. Figure E.3 shows the result of trend extraction. It can be seen that trend signals can represent base pulses perfectly.

After EEMD, the reference and test signals are presented as:

$$\begin{cases} C(t) = \sum_{i=1}^{k} c_i + T_c(t) \\ M(t) = \sum_{i=1}^{k} m_i + T_m(t) \end{cases} \tag{E.10}$$

Generally, $T_c(t)$ and $T_m(t)$ have same number of peaks and valleys. This condition ensures the DTW process in next subsection have a clear physical interpretation.

E.3.3 Compare The Trends of Crash Signals

The trend signal can be treated as a result of low-pass filtering of original signals and a good representation of base signal. In the comparison of trends, two errors, i.e. Time of Arriving (TOA) and magnitude, are proposed.

The difference of trends can be divided into horizontal (i.e. time) and vertical (i.e. value) directions. To make an orthogonal decomposition of discrepancy, dynamic time warping (DTW) is involved. DTW makes an optimal match between two time histories by expanding or compressing time axes. The cost function of DTW is defined in Eqn. (E.11) to punish the distance and local shape between the two points.

$$d(i,j) = \left((i-j)^2 + (T_c(i) - T_m(j))^2\right) |dT_c(i) - dT_m(j)|^{\alpha} \tag{E.11}$$

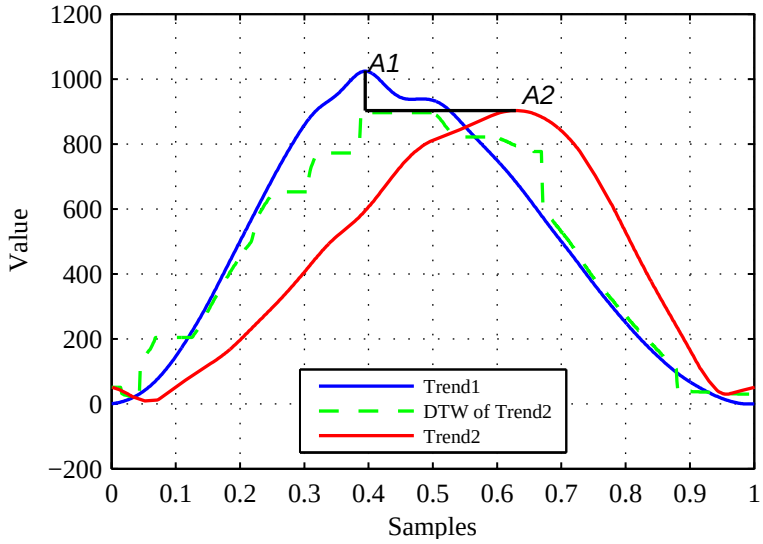

Figure E.4: Comparison of trend signals

where $dT_c(i) = T_c(i) - T_c(i-1)$, $dT_m(j) = T_m(j) - T_m(j-1)$ and α is an adjustable parameter. Figure E.4 shows the correspondence of the trends after DTW. It can be seen that two signals are matched well. Especially, the discrepancy are exactly decomposed along the time and value axes.

Comparing with the original signal, the trends are more suitable for DTW process. Fig. E.5 shows the warping result of original signals. It can be seen that, local oscillations influence the matching significantly and lead unsuitable warping of signals. For example, the peak point of two signals, i.e. M_1 and M_2 are rematched to N_1 and $N2$ respectively, which are obviously unreasonable.

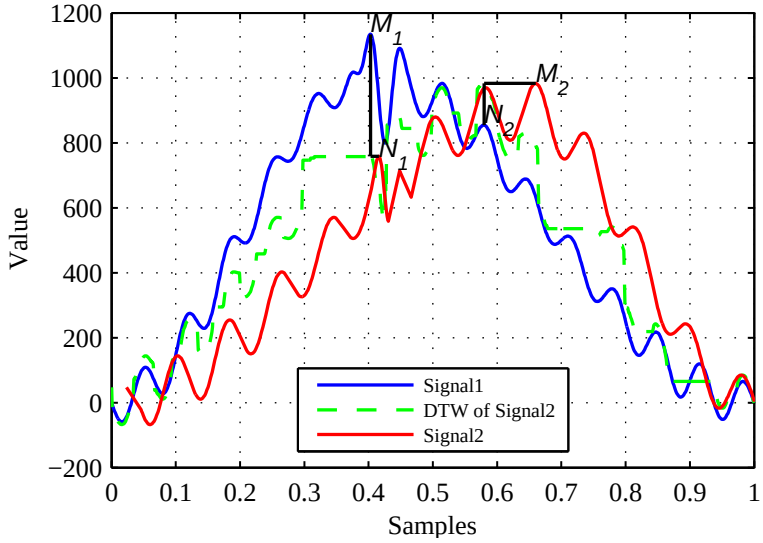

Figure E.5: DTW of original signals

After the DTW, each time point of test signals has one or several corresponding points in reference signals. Assuming $T_m(i)$ are corresponding to $T_c(p) \sim T_c(q)\,(p \leq q)$,

the error of TOA of $T_m(i)$ is

$$e_t(i) = i - \frac{p+q}{2} \tag{E.12}$$

And the error of magnitude is

$$e_v(i) = T_m(i) - \frac{\sum_{k=p}^{q} T_c(k)}{q-p+1} \tag{E.13}$$

Then the discrepancy ratio over the whole time is

$$E_t = \frac{\sum |e_t(i)|}{n^2} \tag{E.14}$$

$$E_v = \frac{\sum |e_v(i)|}{\sum |T_c(i)|} \tag{E.15}$$

where n is the length of time history. And the comprehensive error is

$$E = \sqrt{(E_t^2 + E_v^2)} \tag{E.16}$$

In the example, $E_t = 10.10\%$, $E_v = 12.28\%$ and $E = 15.90\%$. This result is consistent to the observation and Sprague & Geers metric.

E.3.4 Compare The IMFs of Crash Signals

The IMFs are series of high frequency oscillations and present the local features of original signals. According to [25], these IMFs are of physical meaning in crash processes. For this reason, comparing the IMFs can achieve more information of vehicle crashworthiness structure. In the proposed scheme, the error of magnitude and frequency will be compared for validation. However, considering some components in vehicle structure may work in a specified duration, the working period of each IMF should be checked firstly.

According to the property of EEMD, the IMF $x(t)$ is an amplitude modulated-frequency modulated (AM-FM) signal, i.e.

$$x(t) = A(t)\cos(\varphi(t)) \tag{E.17}$$

with $A(t) > 0$, $\dot{\varphi}(t) > 0$. To separate the amplitude modulation component $A(t)$ and frequency modulation component $\varphi(t)$, Huang proposed a normalization scheme in [26]. Fig. E.6 and Fig. E.7 show the IMFs of example signals. As shown, the amplitude functions $A(t)$ are the envelop of IMFs, which are shown by dark line.

The working period is duration $t_a \sim t_b$, when $A(t)$ satisfied $A(t) > A_{th}$. The threshold A_{th} is

$$A_{th} = \theta * \bar{A}(t) \tag{E.18}$$

where $\bar{A}$ is the average of $A(t)$ and θ is the predefined parameter.

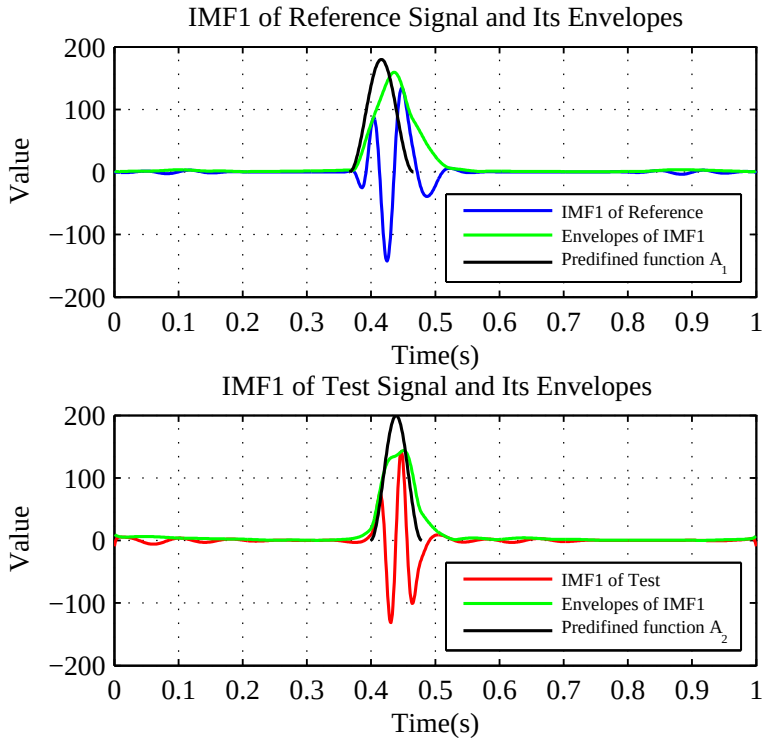

Figure E.6: Comparison of IMF1

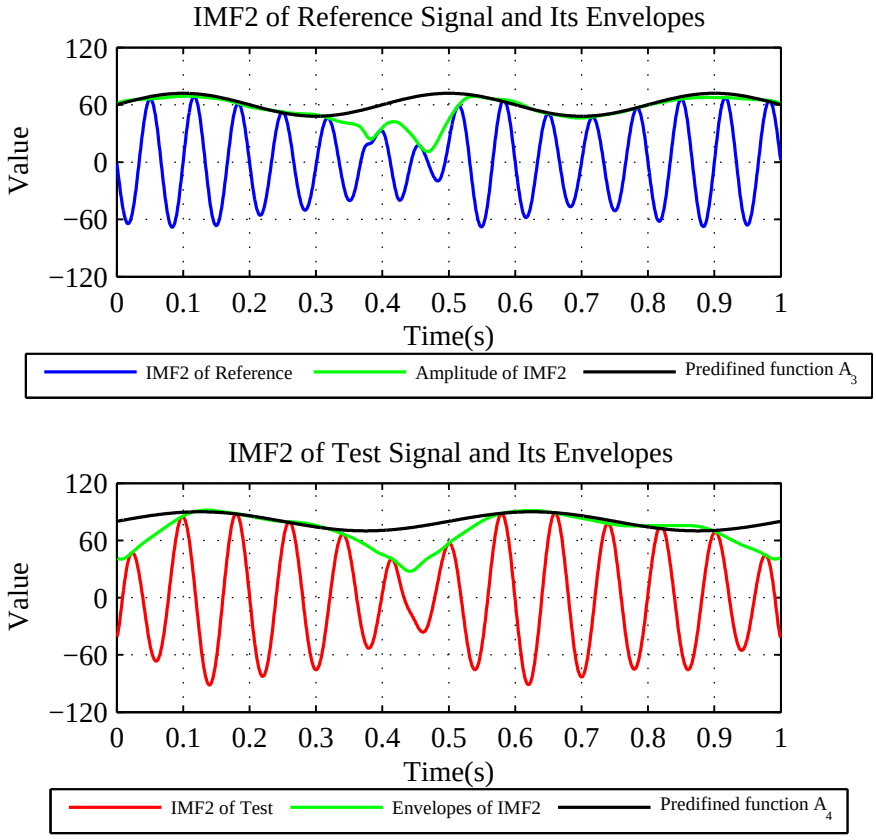

Figure E.7: Comparison of IMF2

In the example case, the refernece IMF1 has working period $0.381 \sim 0.518s$ and test IMF1 $0.376 \sim 0.522s$. The first pair of IMFs are corresponding to the pulse components. The working period of IMF2s are the whole period, which indicates that IMF2s are corresponding to the oscillations.

The errors of IMFs should be calculated only in corresponding working periods of IMFs. The magnitude error of IMFs is defined as the difference of average amplitude, i.e.

$$Ea_i = \frac{\bar{A}_{mi}(t) - \bar{A}_{ci}(t)}{\bar{A}_{ci}(t)} \tag{E.19}$$

where $\bar{A}_{mi}(t)$ and $\bar{A}_{ci}(t)$ are the average amplitude of i-th pair of IMFs.

The instantaneous frequency of $x(i)$ can be calculated by

$$f(t) = \frac{d\varphi(t)}{dt} \tag{E.20}$$

In the examples, the calculated average frequency of reference IMFs are 17.82Hz and 15.00Hz and of test IMFs are 22.881Hz and 12.95Hz.

The discrepancies of frequency are defineded as

$$Ef_i = \frac{\bar{f}_{mi} - \bar{f}_{ci}}{\bar{f}_{ci}} \tag{E.21}$$

where $\bar{f}_{mi}(t)$ and $\bar{f}_{ci}(t)$ are the average frequency of i-th pair of IMFs.

It should be noted that, it is possible that a IMF has no valid working period, which indicates the original signal has no component in the corresponding frequency range. For a pair of IMFs, if both IMFs have no working period, this pair of IMFs can be skipped for comparison. However, if only one IMF has no working period, it may indicate that the component of corresponding frequency is missing in the original signal. In the application of crashworthiness, this may be related to some difference in vehicle structure.

Table E.3: Comprehensive Comparison Metrics

	Metrics	Results
Trend	Time Error	10.49%
	Value Error	12.55%
	Comprehensive	16.35%
IMF1	Magnitude Error	-13.54%
	Frequency Error	28.39%
IMF2	Magnitude Error	28.20%
	Frequency Error	-13.63%

In a short summary, the error metrics of proposed comprehensive comparison scheme are listed in Table E.3 with the comparison result of example case. In addition, the working period of IMFs are in Table E.4.

Table E.4: Working Period of IMFs

		Reference	Test			Reference	Test
IMF1	start	0.381s	0.376s	IMF2	start	0s	0s
	end	0.518s	0.522s		end	1s	1s

E.4 Case Study

To demonstrate the proposed scheme, three cases of vehicle crash with different conditions will be employed. According to relative regulations, a new type of vehicle should be checked in full car crash tests before marketing. Generally, these tests are executed by the New Car Assessment Program (NCAP). To ensure the tests reliable and meaningful, the crashes should be performed in some specified conditions. For example, the FMVSS200 series standards, published by The National Highway Traffic Safety Administration (NHTSA), set the passive safety rules for vehicle crash tests in the US.

In the tests, accelerometers are located on the concerned positions of vehicle body and dummies, such as brake caliper, left rear seat and the head of dummy. These accelerations are recorded as crash responses, which will be used for safety analyses of vehicles. Another source of crash responses are CAE simulations in finite element or multibody software. In this section, the crash responses from CAE software will be compared with those from full car crash, as the common cases of model validation purpose. For simplicity, all signals in this section are sampled by 10kHz and filtered properly.

E.4.1 Case 1

This case is employed to show the basic use of the proposed scheme. Figure E.8 shows the crash responses of left rear seat of Toyota Yaris during a 56 km/h front crash. The first signal (reference signal) comes from NHTSA Test 5677 while another two are from CAE simulations. The FE model of Yaris is published by NCAC and simulated by two different FE softwares. It can be seen that the simulated signals are consistent but have some errors with real crash test. Thus the errors of two simulations are hoped to be similar.

Each signal is decomposed as a trend and three IMFs in the EEMD. The trends are shown in Fig. E.9. After DTW, the trends are rematched as the dashed lines. As shown, both CAE1 and CAE2 trends match the reference trend very well except in the peak area.

Figure E.10 is the comparison of IMFs. It is easy to find a visible discrepancy betweens IMFs, which is corresponding to the error during 0.015$\sim$0.03s of original signals. Other two pairs of IMFs have no significant discrepancy.

Table E.5 lists the calculated errors of this case. Based on this table, some notes can be summarised:

1) By checking the errors, both simulation results match the full car crash test very well.

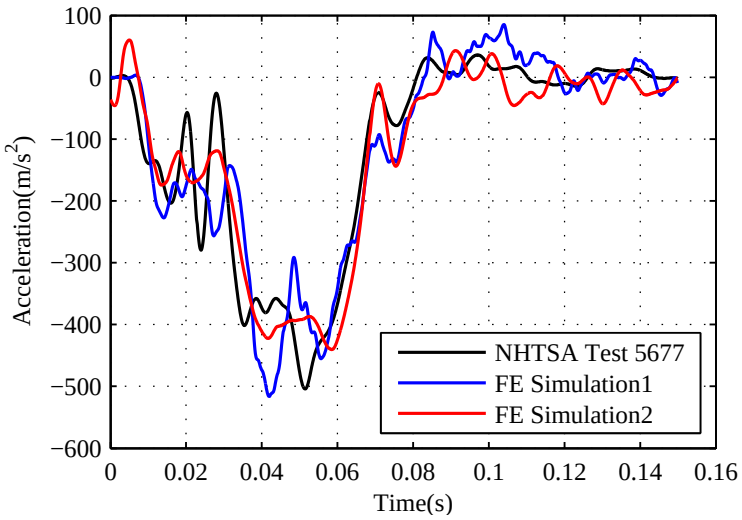

Figure E.8: Crash responses of left rear seat in 56km/h front crash

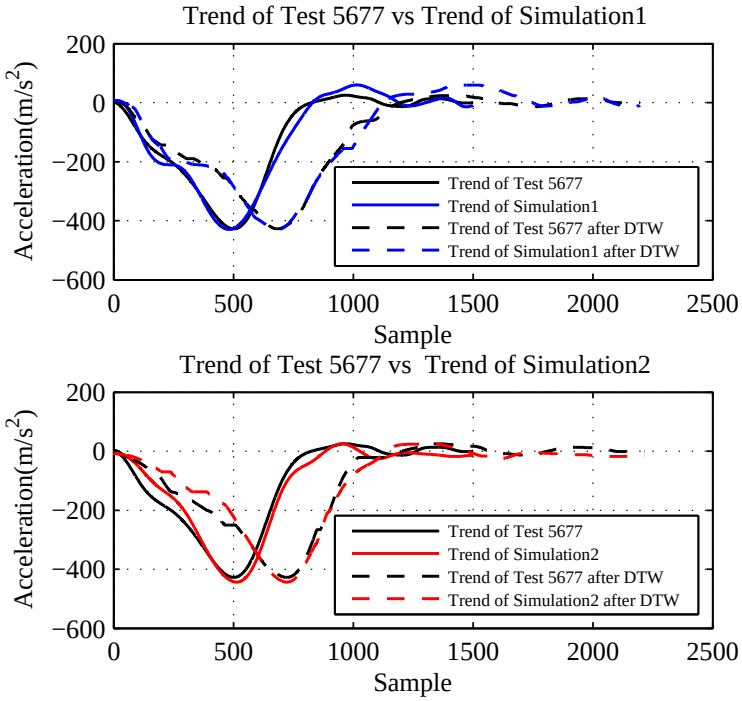

Figure E.9: Comparison of trends in Case1

2) Comparing with the result of S&G, the proposed trend comparison achieves smaller error on time axes and bigger magnitude error. This is consistent with the inspection.

3) According to the IMF comparisons, two simulation results have some errors on details. The most important error happens during 0.015∼0.035s of IMF1. This means neither of these two simulations can describe local oscillations well. However, this is not reflected by the given metrics. This is because the time span for comparison is large and the error only exists on a short period. So it is of

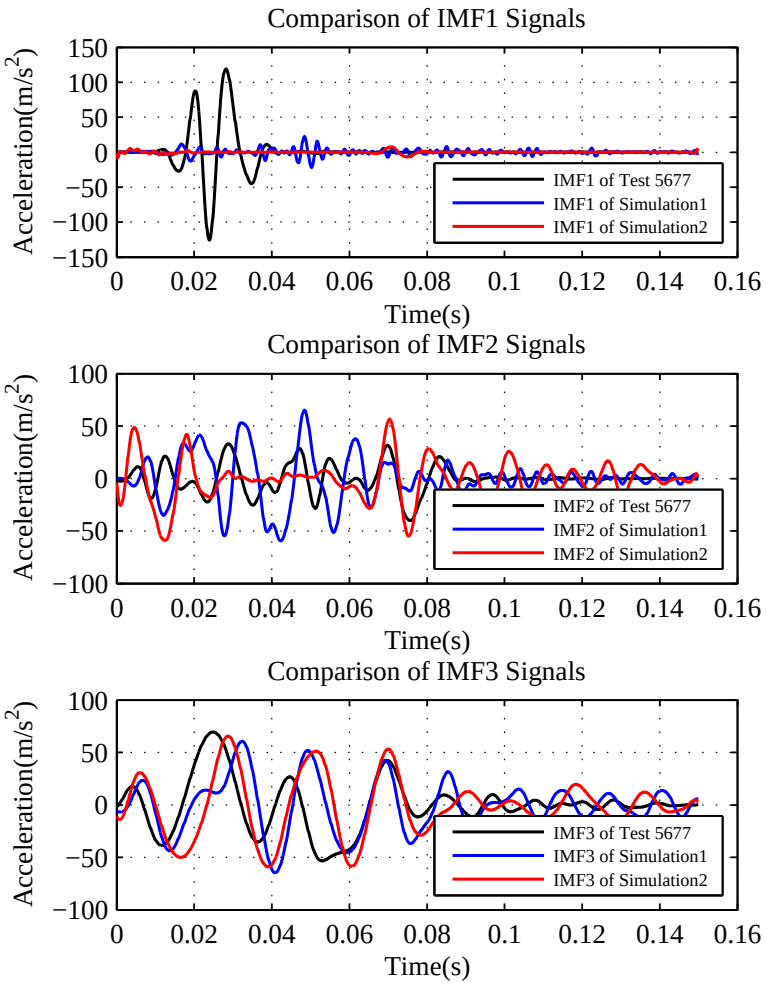

Figure E.10: Comparison of IMFs in Case1

Table E.5: Comparison Result of Case 1

		Simulation 1	Simulation 2
Trend	Time Error	2.50%	2.49%
	Value Error	11.70%	16.91%
	Comprehensive	8.46%	12.08%
IMF1	Frequency Error	135.50%	88.52%
IMF2	Frequency Error	7.11%	-4.44%
IMF3	Frequency Error	75.82%	-7.75%
S&G	Phase Error	7.6%	9.7%
	Magnitude Error	-0.6%	1.4%
	Comprehensive	7.6%	9.8%

importance to trim crash responses properly in the pre-processing process.

4) The errors of two simulation results are quite similar. This is reasonable as they are using the same FE model of vehicle. In addition, the common shortage of the two simulations are the lost of oscillations. This error can be seen as the

problem of FE model, instead of FE solver.

E.4.2 Case 2

Three signals shown in Fig. E.11 are the crash responses of engine top in front crashes, which comes from FE simulations. The initial speeds are 56km/h, 48km/h and 40km/h respectively. The proposed scheme is supposed to check the similarity among them.

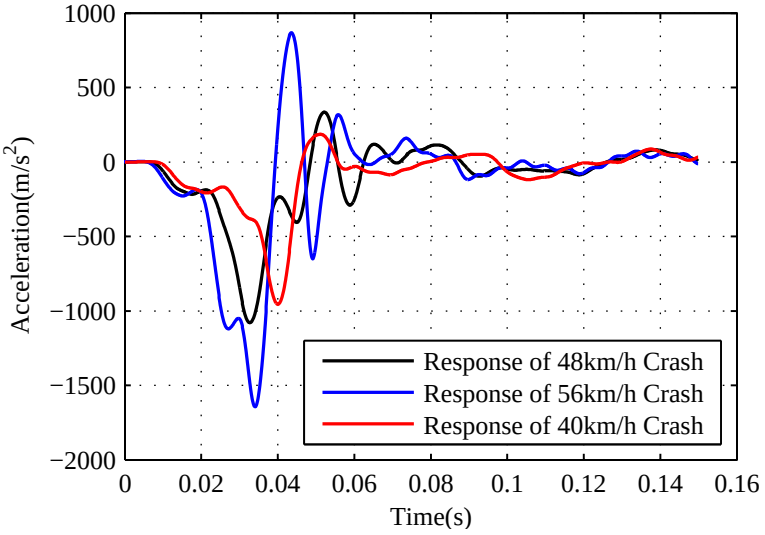

Figure E.11: Simulated responses of engine top in 56km/h front crashes

Table E.6: Comparison Result of Case 2

		48km/h Crash	40km/h Crash
Trend	Time Error	2.87%	5.15%
	Value Error	32.83%	28.15%
	Comprehensive	23.30%	20.24%
IMF1	Frequency Error	94.34%	76.49%
IMF2	Frequency Error	39.99%	105.56%
S&G	Phase Error	24.9%	40%
	Magnitude Error	-36.6%	-48.5%
	Comprehensive	44.3%	62.9%

For the sake of convenience, the crash response of 56km/h crash is set as reference signal. Table E.6 presents the results of comparison. Three points are concluded as follows:

1) The main errors exists on the value of magnitude, i.e. the energy of crash. The calculated errors of 40km/h response are bigger than 48km/h response as expectation. An interesting observation is that the error value is related to the square of velocity.

2) There are very small error of trends on time axes, which is similar to the visual inspection. And comparing to 48km/h crashes, the response of 40km/h crash has a little bigger error of time.

E.4.3 Case 3

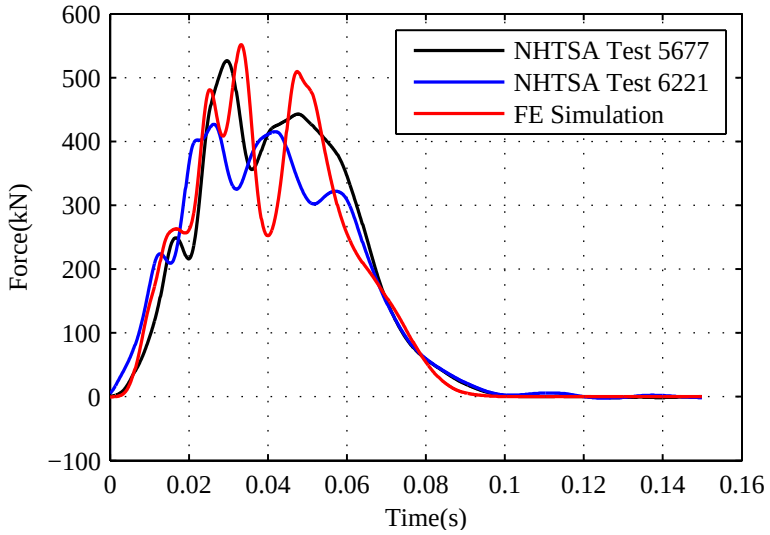

Figure E.12: External forces in 56km/h front crashes

Except the acceleration signals, some other time histories can also be compared by the proposed scheme. This case will show an example of comparison of reaction forces from barrier, which is of meaning in vehicle crash analysis. The force signals ares measured in NHTSA Test 5677(reference), NHTSA Test 6221 and an FE simulation. The crash condition is front crash to a rigid wall in 56km/h. NHTSA Test 5677 used Toyota Yaris for test. While Test 6221 used Toyota Yaris 3-Door Liftback, which is a little different on weight and body shape. The FE simulation used the model of Toyota Yaris in NHTSA Test 5677. Figure E.12 shows the force signals and Tab. E.7 lists the comparison result.

Table E.7: Comparison Result of Case 3

		Test 6221	FE simulation
Trend	Time Error	6.01%	3.77%
	Value Error	7.34%	1.25%
	Comprehensive	6.70%	2.81%
IMF1	Frequency Error	-40.28%	-34.65%
IMF2	Frequency Error	-39.33%	-22.63%
IMF3	Frequency Error	41.09%	133.66%
S&G	Phase Error	6.8%	6.3%
	Magnitude Error	-9.2%	-1.7%
	Comprehensive	11.4%	6.6%

It can be seen that the results of Test 6221 and FE simulation are quite similar. The trends of them match the reference very well, but the details contain errors. The local error of Test 6221 mainly exists in the frequency component, while that of FE simulation exists on the magnitude aspect. This shows the proposed scheme can distinct small difference again.

E.5 Conclusion

This paper presented an EEMD aided comparison scheme for time histories. Different from other existing methods, each signal for comparison is decomposed into a trend signal and several IMFs. The trend signals and each pair of IMFs are compared separately. The advantages of the proposed scheme are as follows:

1) The trend signal represents the based mode of original signal and is not influenced by high frequency disturbance. The comparison of trend signals will provide a robust result to describe the overall difference between test and reference signal.

2) In the comparison of trends, the DTW process helps to find the corresponding relationship between the nodes of reference and test signals. Based on this, the metric of trend comparison contains two orthogonal discrepancy (i.e. the error of time and value) with clear physical meaning.

3) Each pair of IMFs contains the local information on a specific frequency interval. So the comparison of them is to check the local information. A large error of IMF always refers to the lost of local features, such as peak and local vibration.

4) Another advantage of the proposed scheme is that it involves more features into comparison. This makes it possible to provide a comprehensive result. Especially, the measurement of each feature has clear physical meaning. Therefore the proposed scheme is closed to the comparison of SMEs.

5) In different application areas, some parameters in the proposed method should be adjusted properly. For the model validation in vehicle safety engineering, the typical values are given in this paper. Another problem to be improved in the future is that some details cannot be reflected by the given metric and need further analysis of IMFs.

References

[1] H. Sarin, M. Kokkolaras, G. Hulbert, P. Papalambros, S. Barbat, and R.-J. Yang, "Comparing time histories for validation of simulation models: error measures and metrics," *Journal of Dynamic Systems, Measurement, and Control*, vol. 132, no. 6, p. 061401, 2010.

[2] M. H. Ray, M. Mongiardini, and M. Anghileri, "Development of the roadside safety verification and validation program," *Roadside Safety Verification and Validation Program,(Draft)*, 2008.

[3] M. Mongiardini, M. Ray, R. Grzebieta, and M. Bambach, "Verification and validation of models used in computer simulations of roadside barrier crashes," in *Australasian Road Safety Research Policing Education Conference, 2013, Brisbane, Queensland, Australia*, 2013.

[4] "Instrumentation for impact test - Part 1: Electronic instrumentation," Standard, SAE International, 2014.

[5] "Instrumentation for impact test - Part 2: Photographic instrumentation," Standard, SAE International, 2014.

[6] Z. Zhan, Y. Fu, R. J. Yang, and Y. Peng, "Development and application of a reliability-based multivariate model validation method," *International journal of vehicle design*, vol. 60, no. 3/4, pp. 194–205, 2012.

[7] X. Jiang, R.-J. Yang, S. Barbat, and P. Weerappuli, "Bayesian probabilistic PCA approach for model validation of dynamic systems," tech. rep., SAE Technical Paper, 2009.

[8] Y. Fu, X. Jiang, and R.-J. Yang, "Auto-correlation of an occupant restraint system model using a bayesian validation metric," tech. rep., SAE Technical Paper, 2009.

[9] L. Gu and R. Yang, "CAE model validation in vehicle safety design," tech. rep., SAE Technical Paper, 2004.

[10] X. Liu, W. Chen, and M. Paas, "Automated occupant model evaluation and correlation," in *ASME 2005 International Mechanical Engineering Congress and Exposition*, pp. 353–358, American Society of Mechanical Engineers, 2005.

[11] F. La Torre, L. Domenichini, M. Meocci, A. Nocentini, and S. G. Morano, "Evaluation of the vehicle/safety barrier/sign support interaction by means of FEM simulations," *International Journal of Crashworthiness*, no. ahead-of-print, pp. 1–11, 2014.

[12] O. Polach and A. Böttcher, "A new approach to define criteria for rail vehicle model validation," *Vehicle System Dynamics*, vol. 52, no. sup1, pp. 125–141, 2014.

[13] M. H. Ray, M. Mongiardini, and C. Plaxico, "Quantitative methods for assessing similarity between computational result and full scale crash test," in *91th Annual Meeting of the Transportation Research Board, Washington, DC*, Citeseer, 2012.

[14] B. R. Donnelly, R. M. Morgan, and R. H. Eppinger, "Durability, repeatability and reproducibility of the NHTSA side impact dummy," tech. rep., SAE Technical Paper, 1983.

[15] H. Sarin, M. Kokkolaras, G. Hulbert, P. Papalambros, S. Barbat, and R.-J. Yang, "A comprehensive metric for comparing time histories in validation of simulation models with emphasis on vehicle safety applications," in *ASME 2008 International*

Design Engineering Technical Conferences and Computers and Information in Engineering Conference, pp. 1275–1286, American Society of Mechanical Engineers, 2008.

[16] Z. Zhan, Y. Fu, and R.-J. Yang, "Enhanced error assessment of response time histories (EEARTH) metric and calibration process," tech. rep., SAE Technical Paper, 2011.

[17] J. B. Putnam, C. D. Untaroiu, J. Littell, and M. Annett, "Finite element model of the THOR-NT dummy under vertical impact loading for aerospace injury prediction: Model evaluation and sensitivity analysis," *Journal of the American Helicopter Society*, vol. 60, no. 2, pp. 1–10, 2015.

[18] C. Gehre, H. Gades, and P. Wernicke, "Objective rating of signals using test and simulation responses," in *21st International Technical Conference on the Enhanced Safety of Vehicles, Stuttgart, Germany*, 2009.

[19] L. E. Schwer, "Validation metrics for response histories: perspectives and case studies," *Engineering with Computers*, vol. 23, no. 4, pp. 295–309, 2007.

[20] C. C. Chou, J. Le, P. Chen, and D. Bauch, "Development of CAE simulated crash pulses for airbag sensor algorithm/calibration in frontal impacts," in *17th International Technical Conference on the Enhanced safety of Vehicles, Amsterdam*, 2001.

[21] J. R. McCusker, K. Danai, and D. O. Kazmer, "Validation of dynamic models in the time-scale domain," *Journal of Dynamic Systems, Measurement, and Control*, vol. 132, no. 6, p. 061402, 2010.

[22] H. R. Karimi and K. G. Robbersmyr, "Signal analysis and performance evaluation of a vehicle crash test with a fixed safety barrier based on haar wavelets," *International Journal of Wavelets, Multiresolution and Information Processing*, vol. 9, no. 01, pp. 131–149, 2011.

[23] N. E. Huang and Z. Wu, "A review on Hilbert-Huang transform: Method and its applications to geophysical studies," *Reviews of Geophysics*, vol. 46, no. 2, 2008.

[24] Z. Wu and N. E. Huang, "Ensemble empirical mode decomposition: a noise-assisted data analysis method," *Advances in adaptive data analysis*, vol. 1, no. 01, pp. 1–41, 2009.

[25] Z. Wei, H. R. Karimi, and K. G. Robbersmyr, "Analysis of the relationship between energy absorbing components and vehicle crash response," tech. rep., SAE Technical Paper, 2016.

[26] N. E. Huang, Z. Wu, S. R. Long, K. C. Arnold, X. Chen, and K. Blank, "On instantaneous frequency," *Advances in adaptive data analysis*, vol. 1, no. 02, pp. 177–229, 2009.